LABELING AND OPTIMIZATION OF ORGANELLE MARKERS FOR CO-LOCALIZATION WITH YEAST GPCR DIMERS

A THESIS SUBMITTED TO
THE GRADUATE SCHOOL OF NATURAL AND APPLIED SCIENCES
OF
MIDDLE EAST TECHNICAL UNIVERSITY

BY

İLKE SÜDER

IN PARTIAL FULFILLMENT OF THE REQUIREMENTS
FOR
THE DEGREE OF MASTER OF SCIENCE
IN
BIOTECHNOLOGY

SEPTEMBER 2013

Approval of the Thesis

LABELING AND OPTIMIZATION OF ORGANELLE MARKERS FOR CO-LOCALIZATION WITH YEAST GPCR DIMERS

Submitted by **İLKE SÜDER** in partial fulfillment of the requirements for the degree of **Master of Science in Biotechnology Department, Middle East Technical University** by,

Prof. Dr. Canan Özgen _____

Dean, Graduate School of **Natural and Applied Sciences**

Prof. Dr. Nesrin Hasırcı _____
Head of the Department, **Biotechnology**

Assoc. Prof. Dr. Çağdaş Devrim Son _____
Supervisor, **Biology Department, METU**

Assoc. Prof. Dr. Can Özen _____
Co-supervisor, **Biotechnology Department, METU**

Examining Committee Members

Prof. Dr. Mahinur Akkaya _____
Chemistry Department, METU

Assoc. Prof. Dr. Çağdaş Devrim Son _____
Biology Department, METU

Assoc. Prof. Dr. Can Özen _____
Biotechnology Department, METU

Assoc. Prof. Dr. Ayşegül Gözen _____
Biology Department, METU

Assist. Prof. Dr. Bala Gür Dedeoğlu _____
Biotechnology Institute, Ankara University

Date: 02.09.2013

I hereby declare that all information in this document has been obtained and presented in accordance with academic rules and ethical conduct. I also declare that, as required by these rules and conduct, I have fully cited and referenced all material and results that are not original to this work.

Name, Surname: İlke SÜDER

Signature :

ABSTRACT

LABELING AND OPTIMIZATION OF ORGANELLE MARKERS FOR CO-LOCALIZATION WITH YEAST GPCR DIMERS

Süder, İlke

M. Sc., Department of Biotechnology

Supervisor: Assoc. Prof. Dr. Çağdaş D. Son

Co-Supervisor: Assoc. Prof. Dr. Can Özen

September 2013, 105 pages

G-protein-coupled receptors, which are the most versatile chemical sensors, have prominent role in physiologically important cellular processes including cell growth and neurotransmission. Therefore, they are targeted by almost 50% of drugs in the market against diseases such as heart failure, neurological disorders and hypertension. It is well established phenomenon that GPCRs exist and function as dimers. Studies illustrate that dimerization may be favored for receptor activation, signal transduction, trafficking, cell surface mobility and ligand interactions. Even though evidences of homo- and hetero-dimerization accumulated there is no consensus on why GPCRs oligomerize. Since the pharmacological characteristics of the receptors may be altered when oligomerization occurs, the localization and reason of the phenomenon draws great attention. Comprehensive knowledge of the localization of a protein or biological process unravels the function of the protein or process.

Yeast GPCRs, Ste2p, Ste3p and Gpr1p, serve as models for GPCR studies *in vivo*. Since Ste2p is known to form homodimer, dimerization studies have been focused on the receptor for years. Although subcellular fractionation data indicate that Ste2p dimers are found in the ER as many as in the plasma membrane, recent study conducted in our lab points out that the Ste2 dimer does not fluorescence in the ER when labeled with split EGFP. Hence, the aim of the study was to generate fluorescent organelle marker proteins which label the subcellular compartments on the trafficking route of membrane proteins. By co-localizing the markers with split EGFP tagged Ste2 dimer, where the dimerization occurs in living

cells through a noninvasive approach could be identified. Therefore, using short targeting sequences, red ER marker fluorescent protein was constructed in the study. Using resident proteins of the late endosome, the Golgi apparatus and COPII vesicle, related full-length organelle marker proteins were prepared by tagging them at carboxy terminal with mCherry, a red FP. Furthermore, to be used for further studies in our lab, peroxisome markers using resident peroxisome protein were also generated. The visualized subcellular compartments showed characteristic morphologies consistent with previous descriptions. In order to assess the functionality of the organelle markers, they were co-localized with EGFP tagged Ste2p and Gpr1p. All the results were consistent with expectation based on knowledge on membrane protein trafficking. Therefore, it can be confidently suggest that all the markers are valuable resources for co-localization studies in live yeast cells. Moreover, they can serve for organelle marking in live cells without using expensive antibodies or harmful chemicals, identification of localization and thus function of unidentified proteins and monitoring the distribution and dynamics of organelles.

Keywords: Fluorescent organelle marker proteins, co-localization, GPCR oligomerization, intracellular trafficking

ÖZ

MAYA GPKR DİMERLERİNİN KO-LOKALİZASYONU İÇİN ORGANEL İŞARETLEYİCİLERİN HAZIRLANMASI VE OPTİMİZASYONU

Süder, İlke

Yüksek Lisans, Biyoteknoloji Bölümü

Tez Yöneticisi: Doç. Dr. Çağdaş D. Son

Ortak Tez Yöneticisi: Doç. Dr. Can Özen

Eylül 2013, 105 Sayfa

Çok yönlü kimyasal sensör olan G proteinine kenetli reseptörler hücre büyümesi ve sinirsel iletim gibi fizyolojik açıdan önemli biyolojik olaylarda öne çıkan görevlere sahiptir. Bu nedenle; kalp krizi, sinir hastalıkları ve yüksek tansiyon gibi rahatsızlıklara karşı kullanılan ilaçların %50'si GPKR'leri hedeflemektedir. GPKR'lerin dimer hâlinde bulundukları ve fonksiyonlarını yerine getirdikleri bilinmektedir. Çalışmalar; dimerleşmenin reseptör aktivasyonu, sinyal iletimi, hücre işi taşıma, hücre yüzeyi hareketliliği ve ligand etkileşimleri gibi nedenlerle gerçekleştiğini göstermektedir. Homodimerizasyon ve heterodimerizasyon kanıtları bir hayli olsa da GPKR'lerin neden oligomer oluşturduğu üzerinde fikir birliği bulunmamaktadır. Ancak, oligomerleşme gerçekleştiğinde reseptörlerin farmakolojik özellikleri değişebildiğinden olayın lokalizasyonu ve nedeni dikkat çeken konulardandır. Bir protein yahut biyolojik olayın lokalizasyonu üzerine elde edilen kapsamlı bilgi protein ya da olayın işlevinin çözülmesini sağlamaktadır.

Ste2, Ste3p ve Gpr1p maya GPKRleri in vivo GPKR çalışmaları için model olarak kullanılmaktadır. Ste2p'nin homodimer oluşturduğu bilindiğinden de reseptör yıllardır dimerleşme çalışmalarının odağındadır. Hücre içi fraksiyonlanma çalışmaları Ste2p alfa faktör reseptörü dimerlerinin hücre zarında bulunduğu kadar endoplazmik retikulumda da görüldüğünü önermiş olsa da laboratuvarımızda yapılan yakın bir çalışma, bölünmüş EGFP ile işaretlenen Ste2p dimerlerinin endoplazmik retikulumda sinyal vermediğine işaret etmektedir. Bu nedenle, bu çalışmada proteinlerin hücre zarına taşınırken geçtiği organelleri işaretleyen floresan organel işaretleyici proteinlerin hazırlanması amaçlanmıştır. Böylece, bu işaretleyicilerin bölünmüş EGFP ile etiketlenmiş Ste2 dimerleri ile kolokalizasyonu canlı hücrelerde noninvaziv bir yöntemle dimerleşmenin nerede gerçekleştiğini gösterebilecektir.

Bu amaç doğrultusunda, kısa hedefleyici sekanslar kullanılarak kırmızı endoplazmik retikulum işaretleyicileri yapılmıştır. Geç endozom, Golgi ve COPII vezikül işaretleyicileri ise yerleşik proteinlerin C uçlarından mCherry kırmızı floresan proteini ile işaretlenmesi ile oluşturulmuştur. Ayrıca, peroksizom integral zar proteini kullanılarak peroksizom işaretleyicisi de bu çalışmada hazırlanmıştır. Görüntülenen hücre içi bölgeler daha önceki tanımlara uygun karakteristik morfoloji göstermişlerdir. Organel işaretleyicilerin işlevini değerlendirmek için EGFP ile etiketli Ste2 ve Gpr1 reseptörleri ile kolokalizasyonları gerçekleştirilmiş ve hücre zarı proteinlerinin taşınması ile ilgili bilinenlerle tutarlı sonuçlar elde edilmiştir. Dolayısıyla, bu işaretleyicilerin canlı maya hücrelerinde kolokalizasyon çalışmaları için değerli kaynakları olduğu güvenle söylenebilir. Ayrıca bu işaretleyiciler; pahalı antikorlar ya da zararlı kimyasallar kullanılmadan canlı hücrelerde organel işaretlenmesi, karakterize edilmemiş proteinlerin lokalizasyonu dolayısıyla da işlev tayini ve organellerin dağılım ve dinamiklerinin incelenmesi için kullanılabilir.

Anahtar kelimeler: Floresan organel markör proteinler, ko-lokalizasyon, GPKR oligomerizasyonu, hücre içi taşıma

To my family

ACKNOWLEDGEMENTS

I would like to thank first and foremost my thesis advisor, Dr. Çağdaş D. Son, for his support and guidance throughout this research. I am grateful for freedom he has given in the lab and his launching me on the path to becoming an independent researcher.

I would like to thank my co-advisor, Dr. Can Özen, and members of thesis examining committee; Dr. Mahinur Akkaya, Dr. Bala Gür Dedeoğlu and Dr. Ayşegül Gözen for their time, invaluable suggestions and comments which make the final version of the thesis better.

I am really indebted to my ex- and current labmates; Beren Üstünkaya, Giray Bulut, Merve Kasap, Orkun Cevheroğlu, Selin Akkuzu, Sinem Çelebiöven and the last but not least Şerife Şeyda Pirinçci for sharing their knowledge, motivating, assisting and at most camaraderie. Being with them was great pleasure to me. I would also like to thank Burcu Karakaya for her moral and physical support. In the last six months, she was my energy booster, third hand and stand-by brain that enable me to continue.

I would like to acknowledge TÜBİTAK, which financially supports me since the beginning of my undergraduate study, for the support with TÜBİTAK BİDEB 2210 – Domestic Master Scholarship Program.

I would like to thank METU Central Laboratory, Molecular Biology, Biotechnology R&D Center and UNAM for Confocal Microscopy Facilities.

I wish to express my deep appreciation to my dearest friends Alperen Erdoğan, Ezgi Eroğlu, Hilal Gürler, Kemal Sağlam, Nebibe Mutlu, Şerife Şeyda Pirinçci and Uğurcan Özay for turning my life into fun. I also need to thank them for noteworthy discussions we had during my master's study. They taught me that finding friends with the same life style as you is priceless. I hope they will always stand by me even if we might be on the four corners of the world.

I am sure that I cannot find any appropriate words to express my gratitude to my parents for their never ending support and caring even as I followed my ambitions. They are always with me only to encourage, cheer up and love. When I have to cope with any difficulties, talking to them and even thinking of them are enough for me. I hope I make them proud at the end.

TABLE OF CONTENTS

LIST OF TABLES

TABLES

LIST OF FIGURES

FIGURES

LIST OF ABBREVIATIONS

AT	Angiotensin
BRET	Bioluminescence resonance energy transfer
cAMP	Cyclic adenosine monophosphate
COP	Coat protein complex
CXCR	CXC chemokine receptor
$DiOC_6$	Dihexaoxacarbocyanine iodide
DMSO	Dimethyl sulfoxide
dNTP	Deoxyribonucleic acid
EDTA	Ethylenediaminetetraacetic acid
ER	Endoplasmic reticulum
ERES	Endoplasmic reticulum export sites
ERGIC	ER-Golgi intermediate compartment
ESCRT	Endosomal sorting complexes required for transport
EtBr	Ethidium bromide
FP	Fluorescent protein
FRET	Fluorescence resonance energy transfer
GABA	Gamma-Aminobutyric acid
GABABR	Gamma-Aminobutyric acid type B receptor
GAP	Glyceraldehyde 3-phosphate
GDP	Guanosine diphosphate
GEF	Guanine nucleotide exchange factor
GFP	Green fluorescent protein
GPCR	G-protein coupled receptor
GPI	Glycosylphosphatidylinositol
GTP	Guanosine triphosphate
ILV	Intraluminal vesicles
LB	Luria Bertani
LiAc	Lithium acetate
MAPK	Mitogen-activated protein kinase
MAPKK	Mitogen-activated protein kinase kinase
MAPKKK	Mitogen-activated protein kinase kinase kinase
MAT	Methionine adenosyltransferase
mGLU	Metabotropic glutamate
MLT	Medium lacking tryptophan
MLU	Medium lacking uracil
MLTU	Medium lacking tryptophan and uracil
MVB	Multivesicular bodies
OST	Oligosaccharyltransferase
PAGE	Polyacrylamide gel electrophoresis
PCR	Polymerase chain reaction

PDI	Protein disulfide-isomerase
PEG	Polyethylene glycol
PKA	Protein kinase A
PM	Plasma membrane
PRE	Pheromone response elements
PTS	Peroxisome targeting sequence
QD	Quantum dots
RGS	Regulators of G protein signaling
SDS	Sodium dodecyl sulfate
SNARE	Soluble NSF attachment protein receptor
SPC	Signal peptidase complex
SRP	Signal recognition particle
SSTR	Somatostatin receptor
TBE	Tris/Borate/EDTA
TRAPPI	Transport protein particle I
UDP	Uridine diphospate
UGGT	UDP-glucose:glycoprotein glucosyltransferase
YEPD	Yeast Extract-Peptone-Dextrose

CHAPTER I

INTRODUCTION

1.1. G-Protein-Coupled Receptors

Membrane proteins transmit extracellular signal to intracellular responses in order to maintain homeostasis and coordinate cellular activity. G-protein-coupled receptors (GPCRs) is one of the largest and most diverse membrane protein families (Kobilka, 2013; Latek, Modzelewska, Trzaskowski, Palczewski, & Filipek, 2012; Venkatakrishnan *et al.*, 2013). Despite differences in their primary sequence and function, all the receptors possess the same architecture compromising seven transmembrane α-helices, extracellular amino and intracellular carboxy termini (Venkatakrishnan *et al.*, 2013).

GPCRs, represented as nature's most versatile chemical sensors, respond to a wide spectrum of extracellular signals including photons, odorants, amino acids, peptide, proteins, nucleic acids, steroids, fatty acids, protons and ions (Latek *et al.*, 2012). Upon binding of the ligands, GPCRs activate physiologically important cellular processes such as neurotransmission, secretion, cellular differentiation, cell growth and metabolism (Bouvier, 2001). As the processes in which they play substantial roles imply, mutations in the receptors lead to acquired and inherited ailments such as nephrogenic diabetes insipidus, psychological disorders, thyroidism, fertility disorders, and cancer (Schöneberg *et al.*, 2004). Therefore, GPCR agonists or antagonists are commonly used as drugs against many diseases including asthma, hypertension, heart failure and neurological disorders (Bouvier, 2001). Even in 1998, G-protein-coupled receptors were reported as the molecular targets of almost a thousand drugs launched only in the last thirty years (Wilson *et al.*, 1998). Today, they are targeted by nearly 50% of current drugs as well as drugs of abuse (Hipser, Bushlin, & Gupta, 2010; M. C. Overton, Chinault, & Blumer, 2005).

1.1.1. GPCRs in *Saccharomyces cerevisiae*

There are three genes encoding GPCRs in budding yeast (Versele, Lemaire, & Thevelein, 2001) whereas the number is more than 800 in the human genome (Venkatakrishnan *et al.*, 2013). While *STE2* and *STE3* encode proteins that activate pheromone signaling, *GPR1* gene product plays role in glucose sensing in budding yeast.

1.1.1.1. Ste2p, Alpha-Pheromone Receptor

In *Saccharomyces cerevisiae*, a set of sterile (STE) genes, whose mutations bring about inability to mate, are identified (Hartwell, 1980). Among those genes, *STE*2 and *STE*3 encode proteins which are mating type specific G-protein-coupled receptors. In *MAT***α** cells, *STE*3 is expressed and its product recognizes **a**-factor, a peptide pheromone. On the other hand, *STE*2 is expressed in *MAT***a** cells and Ste2p senses **α**-factor, another peptide pheromone. Both Ste2p and Ste3p belongs to D Class of GPCRs, consisting of only fungal mating pheromone receptors (Attwood & Findlay, 1994). Although the yeast pheromone response pathway receptors are highly diverse from other GPCRs with respect to sequence, some heterologous GPCRs expressed in yeast can functionally substitute them being activated by mammalian agonists (Pausch, 1997). Due to the low cost, simplicity, conserved cellular pathways, largely solved signaling pathways of Baker's yeast (Versele *et al.*, 2001) in addition to opportunity of the heterologous expression, well characterized pheromone response pathway, whose elements resemble the counterparts in mammalian cells, has served as a model system to study GPCRs *in vivo* (Pausch, 1997). In order to reveal the GPCR mediated signaling and its regulation, understand ligand-GPCR interactions and deorphanize GPCRs Ste2p has been investigated (Henrik G Dohlman & Thorner, 2001).

Pheromones are substances by which the individuals of the same species communicate with each other. As many vertebrates and insects, fungi secrete pheromone to attract the opposite mating type. The peptide pheromone is sensed by the receptors of the mate and, in turn, leads to physical responses for a successful mating (Xue, Hsueh, & Heitman, 2008).

When 13-amino acid-long mature alpha-factor binds to Ste2p, the alpha-factor receptor, it brings about switch from inactive state to active state conformation. The change, in turn, causes activation of G_{α}, Gpa1p, stimulating the exchange of GDP for GTP. This exchange triggers disassociation of Gα from Gβγ (Ste4p/Ste18p) heterodimer (Whiteway *et al.*, 1989). Ste18 is a protein which anchors the dimer to the membrane whereas Ste4 is the social partner of the complex and inactive when bound to Gα-GDP. All the downstream pheromone signaling responses are induced by the activity of the liberated dimer. The Ste4 component binds to Ste20, which is a member of p21-activated protein kinase (PAK) family, Ste5, adapter and scaffold protein with no catalytic but co-localizing, sequestering

and organizing activity (Dowell, Bishop, Dyos, Brown, & Whiteway, 1998), and Cdc24/Far1 complex, guanine nucleotide exchange factor (GEF) combined with another adapter protein (Peter & Herskowitz, 1994). When $G_{\beta\gamma}$ binds to Far1/Cdc24 heterodimer, Far1 moves with Cdc24 to the plasma membrane, where Cdc42 is permanently anchored. When they come to close proximity, Cdc24 activates Cdc42 for the exchange of GDP for GTP. The activation subsequently leads to the phosphorylation of Ste20p by rendering its binding sites exposed in addition to localization of cytosolic Ste20 to the cell membrane. When $G_{\beta\gamma}$ binds to Ste5p, which is binding platform for mitogen-activated protein kinase (MAPK) module; Ste5, Ste20 and the entire MAPK module become recruited to the membrane to trigger the downstream signaling circuit. The MAPK module consists of Ste11 (MAPKKK), Ste7 (MAPKK) and Fus3 (MAPK). Upon interaction of the dimer with Ste20, Ste20 is activated to phosphorylate Ste11, the first component of MAPK module, located on the scaffold protein, Ste5. Activated Ste11, in turn, activates Ste7, which phosphorylates the last member of the module, Fus3. The phosphoactivated Fus3 activates Far1, which, in turn, inhibits Cdc28/Cln1/2 complex. This inhibition brings about inactivation of cell division control and thus cell cycle arrest in G1 phase (Bardwell, 2004). Activated Fus3 also phosphorylates Ste12/Dig1/Dig2 transcription factor complex. Ste12 is a protein that acts as a transcription factor binding to pheromone response elements (PREs). Before its phosphoactivation, it is repressed by Dig1 and Dig2. Fus3 transfers phosphate group to Dig1 and Dig2 as well as Ste12; therefore, the phosphorylations inhibit the repression of Ste12 by Dig1/2 (Bardwell, 2004). Released Ste12 induces the expression of mating pathway genes such as *STE2*, *FUS3*, *FAR1*; genes of negative feedback regulators of the pathway, which are *SST2*, *MSG5* and *GPA1*; and cell fusion genes including *FUS1*, *FUS2*, *FIG1* and *AGA1* (White & Rose, 2001). Through expression of the genes, Gβγ-Far1-Cdc24-Cdc42 interaction and phosphorylation of Bem1, Bni1, Gic1 and Gic2; yeast cells exhibit polarized growth towards the highest concentration of the pheromone and thus form a pear-like shape termed "shmoo" (Madden & Snyder, 1998). *S. cerevisiae* is non-motile; hence, this chemotactic morphogenesis is crucial for the fusion of mating partners. Upon pheromone binding, in 4 hours, opposite mating partners shmoo, fuse firstly their cell membrane and then nuclei to generate a diploid yeast cell. For the differentiation of vegetatively growing haploid cells to cells with gamete features and later their fusion, 200 genes (almost 3% of yeast genome) are expressed (Bardwell, 2004) (Figure 1.1).

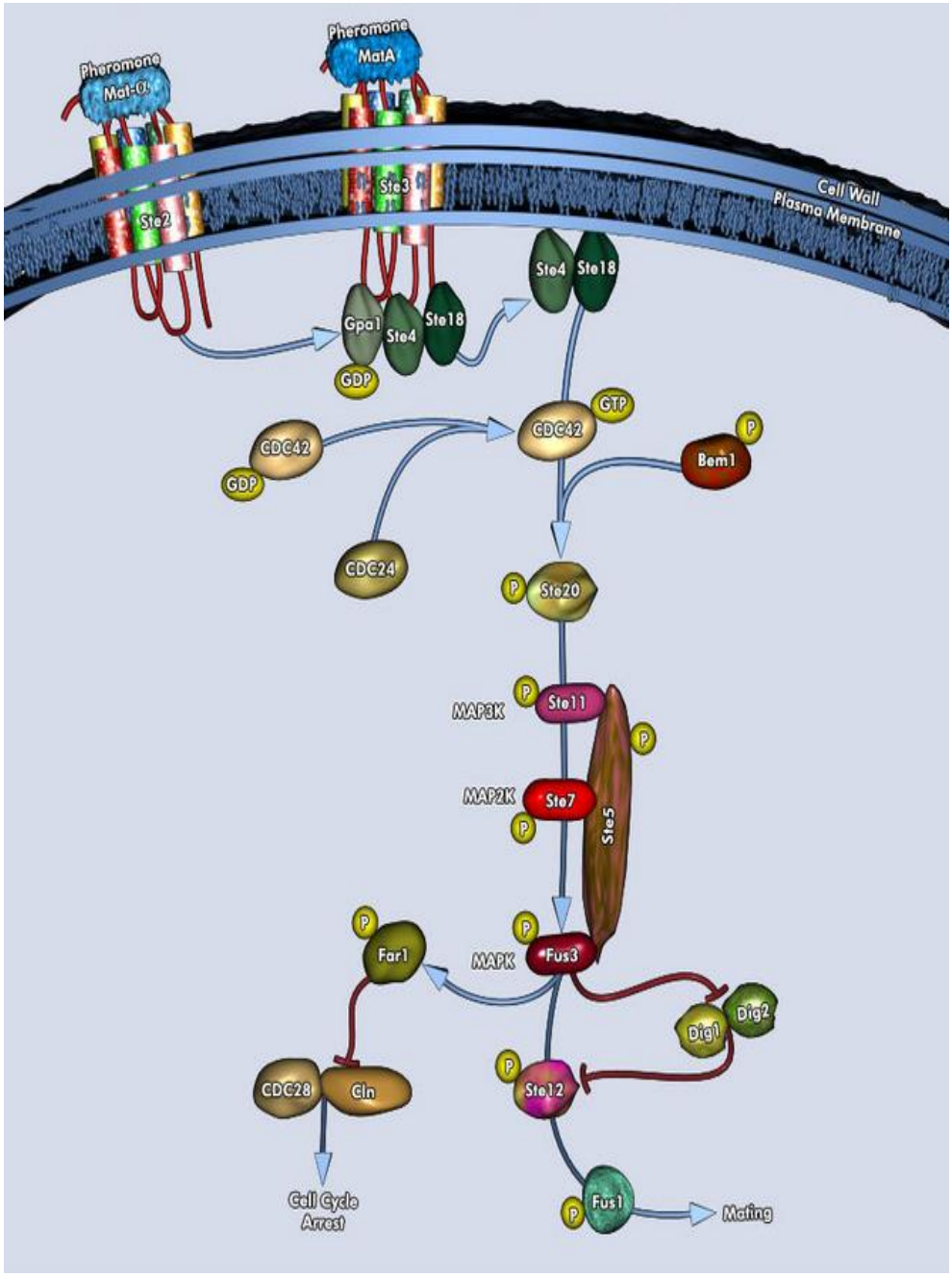

Figure 1.1 Pheromone Response Pathway in *S. cerevisiae* (Retrieved from **http://www.qiagen.com/products/genes%20and%20pathways/Pathway%20Details.aspx?pwid=283** on 01.08.2013)

Yeast pheromone response pathway is modulated in many ways to enhance desensitization, recovery and adaptation. To begin with, protein kinase members of the pathway are regulated by either autoinhibition or phosphorylation of activation loops. For instance, Ste20 and Ste11 have autoinhibitory domains to be inactive whereas Ste20, Ste11, Ste7 and MAPKs are activated by phosphorylation (Bardwell, 2004) as mentioned above. Modification of the pheromone receptor plays also prominent role in internalization and endocytosis. Continued presence of the pheromone leads to desensitization throughhyperphosphorylation of C terminal residues followed by ubiquitylation, internalization and vacuolar degradation (Versele *et al.*, 2001). Besides, it is reported that the phosphorylation of receptor tail lowers the sensitivity of Ste2 regardless of its endocytosis (Bardwell, 2004). Furthermore, Fus3 autocontrol its activation duration and intensity in order to prevent signal leak into other pathways. Before phosphoactivation of Kss1, its inactive form also interacts with Ste12 so as to repress the transcription of mating specific genes. There are some GTPase acceleration proteins (GAPs) to check the Cdc42 activity. Moreover, there are proteins named as regulators of G-protein signaling (RGSs). Sst2 is a well-studied RGS protein which is phosphostabilized by MAPKs following the kinases activation upon ligand binding. Stabilized Sst2 directly binds to Ste2 and acts as GAP to hydrolysis GTP of Gpa1 and hence causes the retrimerization of G protein. Since the pathway is dependent on kinase activity, phosphatases such as Ptp2, Ptp3 and Msg5 play role in inhibition of the cascade. Bar1/Ssst1 complex is Mat**a** specific extracellular protease, which is secreted to degrade alpha-factor. There are two other proteins that take action on the signaling; which are Afr1, which leads to alpha factor resistance by a signaling-independent way, and Asg7, Mata specific protein that also inhibits the pheromone response (Bardwell, 2004). Furthermore, a1 encoded by MATa and α2 encoded by MATα generate a dimer in fused cells in order to repress the transcription of pheromone response pathway genes (Herskowiitz, 1989).

1.1.1.2. Gpr1p, Glucose Sensing Receptor

As many organisms, primary carbon and energy source of Baker's yeast is glucose. When *Saccharomyces cerevisiae* cells grow on glucose with no limitation of other nutrients, they prefer to metabolize glucose anaerobically, even under aerobic conditions, rather than to fully oxidize glucose to water and carbon dioxide since fermentation proceeds at higher rates and the ethanol product facilitates the survival of the yeast against its alcohol-sensitive competitors (Busti, Coccetti, Alberghina, & Vanoni, 2010). In order to maintain the efficiency, yeast cells have developed several sophisticated mechanisms to sense the glucose amount and change in its environment, which are cyclic AMP (cAMP)/protein kinase A (PKA) pathway, Rgt2/Snf3-Rgt1 pathway and Snf1 involved repression pathway. The distinct pathways are connected in order to modulate and coordinate cell growth and cell cycle (Busti *et al.*, 2010).

cAMP/PKA pathway is the major glucose signaling pathway in budding yeast and regulates many mechanism from proliferation and metabolism to morphogenesis and development depending on sugar availability. There are two G-protein related systems to control adenylate cyclase acitivity, which are Ras pathway and Gpr1-Gpa2 pathway (Zaman, Lippman, Zhao, & Broach, 2008). Ras1 and Ras2 are small monomeric GTP binding proteins. Their activity is controlled by GEFs, specifically Cdc25 and Sdc25, and GAPs, IraI and Ira2. Glucose in the extracellular medium of *Saccharomyces cerevisiae* triggers the GTP bound Ras protein production *(*Busti *et al.*, 2010). Then, Ras-GTP directly binds to adenylate cyclase (Cyr1) to stimulate cAMP production. Ras-dependent increase in cAMP level in the cell activates PKA, which is serine/threonine kinase with two catalytic subunits encoded by *TPK1*, *TPK2* and *TPK3* and two regulatory subunits encoded by *BCY1* in its inactive state. In addition to Ras system, GPCR module, composed of Gpr1 and Gpa2, activates PKA. Gpr1 is a GPCR with a long third cytoplasmic loop and long C terminal tail and does not belong to any known GPCR class (Xue *et al.*, 2008). Gpa2 is Gα, which is activated upon glucose or sucrose binding to the Gpr1. GTP bound Gpa2 then stimulates cAMP synthesis during the transition from respiration to fermentation on glucose (Rolland, Winderickx, & Thevelein, 2002). The G_{α} protein is atypical since there are still no known canonic G_{β} and G_{γ} proteins to heterodimerize. Asc1p is a protein which is not homolog of classical G_{α} proteins but contains their characteristic structure. Recently, it is suggested that it can act as $G_{\beta\gamma}$ heterodimer since it binds to both inactive Gpa2 to inhibit phosphorylation of the G_{α} and also Cyr1 to lower cAMP generation (Zeller, Parnell, & Dohlman, 2007). Krh1 and Krh2 kelch proteins were thought to work as Gβγ; however, they downregulate the PKA pathway (Peeters, Versele, & Thevelein, 2007). According to the model in which Krh1/2 is Gβ, Gpg1, which activates PKA pathway, was thought to be Gγ (Zeller *et al.*, 2007). Rgs2s is another protein that has a role in triggering the GTPase activity of Gpa2 and so downregulating the cAMP signaling (Busti *et al.*, 2010; Versele *et al.*, 2001). Activation of cAMP/PKA pathway by G-protein dependent ways, in turn, leads to transcription genes in ribosome biogenesis (Neuman-Silberberg, Bhattacharya, & Broach, 1995), repression of stress responsive genes (Martínez-Pastor *et al.*, 1996) in addition to promoting fermentation and targeting enzymes in carbon and energetic metabolism *(*Busti *et al.*, 2010). Although mechanism has not been known yet, glucose internalization and glucose phosphorylation are crucial for glucose induced cAMP/PKA pathway activation. Furthermore, GPCR module is not necessary for acidification induced PKA activation and does not control basal cAMP level as Ras proteins. Gpr1p-dependent cAMP signaling can be initiated by only D-glucose and sucrose whereas mannose acts as antagonist of the pathway. The affinity of Gpr1 to glucose is low; 20 mM of glucose is required for activation of the pathway *in vivo*. This low affinity supports that the function of GPCR module in glucose sensing is restricted to stimulation of cAMP synthesis during transition from fermentative to aerobic growth. On the other hand, Gpr1 has high affinity to sucrose and 0.5mM in adequate to signaling activation, suggesting that under low glucose concentration, sucrose is determined to survive (Busti *et al.*, 2010; Rolland *et al.*, 2002; Versele *et al.*, 2001).

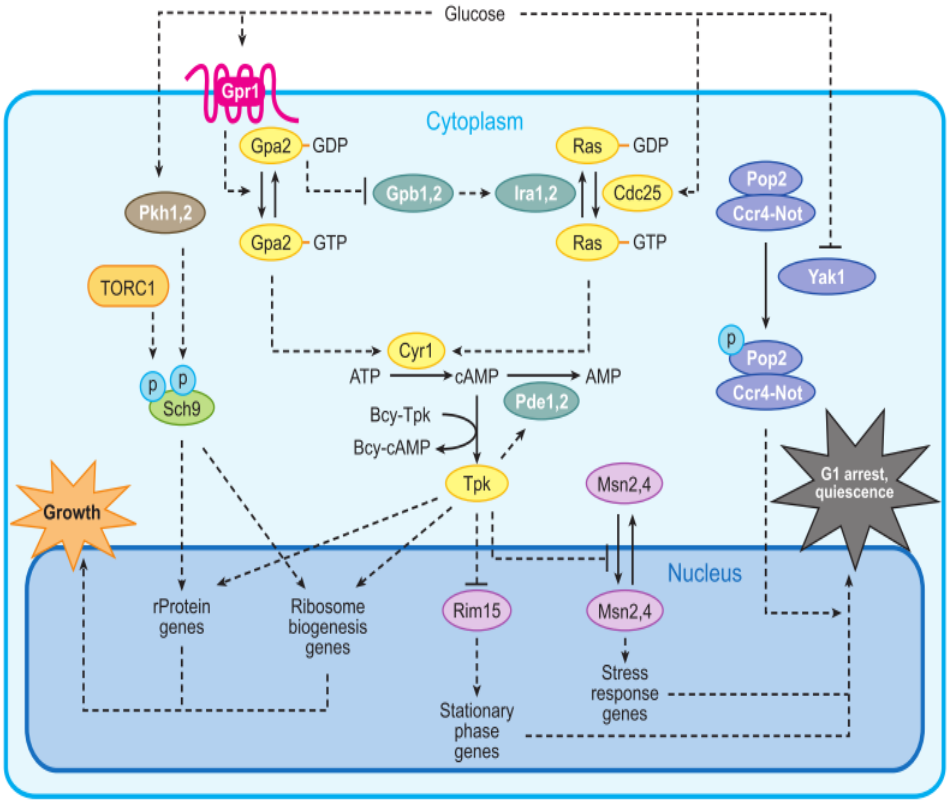

Figure 1.2 G-protein dependent glucose sensing pathway in *S. cerevisiae* (Busti *et al.*, 2010)

1.1.2. Oligomerization of GPCRs

Including cytosolic and nuclear DNA-binding receptors, most receptors exist and function as dimers (Heldin, 1995). Receptors can oligomerize with either identical (homooligomerization) or distinct receptors (heterooligomerization) (Ferré, Baler, Bouvier, & Caron, 2009). Studies on dimerization of distinct receptor types elucidate the probable reasons why receptors need to dimerize: ligand recognition, receptor activation, signal transduction, trafficking and cell surface mobility (Lohse, 2010) (Table 1.1).

Table 1.1 Mechanistic Effects of Receptor Dimerization (Lohse, 2010; M. C. Overton *et al.*, 2005)

Mechanism	Properties Gained by Dimerization
Ligand Recognition	• Specificity due to ligand interaction with more than one subunit • Enhanced affinity due to multiple interaction sites • Ligand diversity owing to different dimerizing partners
Receptor Activation	• Crossphosphorylation as activation • Change in distance between subunits as activation
Signal Transduction	• Crossregulation of activity in protomers • More than one interaction sites and specificities for intracellular signaling proteins
Trafficking	• Changes in trafficking to target to target sites • Crossregulation in receptor internalization
Cell Surface Mobility	• Crossregulation in cell surface mobility

On account of the characteristic structure of GPCRs, GPCRs can carry out a great deal of rearrangements and movements that successively facilitate transmission of activation signal across the membrane. In addition, its tight packing provides ligand specificity and interaction with G proteins leads to a suitable signaling. Therefore, GPCRs were traditionally considered to exist and function as monomers (Chabre, Deterre, & Antonny, 2009; Chabre & Maire, 2005). Consistent with the hypothesis, single rhodopsin, β2-adrenergic and μ-opioid receptors have been shown to be able to activate signaling with physiological speed *in vitro* (Vilardaga, Agnati, Fuxe, & Ciruela, 2010).

On the other hand, evidences from functional complementation, co-precipitation, SDS-PAGE, antibodies targeting more than one receptors, crosslinking, atomic force microscopy, FRET and BRET studies of GPCRs have been accumulated to state that GPCRs exist as dimers (Bouvier, 2001; Lohse, 2010). The early evidences of oligomerization are from radio-ligand binding studies conducted in 1970s (Salahpour, Angers, & Bouvier, 2000). Unraveling the rhodopsin homodimers in native membranes by atomic force microscopy (Fotiadis *et al.*, 2004) and results of fluorescence and bioluminescence energy transfer studies *in vivo* or *in vitro* have been the most satisfying proofs of GPCR oligomerization.

The first indication of heterodimerization is obligate dimer of $GABA_BR1$ and $GABA_BR2$, metabotropic receptors of gamma-amminobutyric acid (GABA) (Kaupmann *et al.*, 1998). In addition, $GABA_B$ receptors has been determined as tetramer and disruption of the oligomer led to increase in signaling, meaning that tetramerization of GABA receptors play role in regulation of the signaling (Lohse, 2010). Although dimerization and/or higher order oligomerization of receptors are well established phenomenon for GPCRs, there is no shared idea for the reason of oligomerization.

There are many examples suggesting that oligomerization is important in signal transduction. Baneres and Parello employed phase neutron scattering method to investigate leukotriene B_4 (BLT_1 receptor) dimers and found that the dimer engages with one G-protein upon ligand binding (Milligan, 2007). This finding suggests that GPCRs dimerize in order to 2:1 stoichiometry with bound G-protein. As mentioned earlier, $GABA_BRs$ form tetramer and if the oligomer structure is disrupted signal is multiplied compared to the former form. This illustrates that tetramer formation presumably inhibits signaling of all receptors and so modulated the action of γ-aminobutyric acid receptors (Kaupmann *et al.*, 1998).

Furthermore, there are mounting evidences of the fact that oligomerization is required for receptor activation. For instance, agonist binding to one protomer of metabotropic glutamate (mGlu) receptor dimer induces partial activation whereas they are fully activated when they are stimulated by binding of two agonists, suggesting that dimer formation is required for full activation. In addition, according to dimer symmetry, activation and signaling may assigned to each protomer as ligand binding protomer and G-protein coupling one or both protomer functions in activation and signaling in additive manner (Kniazeff *et al.*, 2004).

One of the most studied mechanisms acquired by oligomerization is ligand recognition. To illustrate, dimer of TIR2 and TIR3 taste receptors is involved in sweet taste perception TIR1/TIR3 dimer perceives umami taste, revealing that different combination of taste receptors brings about modulation of ligand binding properties (Li *et al.*, 2002). In addition, single α_{2A}-adreneergic receptor responds only to noradrenaline, when co-expressed with μ-opioid receptor its response only to noradrenaline decreases in the presence of morphine although it remains the same in the absence of morphine. This suggests that μ-opioid receptor negatively regulate acitivity of alpha2a receptors and thus the dimerization may affect the ligand affinity as well as receptor activation (Lohse, 2010). Moreover, ligand binding, functional and trafficking properties of δ- and κ-opioid receptors markedly differ with those of individual receptors. The pharmacological properties of the heterodimer is so distinct that the heterodimer, which is involved in morphine mediated analgesia, is thought to open a new door into regulation of analgesia and addiction (Jordan & Devi, 1999). Furthermore, it is reported that significantly increased number of heterodimer of AT1 angiotensin receptor and B2 bradykinin receptor is detected in preeclamptic hypertensive women. This heterodimerization causes reduced affinity to B2 agonist and is thought to be target of drugs despite what triggers the dimerization is not known (Hipser *et al.*, 2010).

Besides, evidences indicate that GPCR oligomerization is required for receptor maturation and/or trafficking to plasma membrane. $GABA_BR1$ and $GABA_BR2$ receptors are the first

known supporting examples of the idea. If R2 is not expressed in the cell, $GABA_BR1$ cannot exit from the endoplasmic reticulum since the heterodimerization leads to mask ER retention signal of R1 protomer. Thus, heterodimerization of GABA receptors is crucial for the receptor maturation. Since mutants of V_2-Vasopressin receptor are also retained in the ER as dimer it is suggested that quiet statically dimerized GPCRs, as $GABA_BR$ and V_2Rs, dimerize in the early stages of their biogenesis and are controlled in quality control check points (Lohse, 2010). Cell fractionation studies of β2-adrenergic receptor dimerization are illustrated that the dimer has been determined also in the ER (Salahpour *et al.*, 2004).

In addition to variety in the reason of GPCR dimerization, whether oligomerization is constitutive or not is not clearly known. For instance, oligomerization of chemokine (CXCR2) vasopressin, oxytocin and δ-opioid receptors is not affected by agonist and antagonist binding. Nevertheless, agonist binding to somatostatin receptor (SSTR5), gonadotropin-releasing hormone receptor and luteinizing hormone receptor has caused changes in FRET and BRET. This may indicate that their oligomerization is not constitutive for some GPCRs or ligand binding has induced conformational change which leads to significant angle alteration of RET pairs.

As yeast offer simplicity to study conserved eukaryotic mechanisms, dimerization of yeast GPCRs has been studying since late 1980s. The first evidence comes from a study on Ste2 receptors, whose C-tail is truncated. Carboxy terminus of Ste2p carries DAKSS endocytosis signal and its lack leads to loss of desensitization and endocytic downregulation. In the study, when the mutants were expressed with wild type alpha pheromone receptors, desensitization and downregulation of the receptors were partially regained, implying that Ste2p form homodimers (Reneke, Blumer, Courchesne, & Thorner, 1988). The homodimer of Ste2p was also detected as SDS-resistant and but detergent use seemed to disrupt the structure (Yesilaltay & Jenness, 2000); therefore, noninvasive methods like FRET was opted to study dimerization in yeast. Homodimerization was illustrated by FRET using CFP and YFP tagged receptors in native cells and membrane fractions (M. Overton & Blumer, 2000). The study hypothesizes that dimerization is constitutive since agonist binding does not alter FRET efficiency and that the complex is specific since there is no detected interaction with other membrane proteins. Moreover, G-protein activation was also showed not to affect FRET efficiency and Ste2p homooligomeric complex is regarded as functional unit. In 2002, Overton and Blumer employed subcellular fractionation and FRET so as to investigate where the oligomerization occurs. FRET efficiencies in subcellular fractions obtained from the cell membrane and the ER was determined as the same, suggesting that Ste2p oligomerizes during its biogenesis. Considering that Ste2p homodimer is internalized as dimer (Yesilaltay & Jenness, 2000), oligomerization has been suggested to occur throughout birth, life and death of alpha pheromone receptors (M. C. Overton & Blumer, 2002). In the help of mutagenesis and FRET, first transmembrane helix (TM1) of Ste2p was stated to be crucial for oligomerization and N-terminal domain and second transmembrane domain (TM2) were illustrated to be involved in facilitation of dimerization. Later studies showed that GXXXG motif within TM1 is exposed to lipid bilayer and so can be the direct interaction site. Nevertheless, TM1 containing the motif is not enough for dimerization since

it cannot form homodimer but TM1, TM2 and N terminal domain can do so. Amino acid substitutions in the motif also led to retention in the intracellular compartments but retention was not sufficient to impair signaling (M. C. Overton *et al.*, 2005). The motif can play role in trafficking, however, the intracellular trafficking of Ste2p has not been elucidated yet. When Ste2 mutants which are defective in G-protein coupling or ligand binding were coexpressed, signaling could not be recovered; thus, Ste2 protomers may be independently activated (M. C. Overton *et al.*, 2005). In the study, they also showed that Ste2 receptors in dimer may cooperate to interact and/or activate G proteins. Consistent with early studies, BRET experiments, using full length Ste2p in contrast to FRET studies, showed that for proper signaling two functional receptors are required (Gehret, Bajaj, Naider, & Dumont, 2006). To investigate the specific role of ligand in Ste2p dimerization, using atomic force microscopy and dynamic light scattering coupled with chemical crosslinking, it is suggested that even if the dimerization is constitutive agonist binding stabilizes the dimer and may induce higher order oligomerization (Shi, Paige, Maley, & Loewen, 2009). Furthermore, in addition to TM1, Cys residues from TM4 are indicated to be involved in homomeric contacts. Since TM1 and TM4 are far away to interact, Ste2p has been thought to form higher oligomers not only dimers (H. X. Wang & Konopka, 2009).

Although dimerizations of Ste2 and Ste3 receptors have been intensively studied there is no record of Gpr1 oligomerization up to now.

1.1.3. Biogenesis and Trafficking of Yeast GPCRs

Membrane proteins are sorted to plasma membrane along with secretory pathway. When the hydrophobic signal sequence of GPCRs is synthesized on ER associated polysomes, nascent protein is recognized by signal recognition particle (SRP) and a complex consisting of ribosome, nascent chain and SRP is formed. Then, SRP directs the complex to SRP receptor, localized on the ER and encoded by *SRP101* and *SRP102*, thereby transferring the protein that is being translated to Sec61 translocons. The cotranslational translocation (Figure 1.3 A) of membrane proteins is preferred although their posttranslational translocation (Figure 1.3 B) is also suggested to occur in the complete loss of SRP dependent route.

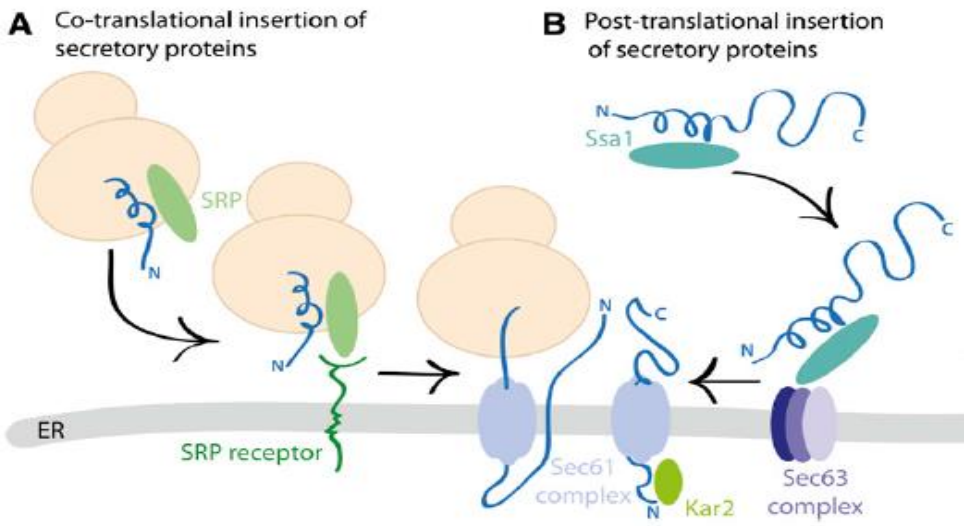

Figure 1.3 Membrane translocation of GPCRs (Barlowe & Miller, 2013)

Signal peptidase complex (SPC), which is thought to be very close to translocon exit site, cleaves the N-terminal signal peptide of the polypeptides and this endoproteolytic cleavage appears to be essential for maturation of proteins that have N terminal signal sequence and are trafficked to plasma membrane. Proteins having multiple transmembrane domains are located into the membrane during the translocation presumably its alternating signal and anchor sequences. The anchor sequences attach the hydrophobic domains of the protein to the lipid bilayer and hydrophilic regions are exposed to cytosol. After cleavage, N-linked glycosylation is catalyzed by oligosaccharyltransferase (OST), complex consisting of eight integral membrane proteins, in the ER (Barlowe & Miller, 2013). In order to help protein folding and quality control in the ER, the three terminal glucose residues of 14-residue N-linked oligosaccharide is trimmed by glucosidase I and glucosidase II. If the polypeptide is not fully folded, UDP-glucose; glycoprotein glucosyltransferase (UGGT) attaches one glucose to the end of glycan. Calnexin subsequently binds to unfolded protein for proper folding. Protein disulfide isomerases, such as Pdi1p, Mpd1p, Eug1p and Eps1p, exchange electrons in order to form, reduce and isomerize disulfide bonds, thereby assisting correct protein folding in the ER lumen (Laboissière, Sturley, & Raines, 1995). The protein disulfide isomerases have been suggested that they interact with ER folding machinery and direct proteins to interact with ER chaperons. During translocation and modifications in the ER, Kar2p, Hsp70 protein, is also involved in protein folding in concert with PDI, calnexin and glycan trimming pathways (Barlowe & Miller, 2013). Kar2 also has role in ER associated degradation of unassembled and misfolded proteins in the cytosol via ubiquitin- and proteasome-dependent pathways (Smith, Ploegh, & Weissman, 2011).

It is well established that proteins, whose synthesis and modification are terminated, are deposited into a transport vesicle which buds off from one compartment, passes the

cytoplasm and fuses with a downstream organelle. The transport of membrane proteins is mediated by COPII vesicles which do not randomly form all over the ER; instead, they form at discrete sites, ER exit sites (ERES), which are marked by COPII coat proteins and accessory proteins, Sec16 and Sec12 (Barlowe & Miller, 2013). In mammalian cells, the Golgi apparatus and ER-Golgi intermediate compartment (ERGIC) are very close to ERES, meaning that COPII vesicles do not move long to the downstream compartment (Spang, 2008). COPII machinery contains five proteins, which are Sar1, Sec23, Sec24, Sec31 and Sec13, and the coat is formed by sequential activation and recruitment of the proteins. The assembly is initiated by activation and recruitment of Sar1p, small G protein, by exchange of its GDP for GTP by membrane bound GEF, Sec12. Binding of Sar1p to the ER membrane triggers the first membrane curvature. In addition, Sar1p recruits Sec23/Sec24 heterodimer to the membrane. Sec23 acts as GAP for Sar1p whereas Sec24 is cargo binding protein that functions by either binding directly to sorting signals of cargoes or adaptor proteins, which are bound to cargo. Sar1/Sec23/Sec24 then recruits heterotetrameric complex of Sec31, which stimulates the GAP activity of Sec23, and Sec13, which provides structural rigidity to the coat. The Sec31/Sec13 complex assists in deformation of the membrane and stabilization of polymerizing coat. The fully assembled coat has two distinct layers: "inner" membrane layer of Sar1/Sec23/Sec24 and "outer" membrane layer of Sec31/Sec13 (Figure 1.4) (Barlowe & Miller, 2013; Sato & Nakano, 2007; Spang, 2008).

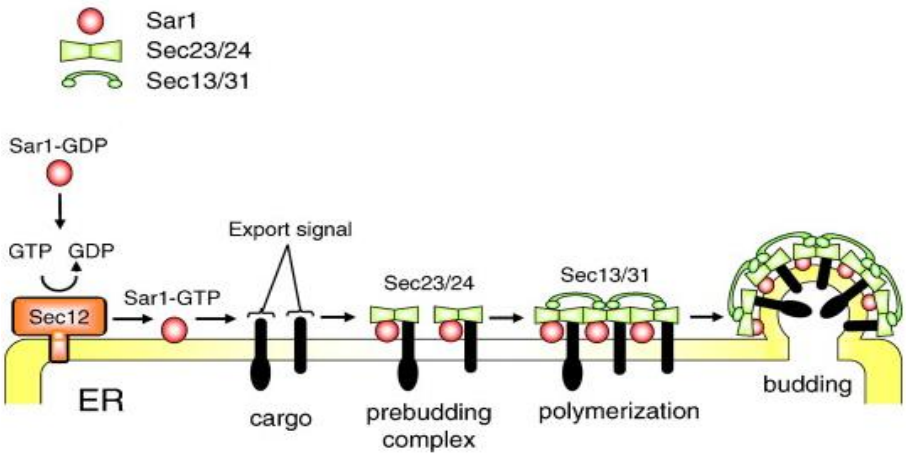

Figure 1.4 CopII vesicle formation (Sato & Nakano, 2007)

Although directional trafficking in a nonspecific manner gained favor, more selective packaging of some cargoes is considered. It is known that Sec24 has multiple binding sites

and together with its isoforms, it binds to many different sorting signals of cargoes and some adaptor proteins. Erv26 and Erv14 adaptors/receptors play role in interaction of COPII coat and transmembrane proteins to be exported (Barlowe & Miller, 2013). Although there are some points to be elucidated in coat shedding it is suggested that GTP hydrolysis required for coat disassembly is not carried out until the coatomer fully forms and correct membrane curvature is presented. Shedding of the coat may occur during transport of the vesicle to the downstream compartment or at the acceptor organelle during tethering (Spang, 2008). Then, budded vesicles tether to Golgi membranes by the aid of Ypt1, a GTPase, Uso1 and transport protein particle I (TRAPPI), tethering proteins (Cai, Chin, Lazarova, Menon, & Fu, 2008). Sed5, Bos1, Bet1 and Sec22 SNARE proteins, which form four helix coiled coil structure, and Sly1, SNARE binding protein, are required for fusion of COPII vesicles with Golgi membranes (Barlowe & Miller, 2013). TRAPPI is suggested to coordinate fusion and tethering by binding both COPII subunits Sec23, Ypt1 GTPase and SNARE proteins (Figure 1.5).

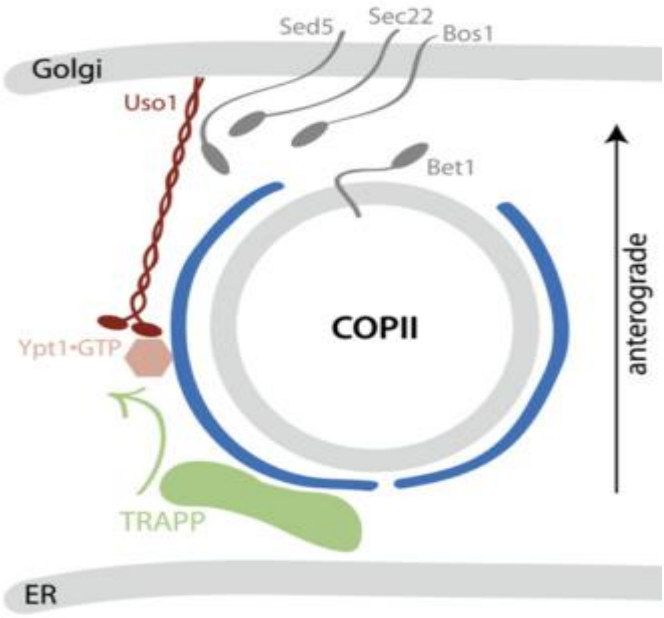

Figure 1.5 Vesicle tethering and fusion (Barlowe & Miller, 2013)

As depicted in Figure 1.6, individual golgi cisternae are dispersed throughout the cytosol in *Saccharomyces cerevisiae*. When the membrane proteins are delivered to cis Golgi, Golgi cisternae containing the cargoes form at cis-face of the Golgi apparatus and mature into medial and then trans compartment, suggesting that rather than vesicle transport between distinct compartments of Golgi complex Golgi cisternae are the carriers of cargo proteins (Papanikou & Glick, 2009). In the Golgi apparatus, mannosyltransferases add α-1,6-mannose, α-1,2-mannose and α-1,3-mannose sequentially (Barlowe & Miller, 2013). In the cisternal maturation model, when the protein processing is completed, the glycosylation and processing proteins are returned to previous preceding cisternae by COPI vesicles. Furthermore, other ER resident proteins containing HDEL or KKXX motif, which are ER retrieval/retention signals, are retrieved back to ER by retrograde transport mediated by COPI vesicles.

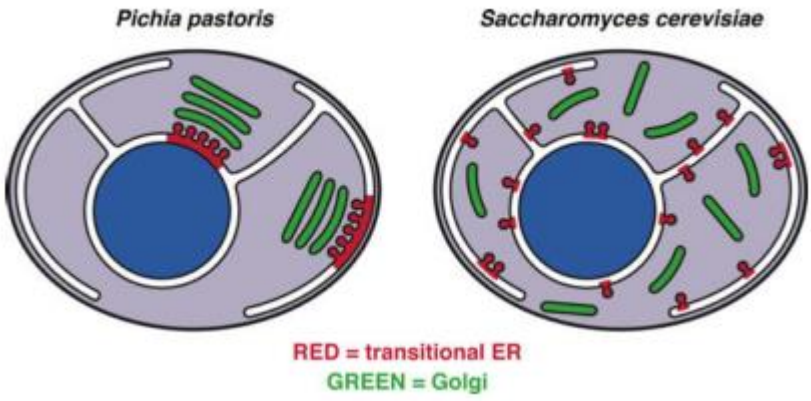

Figure 1.6 Golgi organization in two budding yeast (Papanikou & Glick, 2009)

In budding yeast, two routes are suggested for trans-Golgi network to plasma membrane. While periplasmic enzymes are generally transported through clathrin coated vesicles, most likely passing firstly from endosomal compartments, plasma membrane and GPI-anchored proteins are transported in a lipid raft dependent manner (Surma, Klose, & Simons, 2012; Zabrocki *et al.*, 2008) (Figure 1.7). Ergosterols, sphingolipids and GPI-anchored proteins are suggested to have crucial roles in lipid raft associated transport. Oligomerization of Pma1, hydrogen exporting ATPase, is also suggested to enhance the affinity for lipid rafts (Lee, Hamamoto, & Schekman, 2002). Cargo proteins associated with lipid rafts are targeted to lipid raft transport carriers and lipid rafts cluster into raft platform by the help of clustering agents. Membrane is bended and vesicle buds by driving force of the increasing

line tension between the domains as well as auxiliary proteins. Despite that cytoskeletal elements are thought to be involved in the vesicle generation, it is not clearly understood yet (Surma *et al.*, 2012) (Figure 1.7). Finally, the carriers are trafficked to docking sites in the PM.

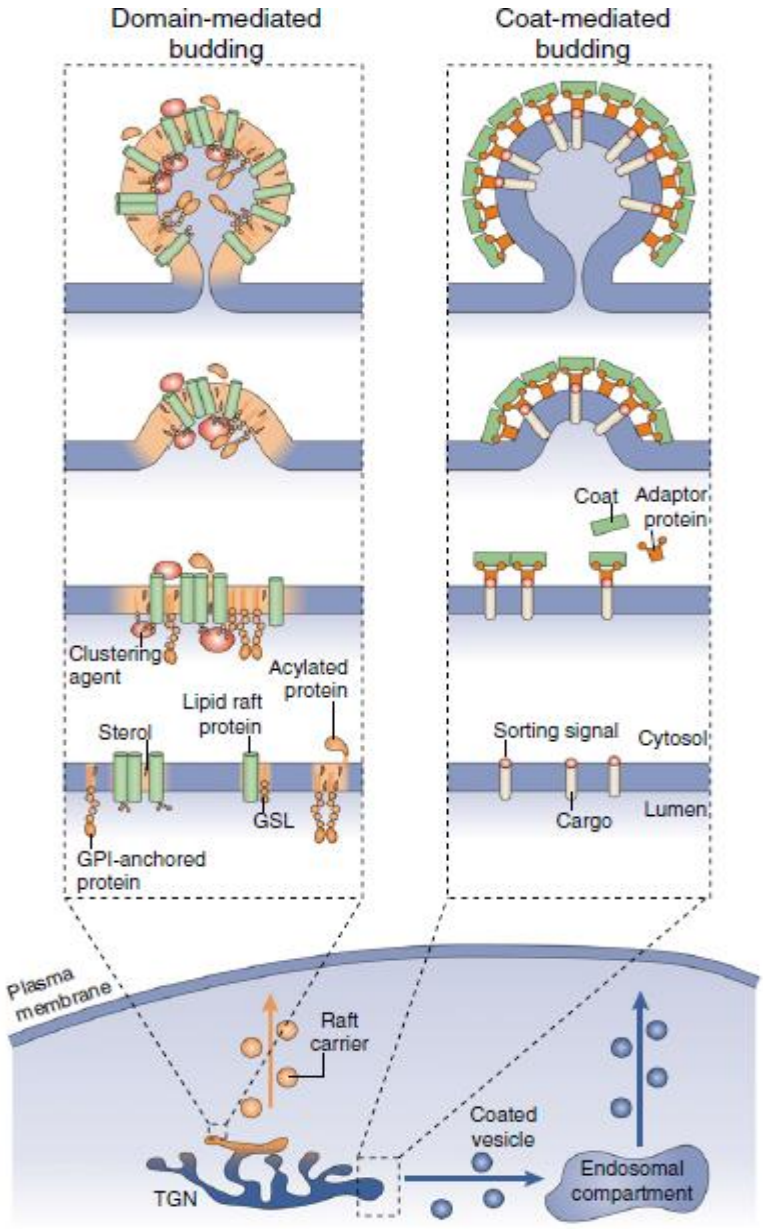

Figure 1.7 Trafficking from trans-Golgi network to plasma membrane and generation of two transport carriers (Surma *et al.*, 2012)

In general, the vesicles formed through endocytosis fuse with early endosomes. The cargo of the vesicles can be directed back to plasma membrane or early endosomes undergo maturation to late endosome and finally transported to yeast vacuoles to be degraded via endosomal sorting complexes required for transport (ESCRT) (Solinger & Spang, 2013). Upon agonist binding, alpha-factor receptor is known to be monoubiquitinated and thus internalized into endocytic vesicles (Hicke, 1997). Regardless of clathrin coated vesicle transport, all endocytosed materials are transported to early endosome. ESCRT machinery recognizes ubiquitinated cargoes and deubiquitinates before packing cargoes into intraluminal vesicles (ILVs). ILVs bud into the late endosome and multivesicular bodies (MVBs) are generated by five ESCRT complexes (William M Henne, Buchkovich, & Emr, 2011). ESCRT-III, composed of Vps20, Snf7/Vps32, Vps24 and Vps2, is regarded as minimal machinery required for formation of ILVs *in vitro* (Wollert & Hurley, 2010). Then, the MVBs deliver the cargo to vacuoles for degradation (William M Henne *et al.*, 2011).

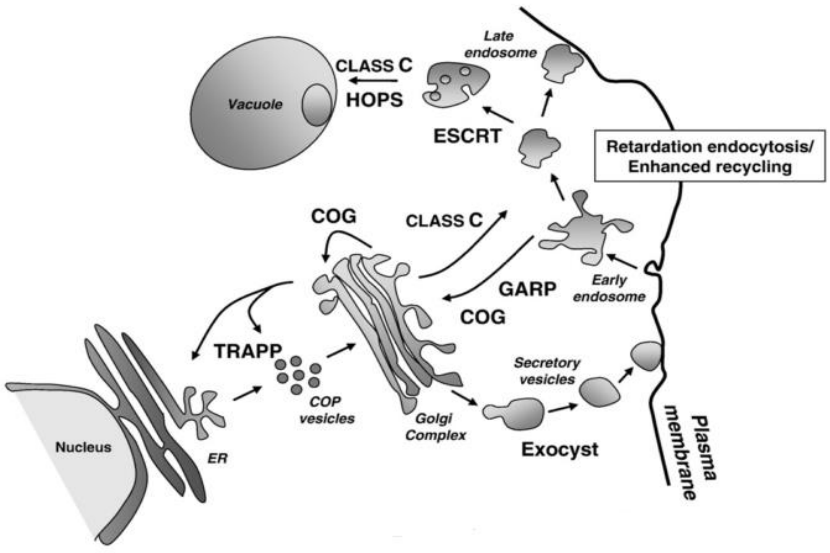

Figure 1.8 Overall trafficking in *Saccharomyces cerevisiae* (Zabrocki *et al.*, 2008)

1.2. Protein Localization

As described below, eukaryotic cells compartmentalize to carry out distinct metabolic processes and the roles of organelles are defined by resident proteins of the compartments

(Lunn, 2007). Therefore, to understand the role of uncharacterized protein in biological processes it is invaluable to elucidate the subcellular localization of protein of interest. Furthermore, to identify different organelles and study their dynamics and special organization is crucial for elucidating organelle function, biogenesis and maintenance in addition to determining trafficking pathways (Terasaki, Loew, Lippincott-Schwartz, & Zaal, 2001). There are two strategies for detecting of protein localization: experimental determination and computational prediction (Nelson, Cai, & Nebenführ, 2007).

1.2.1. Protein Localization Methods

The commonly used biochemical approaches are subcellular fractionation, immunocytochemistry, immunofluorescence and co-localization by fluorescent organelle markers.

1.2.1.1. Subcellular Fractionation

Subcellular fractionation is a technique by which organelles are separated depending on their physical properties. In the method, cells are firstly homogenized by osmotic shock, sonication or mechanical shearing and then exposed to differential centrifugation (repeated centrifugation at higher speeds for each step) that separates cells according to size. Then, density gradient centrifugation is applied to separate fractions according to the density. Depending on the aim of the fractionation, from sucrose to nycodenz, non-ionic, iodinated derivative of 3-iodobenzoic acid, many stable, inert and nonionic media can be utilized for the step. The step-wise centrifugation resolves cell lysate into a few fractions containing mainly (1) plasma membrane, nuclei, heavy mitochondria and cytoskeletal elements; (2) lysosomes, peroxisomes and light mitochondria; (3) the Golgi apparatus, the ER, endosomes and microsomes and (4) cytosol. The fractions are gingerly collected either by hand or machines. In order to gather information from the purified fractions, downstream methods such as western blotting, enzyme assays, electron or light microscopy are preferred depending on the further purpose (Harford & Bonifacino, 2009; Huber, Pfaller, & Vietor, 2003).

Despite simplicity and speed of the approach, it is obvious that cellular compartments possess the similar physical characteristics and thus they cofractionate to some extent. Moreover, to fairly purify proteins from the fractions needs detergents and chemicals which interfere with the nature of proteins. The method also needs further analysis, to illustrate western blotting. Western blotting has in turn disadvantages such as use of expensive antibodies, time consuming labeling and washing steps and non-specific labeling.

Subcellular fractionation also cannot take advantage of determination live cell localization and monitoring.

1.2.1.2. Immunocytochemistry

Another method that can be utilized to determine the specific protein in yeast is immunocytochemistry. By the aid of the method, the localization of a known protein (antigen) is determined using antibodies directed to the antigen. In this technique, the cells should be fixed using fixatives differing with respect to advantages and disadvantages. Then, the cells are embedded onto materials to preserve cell integrity. Embedded cells subsequently sectioned and incubated with primary antibodies that are against the protein of interest in the cell. Then, the excess amount of primary antibody is washed out and fluorescent or stain tagged secondary antibodies raised against the first antibody is applied onto the cells. According to the tag of secondary antibody, the cells are examined to determine the localization. In the method, positive and negative controls play central role in reliability of the approach since the immunoreactivity is high possibility and so it is hard to understand whether the protein is in the cell or in that compartment. Using expensive antibodies, complexity of preparation of the cells, choose of fixatives and embedding material are other disadvantages of the method over advantages like possibility to design antibodies against the native, specific conformation of protein. The power of the technique is also restricted with the resolution of fluorescence microscope or efficiency of the dye used (Javois, 1999).

1.2.1.3. Computational Approaches

There are well established targeting and retrieval/retention signals of proteins that are target of some transport proteins or machineries, which carries proteins to the target subcellular compartments depending on the postal codes. Computational approaches mainly use the information of these sequences, which are revealed by experimental methods. Nevertheless, most of the targeting sequences, especially of yeast proteome, are poorly defined and do not highly contribute to prediction programs (Emanuelsson & von Heijne, 2001). Moreover, these methods have not yet had the ability of providing information about the localization of a biological event such as dimerization.

1.2.1.4. Co-localization with Quantum Dots and Fluorescent Dyes

Quantum dots (QDs) are inorganic nanocrystals that give fluorescent signals with high quantum yield, high extinction coefficient and at sharp and distinct wavelengths. QDs have attracted the attention of biologists when they are coated enabling water solubility and conjugation with proteins or protein targeting molecules. Owing to photostability capability, QDs allow repeated imaging. Moreover, they are very useful for electron microscopy based approached because of their electron density and size. On the other hands, their multiple emission spectra lower the use for dual coloring. Moreover, use of majority of QDs is restricted to permeabilized cells or extracellular proteins since they are large enough not to penetrate into cells especially when tagged with targeting proteins (Giepmans, Adams, Ellisman, & Tsien, 2006).

Fluorescent dyes like FM4-64 and dihexaoxacarbocyanine iodide ($DiOC_6$) are also preferred molecules to label subcellular compartments and visualization of living cells. $DiOC_6$ is a fluorescent dye for staining the ER. It is positively charged molecule that passes across the cell membrane (Terasaki, Song, Wong, Weiss, & Chen, 1984). However, when low concentration is used, the dye accumulates in mitochondria while at higher concentrations, it stains the ER with other membrane bound organelles. Furthermore, it is useful only in cells where the ER structure can easily be distinguished from other organelles. Therefore, it is not much reliable to use in co-localization studies. FM4-64 is another fluorescent dye which is used to monitor endocytic pathways since it preferentially stains the membranes of endocytic vesicles and endosomes. However, as $DiOC_6$, the changes in its concentration lead to staining of other membrane bound organelles (Fischer-Parton *et al.*, 2000).

1.2.1.5. Co-localization with Fluorescent Organelle Markers

Today, cell biology takes advantage of fluorescence at many levels. Fluorescence was mainly used for labeling antibodies which are used in immunoassays at first. The discovery, cloning and heterologous expression of green fluorescent protein (GFP) from the jellyfish *Aequorea victoria* have made a scientific breakthrough in live cell imaging. In the advent of fluorescent proteins (FPs), uses of fluorescently tagged proteins for noninvasive imaging of protein expression, function and activity in living cell get accelerated (Giepmans *et al.*, 2006; Nelson *et al.*, 2007). After GFP, some other variants mostly obtained from marine coelenterates have been discovered and thoroughly studied. The studies on the fluorescent proteins have enhanced the brightness, photostability and folding efficiencies, varied their spectra and lowered the tendency to oligomerize (Shaner, Steinbach, & Tsien, 2005). Consequently, genetic fusion of FPs to the coding regions of specific proteins provides easy and convenient method to identify subcellular distributions in live cells (Dixit, Cyr, & Gilroy, 2006; Nelson *et al.*, 2007). Even though the fluorescence patterns provide evidence

on whether the protein is resident, the distributions should be compared with previously described characteristic morphologies of the subcellular compartments and especially with organelle markers expressed in the same cell (Nelson *et al*., 2007).

Organelle markers are mostly fusion proteins utilized in noninvasive organelle labeling without antibodies or chemicals, studies on organelle dynamics and morphology, monitoring intracellular trafficking, fraction tracking in cell lysates and protein co-localization in specific organelles.

Organelle markers are generally generated by fusion of organelle resident proteins with fluorescent proteins in the genetic level. However, by the identification of some targeting sequences, they can be also constructed by addition of targeting sequences to the appropriate site of gene of fluorescent proteins. Although the targeting/retention sequences in higher eukaryotes are well established and so more confidently used for organelle marker generation, there are only few well known sequences for budding yeast and they are elucidated due to the unravel of them in other eukaryote models.

The most established sorting signal in yeast is HDEL tetrapeptide, which provides the retention of proteins in the ER as well as retrieval from the Golgi. It is known that many proteins cannot exit the ER unless their HDEL sequences are masked by proper folding and processing. In order to illustrate the efficiency of HDEL, invertase, a secreted protein, was linked at the extreme C-terminus with (FE)HDEL sequence and with linker plus FEHDEL. As a result of the addition, the secretion was suppressed and the six amino acids were suggested to be sufficient for prevention of secretion (Pelham, Hardwick, & Lewis, 1988). Studies of KDEL (ER retention/retrieval sequence) and HDEL accumulated the evidence that the fusion to C-terminus of any proteins leads to the ER localization. However, for proteins expressed in the cytoplasm such as plasmid encoded proteins, another sequence is required for ER sorting. Since the biogenesis of all proteins is highly conserved and well identified, the signal sequence of any yeast protein can be suggested to serve as ER targeting sequence. Signal sequence of SUC2 encoding invertase is prominent candidate since it is well established for the aspect (Carlson, Taussig, Kustu, & Botstein, 1983; Rothe & Lehle, 1998). Moreover, the targeting of peroxisome in *Saccharomyces cerevisiae* is one of the topics which are heavily studied. As a consequence, peroxisome targeting sequences can be reliably known. Peroxisome targeting sequence 1 (PTS1) is a tripeptide, SKL and its variants that can be summarized as (A/S/C)-(K/R/H)-L. The C-terminally located short peptide direct the proteins to the peroxisomal lumen (Y. Wang *et al*., 2009). Although PTS2, located to be in N terminus, seems to need some more evidences to be identified in detail, the N terminal 40-50 amino acids of Pex3 is suggested to direct proteins to the peroxisome in *A. thaliana* and human, indicating that it can be useful for peroxisome targeting in budding yeast (Akiyama, Ghaedi, & Fujiki, 2002).

1.3. Aim of the Study

G-protein-coupled receptors, which are the most versatile chemical sensors, have prominent role in physiologically important cellular processes. It is well established phenomenon that GPCRs exist and function as dimers. Studies illustrate that dimerization may be favored for receptor activation, signal transduction, trafficking, cell surface mobility and ligand interactions. Despite that Ste2p, a yeast GPCR, is known to homodimerize where it dimerizes is controversial. While subcellular fractionation data indicate that Ste2p dimers are found in the ER as many as in the plasma membrane, recent study conducted in our lab points out that the Ste2 dimer does not fluorescence in the ER when labeled with split EGFP. In order to settle the conflict, co-localization of fluorescently tagged yeast GPCR dimers with fluorescent organelle marker proteins was an easy and convenient approach. Hence, we aimed at

- generating fluorescent organelle markers which label the subcellular compartments, namely, the ER, the Golgi apparatus, late endosome, COPII vesicle, on the trafficking route of yeast membrane proteins.
- generating peroxisome marker which useful for checking whether the membrane proteins were processed in peroxisome or can be used for any other co-localization studies in budding yeast.
- visualizing subcellular compartments in live yeast cells.
- co-localizing split EGFP tagged Ste2p and Gpr1p with labeled organelles in order to assess the functionality of the fluorescent organelle marker proteins. In addition, the acquired data would additionally be used for comparison with co-localization of the Ste2p and Gpr1p dimer in a further study.

Although there are many organelle markers generated over the years, the majority of them are GFP tagged. Moreover, many markers are chromosomally tagged and thus it is useless for studies requiring special mutant strains such as Ste2 knocked down cells. Moreover, the markers are found in different vector systems and thus collecting them from different sources leads to inconsistency especially with respect to expression. Therefore, red fluorescent marker proteins, which can be combined with any GFP tagged proteins for co-localization, were developed for many purposes from monitoring intracellular trafficking to tracking protein in fractions.

CHAPTER 2

MATERIALS AND METHODS

2.1. Materials

2.1.1. Yeast Strain, Media and Cultivation Conditions

Saccharomyces cerevisiae strain DK102 (*MAT***a** ura3-52 lys2-801^{am} ade2-101^{oc} trp1-Δ63 his3-Δ200 leu2-Δ1 ste2::HIS3 sst1-Δ5) was used for the expression of fluorescent protein tagged organelle markers and receptors throughout the study (H G Dohlman, Goldsmith, Spiegel, & Thorner, 1993; Sikorski & Hieter, 1989). The strain was kindly gifted by Prof. Dr. Jeffrey M. Becker from University of Tennessee, Knoxville, USA.

S. cerevisiae DK102 was grown in liquid YEPD (Appendix B) medium at 30°C in a shaking incubator (Zheiheng) at 200 rpm overnight for yeast transformation studies. For short term storage, the yeast strain was maintained on the YEPD solid medium at 4°C. In order to prepare long term stocks, 87% (w/V) glycerol was mixed with a specific amount of aliquot of culture in YEPD broth until the final glycerol concentration was 15% (V/V). These glycerol stocks were stored at -80°C.

For yeast selection purposes, MLT (Medium lacking tryptophane), MLU (Medium lacking uracil) and MLTU (Medium lacking tryptophane and uracil) were used (Appendix B). Transformants grown on these solid media were incubated at 30°C for 2-3 days. Short and long term yeast stocks in these media were also prepared as expressed in the previous paragraph.

To prepare all these media, their ingredients were dissolved in distilled water and sterilized by autoclaving at 121°C for 20 minutes.

2.1.2. Bacterial Strain, Media and Cultivation Conditions

Escherichia coli TOP10 strain was used for amplification of the plasmids. LB (Appendix A) liquid and solid media were used to grow the cells at 37°C for 12-16 hours in a rotary shaker at 200 rpm or an incubator, respectively. Ingredients of LB medium were dissolved in distilled water, the pH of the medium was adjusted to 7.4 and the medium was autoclaved at 121°C for 20 minutes. After cooling of the medium, ampicillin was added into LB medium to the final concentration of 100 µg/mL in order to select the transformant cells. *E. coli* cells were preserved on agar plates at 4°C for a short time while 15% (V/V) glycerol stocks were stored at – 80°C for long term.

2.1.3. Plasmids

Yeast organelle marker genes were purchased in pBY011 parental vector from Harvard Medical School (MA, USA) (Appendix C). All the constructs were cloned into either pBEC1 or pNED1 bacteria-yeast shuttle vectors (Appendix C), which were gifts of Prof. Dr. Jeffrey M. Becker, University of Tennessee Knoxville, USA.

2.1.4. Other Materials

The chemical used throughout the study were purchased from Applichem (Darmstadt, Germany), Merck (Darmstadt, Germany) and Sigma-Aldrich Co. (NY, USA). All the restriction enzymes used throughout the study were from New England Biolabs (Hertfordshire, UK). Phire Hot Start II DNA Polymerase, which was utilized in PCR amplifications, was purchased from Finnzymes (Vantaa, Finland). T4 DNA ligase was from Fermentas (Ontario, Canada). Primers used in the study were synthesized in Integrated DNA Technologies (Iowa, USA) or Alpha DNA (Quebec, Canada). Plasmid isolation and PCR purification kits were ordered from Fermentas (Ontario, Canada) while gel extraction kit from QIAGEN (Düsseldorf, Germany).

Live cells were visualized under Zeiss 510 laser scanning microscope (UNAM, Bilkent University) and Leica DMI 4000 fluorescence microscope.

2.2. Methods

2.2.1. Preparation of Competent *E. coli* Cells

2.2.1.1. Preparation of Competent *E. coli* Cells by $RbCl_2$ Method

E. coli TOP10 cells were streaked onto LB agar plate and incubated for 12-16 hours at 37°C. On the following day, a single colony was picked and inoculated into 5mL of LB broth and was incubated by shaking overnight at 200 rpm and 37°C. This bacterial culture was transferred into a sterile flask containing 100 mL of liquid LB medium. The subculture was shaken at 200 rpm and 37°C until the OD_{600} became between 0.48 and 0.75. Reaching the target OD_{600} value, the culture was transferred to two 50 mL falcon tubes and chilled on ice for 5 minutes and then centrifuged at 6000 rpm for 5 minutes at 4°C. After discarding supernatant, pellet was resuspended in 20 mL ice cold Transformation buffer I (Appendix E). The resuspension was incubated in ice for 5 minutes before centrifugation at 6000 rpm for 5 minutes at 4°C. Supernatant was decanted and the pellet was dissolved in 2 mL of Transformation buffer II (Appendix E). The bacterial solution was kept on ice for 15 minutes and, at the end, 100 µL of aliquots were distributed into 1.5 mL eppendorf tubes and frozen in liquid nitrogen. Until use, the competent *E. coli* cells were stored at -80°C.

2.2.1.2. Preparation of Competent *E. coli* Cells by $CaCl_2$ Method

E. coli TOP10 cells were streaked onto LB agar plate and incubated overnight at 37°C. Then, a single colony taken from the plate was inoculated into 5 mL of liquid LB medium and shaken for 12-16 hours at 200 rpm and 37°C. The culture was subcultured in 50 mL of LB broth in an autoclaved 250 mL Erlenmeyer flask and then incubated in a shaker at 200 rpm and 37°C for 2-3 hours (OD_{600} should be around 0.5). The bacterial culture, at the required OD_{600}, value was transferred to a 50 mL falcon tube and chilled on ice for 15 minutes. Afterwards, it was centrifuged at 4100 rpm for 7 minutes at 4°C. After decanting supernatant, the pellet was dissolved in 15 mL of sterile 1.0 M $CaCl_2$ solution, which was stored at 4°C, and kept on ice for 15 minutes. Then, it was centrifuged again at 4100 rpm for 7 minutes at 4°C. Supernatant was discarded and pellet was resuspended in 4 mL of ice cold $CaCl_2$-glycerol solution, whose 15% (V/V) content was glycerol. Finally, the suspension was aliquoted into 100 µL in 1.5 mL eppendorf tubes and frozen in liquid nitrogen. The prepared competent bacteria were stored at -80°C.

2.2.2. Transformation of competent *E. coli* cells

Previously prepared competent bacterial cells were taken from – 80°C and thawed on ice for 10-15 minutes. Then, 25-50 ng of plasmid DNA or 10 µL of ligation or digestion product was added onto the competent cell suspension. After incubation on ice for 30 minutes, the cells were heat shocked at 42°C for 90 seconds. Following the heat shock step, the cells were chilled on ice for 5 minutes. Afterwards, 900 µL of prewarmed LB broth was added onto the cells and bacteria were shaken at 200 rpm at 37°C for 1 hour. Then, the cells were harvested by centrifugation at 6000 rpm for 3 minutes. 800 µL of the supernatant was removed and the pellet was dissolved by pipetting in the remaining supernatant. 100 µL of the suspension was spreaded onto LB agar plate, consisting of ampicillin, using glass beads. The plates were incubated at 37°C for 12-16 hours. To screen recombinants, single colonies were picked from the plates and examined.

2.2.3. Plasmid Isolation from *E. coli*

A single colony was taken from selective fresh agar plate and inoculated into 4 mL of LB broth supplemented with 100 mg/mL ampicillin. The inoculum was incubated by shaking at 200 rpm for 12-16 hours at 37°C. On the following day, plasmid DNA was isolated from the culture using Thermo Scientific® GeneJET Plasmid Miniprep Kit according to manufacturer's instructions.

2.2.4. Restriction Enzyme Digestion

All restriction enzyme digestion reactions for either controlling the constructs generated or cloning were prepared following NEB's instructions.

2.2.5. Ligation

Digested gel extraction products and plasmids were ligated *in vitro* using T4 DNA Ligase (Thermo Scientific®) according to manufacturer's instructions. The amounts of ligation reaction components were calculated considering the sizes of insert and vector and taking the molar vector to insert ratio as 1:5.

2.2.6. Polymerase Chain Reaction

In order to append mCherry (Accession Number: ACO48282, 711bp) to the 3' end of SNF7 (Accession Number: CAA97548.1, 723 bp) and SEC13 (Accession Number: AAB67426.1, 894 bp) genes in pBY011 expression vector through PCR integration method, mCherry was amplified conducting PCR, whose optimized conditions were tabulated below.

Table 2.1 Optimized PCR Conditions to Amplify mCherry or EGFP with Flankings Homologous to Downstream of SNF7 and SEC13 in pBY011

Reagent	Amount (µL)
Phire Hot Start II DNA Polymerase	1
5X Phire Reaction Buffer	10
dNTPs (25 mM)	0.4
Forward Primer (20 mM)	1.25
Reverse Primer (20 mM)	1.25
DMSO	1
Template DNA (500 ng/µL)	0.4
Nuclease-free Water	34.7

98°C for 30 s

98°C for 5 s
61°C for 5 s
72°C for 10 s
} x 35 cycles

72°C for 60 s

In order to transfer SNF-mCherry and SEC13-mCherry fusions from pBY011 to pBEC vector, primers were designed to generate BamHI and KpnI cut sites at 5' and 3' end of the each fusion gene, respectively. The optimized PCR conditions were as follows:

Table 2.2 Optimized PCR Conditions to Add Cut Sites at each end of SNF7-mCherry and SEC13-mCherry

Reagent	Amount (µL)		
Phire Hot Start II DNA Polymerase	1	98°C for 30 s	
5X Phire Reaction Buffer	10	98°C for 5 s	x 35 cycles
dNTPs (25 mM)	0.4		
Forward Primer (20 mM)	1.25	59°C for 5 s	
Reverse Primer (20 mM)	1.25		
DMSO	1.5	72°C for 15 s	
Template DNA (500 ng/µL)	0.3	72°C for 60 s	
Nuclease-free Water	34.3		

In order to generate organelle marker proteins fusing targeting sequences or organelle resident proteins to mCherry, the fluorescent gene (with or without stop) was amplified with overhangs containing BamHI and EcoRI cut sites through PCR with the conditions stated below (Table 2.3). Thus, it could be cloned between aforementioned cut sites in the pBEC vector.

Table 2.3 Optimized PCR Conditions to Amplify mCherry with Flankings Consisting of BamHI and EcoRI cut sites

Reagent	Amount (µL)		
Phire Hot Start II DNA Polymerase	1	98°C for 30 s	
5X Phire Reaction Buffer	10	98°C for 5 s	x 35 cycles
dNTPs (25 mM)	0.4		
Forward Primer (20 mM)	1.25	58°C for 5 s	
Reverse Primer (20 mM)	1.25		
DMSO	2	72°C for 15 s	
Template DNA (300 ng/µL)	0.5	72°C for 60 s	
Nuclease-free Water	33.6		

To embed signal sequence of SUC2 gene to the 5' end and HDEL, ER retention signal, to the 3' end of mCherry in pBEC, the signal sequence and HDEL cDNA sequences were cloned as primer dimer according to the PCR protocol (Table 2.4).

Table 2.4 Optimized PCR Conditions to Amplify HDEL and SUC2's Signal Sequence

Reagent	**Amount (µL)**
Phire Hot Start II DNA Polymerase	1
5X Phire Reaction Buffer	10
dNTPs (25 mM)	0.4
Forward Primer (20 mM)	4
Reverse Primer (20 mM)	4
DMSO	1
$MgCl_2$	0.5
Nuclease-free Water	29.1

98°C for 30 s

98°C for 5 s
59°C for 5 s
72°C for 15 s
x 35 cycles

72°C for 60 s

In order to tag ANP1 (Accession Number: AAB64764.1, 1326 bp) with mCherry, SpeI and BamHI cut sites were appended to the 5' and 3' end of ANP1, respectively, following the protocol mentioned below. Besides, the same protocol was used to amplify PEX3 (Accession number: AAB65006.1, 1503 bp) with overhangs homologous to the upstream of mCherry in pBEC.

Table 2.5 Optimized PCR Conditions to Amplify ANP1 and PEX3 As Specified Above

Reagent	Amount (µL)
Phire Hot Start II DNA Polymerase	1
5X Phire Reaction Buffer	10
dNTPs (25 mM)	0.4
Forward Primer (20 mM)	1.25
Reverse Primer (20 mM)	1.25
DMSO	1.5
$MgCl_2$	0.5
Template (400 ng/µL)	0.3
Nuclease-free Water	33.8

98°C for 30 s

98°C for 5 s
58°C for 5 s
72°C for 15 s
} x 35 cycles

72°C for 60 s

2.2.7. Agarose Gel Electrophoresis

Agarose gel electrophoresis was conducted so as to control the sizes of DNA fragments which were either amplified by PCR or digested. 0.8 % (w/V) agarose gel concentration was preferred to run DNA fragments which were longer than 3 kb whereas 1.5 % concentration was used for DNA samples at the lengths between 500-3000 bp and 3% was for fragments less than 500 bp. The gel was prepared by dissolving determined amount of agarose in 1 X TBE (Appendix E) and then melting the gel in a microwave oven. After cooling, EtBr was added onto the gel to visualize the DNA bands under UV light. DNAs were mixed with 6 X loading dye (Fermentas®, Cat#R0611, Appendix E) to the final concentration of 1 X before loading onto the gel wells. To determine the molecular weights of DNA bands, GeneRuler^{TM} 1 kb DNA Ladder, 100 bp plus DNA Ladder and 50 bp DNA Ladder (Fermentas) were used according to the expected band sizes. The gels, which run at 80-100 V, were photographed via Vilber Lourmat Gel Imaging System.

2.2.8. DNA Fragment Extraction from Agarose Gel

PCR or digestion products controlled through gel electrophoresis were extracted from agarose gel using QIAGEN® Gel Extraction Kit (Cat#28704) according to manufacturer's instructions if the bands had been at the expected sizes.

2.2.9. Determination of DNA Amount

NanoDrop 2000 spectrophotometer (Thermo Scientific®) was used in order to detect the concentration of nucleic acids. 1.5 µL of plasmid DNA or gel extraction product was loaded onto micro-volume pedestal and measured using the software.

2.2.10. PCR Integration Method

Generation of endosome (SNF7) and secretory pathway (SEC13) fluorescent markers in pBY011, peroxisome (PEX3) and ER markers in pBEC were carried out using PCR integration method.

The technique includes two successive PCRs, through which the first PCR product is used as the double stranded primer during the second PCR. The first reaction was carried out as stated above and its product was the gene with 30-bp long overhangs, homologous to planned integration site within a plasmid of interest. To embed the gene between any desired two nucleotides in the target plasmid, 1:5 template (plasmid of interest) to insert (first PCR product) ratio was used in the second PCR and the whole plasmid containing its new insert was amplified following optimized PCR conditions were applied.

Table 2.6 PCR Conditions for the Second PCR of PCR Integration Method

Reagent	Amount
Phire Hot Start II DNA Polymerase	1 µL
5X Phire Reaction Buffer	10 µL
dNTPs (25 mM)	1 µL
DMSO	1.5 µL
Template	50 ng
First PCR Product	250 ng
Nuclease-free Water	Up to 50 µL

98°C for 30 s

98°C for 30 s

51°C for 1 min

68°C for 2 min/kb

x 18 cycles

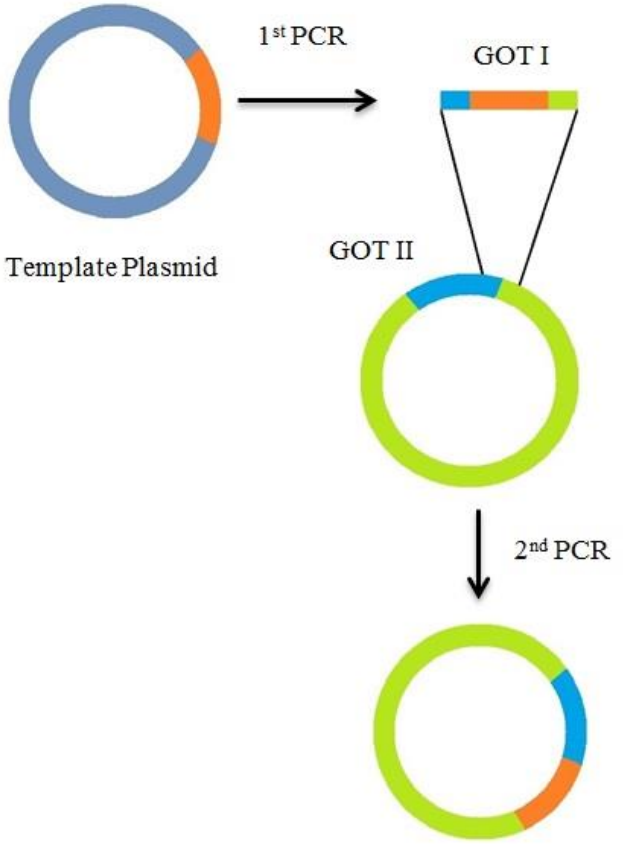

Figure 2.1 Representative scheme for PCR integration method (GOT I: Gene of interest I; GOT II: Gene of interest II)

2.2.11. High Efficiency Yeast Transformation Using LiAc/SS carrier DNA/PEG Method

In order to introduce engineered plasmids into yeast cells, the LiAc/ssDNA/PEG method (Gietz, St Jean, Woods, & Schiestl, 1992) was applied with some modifications. All required solutions (Appendix E) were either filter or heat sterilized before use.

Saccharomyces cerevisiae DK102 cells were grown overnight in 5 mL of appropriate yeast liquid medium by shaking at 30°C and 200 rpm in a shaking incubator (Zheiheng). On the following day, the grown cells were counted using hemocytometer and subcultured to reach cell densitiy of 5 x 10^6 cells/ mL culture in 50 mL appropriate medium. Until the cell density reached 2 x 10^7 cells / mL culture, the yeast cells were shaken at 30°C and 200 rpm. When the concentration was obtained, 50 mL culture was transferred from Erlenmeyer flask to a sterile 50 mL falcon. Then, the cells were centrifuged at 4000 rpm for 5 minutes. In the meantime, salmon sperm DNA (ssDNA) was kept in boiling water for 5 minutes and then

incubated on ice until use. The supernatant was discarded and the pellet was resuspended with 25 mL of sterile distilled water. Afterwards, the cells were harvested again at 4000 rpm for 5 minutes. The supernatant was decanted over immediately and the cells were dissolved in 5 mL of 100 mM LiAc. The culture, in turn, was centrifuged at 4000 rpm for 8 minutes and the supernatant was removed and the following solutions were added onto the pellet by pipetting in the given order:

240 µL of PEG 3350 (50% w/V)

36 µL of 1.0 M LiAc

25 µL of ssDNA

0.1-10 µg plasmid DNA in 50 µL of diluted plasmid DNA for each tube

The mixtures were vortexed until the cell pellet disappeared. Then, the tubes were incubated at 30°C for 30 minutes. It was followed by heat shock at 42 °C for 25 minutes. After that, the cultures were centrifuged at 4000 rpm for 3 minutes and the supernatant was immediately discarded. The pellet was resuspended in 1 mL of sterile dH_2O and 200 µL of the suspension was spread onto selective agar medium using glass beads. These plates were left in a 30°C incubator for 2-3 days. In the third day, 4 colonies were picked from each plate and streaked onto the same selective agar medium for further analysis and short term storage at 4°C.

2.2.12. Imaging with Laser Scanning Confocal Microscope and Fluorescence Microscope

Before visualization of yeast cells, a single colony was picked from streak plate or glycerol stock. The cells were grown for 12-16 hours at 30°C and 200 rpm by shaking. Next morning, the cells were subcultured in 5 mL of fresh selective medium and the culture was shaken for 4-5 hours at 200 rpm and 30°C.

To detect the fluorescent signal in live yeast cells, microscopy was performed on Leica DMI 4000 inverted wide field fluorescence microscope with HCX APO U-V-I 100.0 x 1.30 oil immersion objective. Images were acquired by DFC360 FX camera. For mCherry, C145098 filters; for EGFP, C145096 coded filters were used. Configuration settings are depicted below.

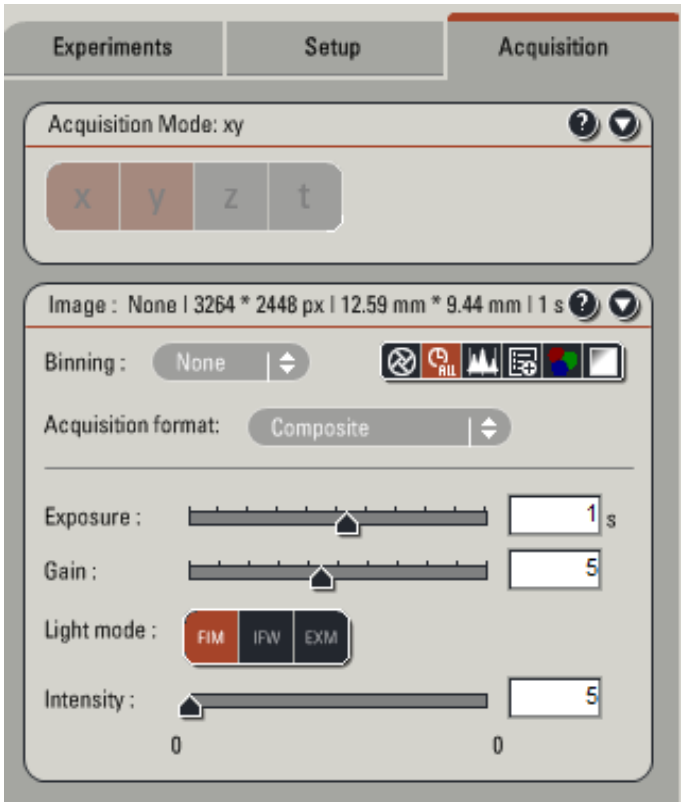

Figure 2.2 Configuration settings for mCherry visualization by inverted wide field fluorescence microscope

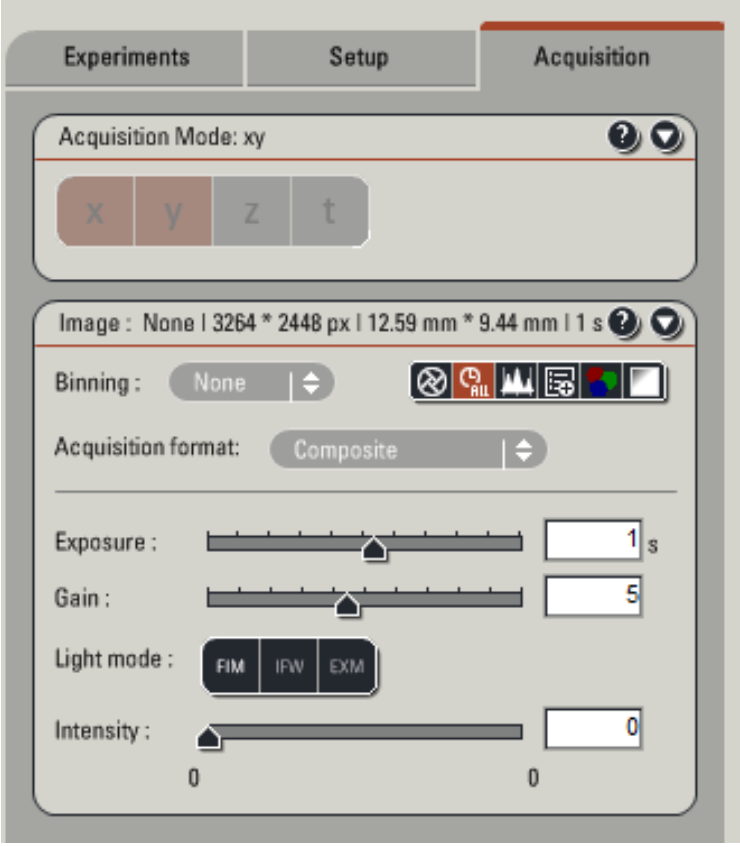

Figure 2.3 Configuration settings for EGFP visualization by inverted wide field fluorescence microscope

Moreover, yeast cells were also examined using Zeiss LSM 510 confocal microscope with an objective Plan-Apochromat 63x/1.40 Oil DIC M27. Filters used for mCherry were LP 650 and LP 585 whereas BP 505-550 for imaging of EGFP tagged proteins.

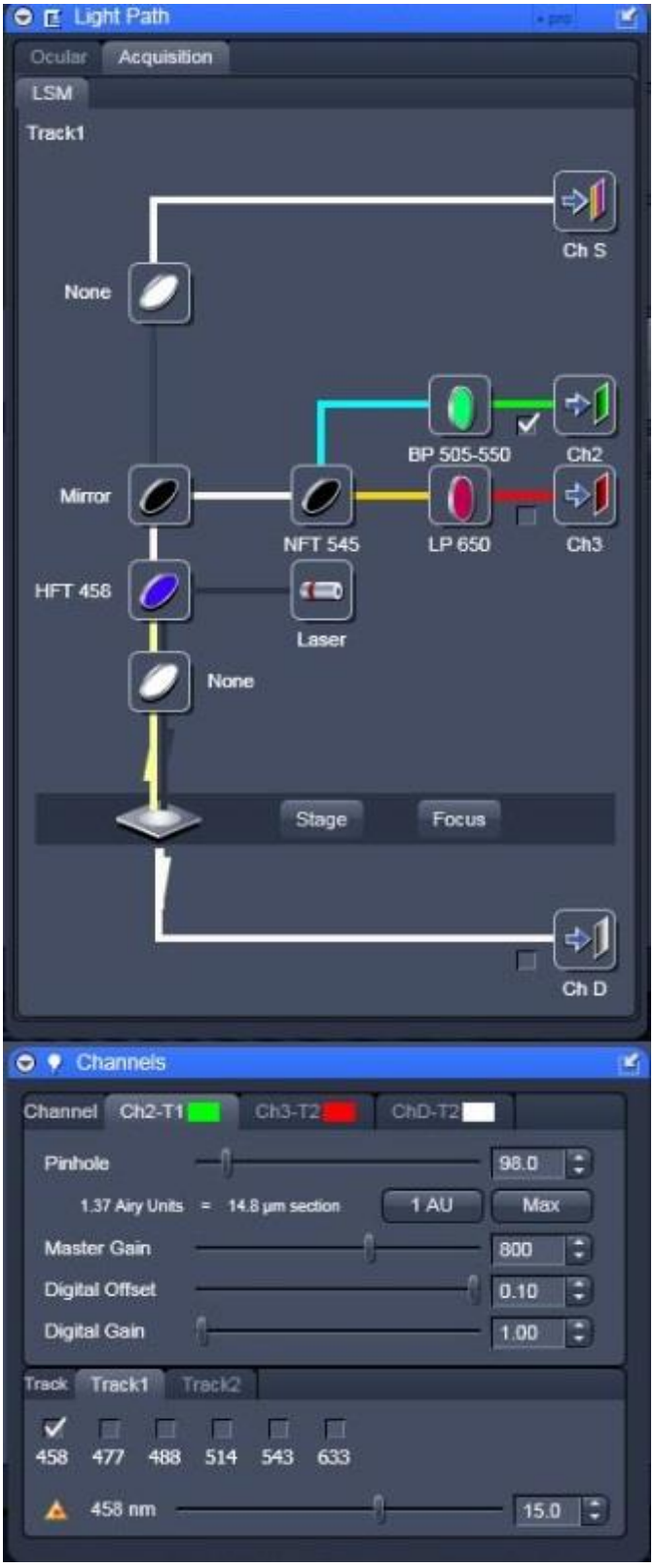

Figure 2.4 Configuration setting for EGFP visualization by confocal microscope

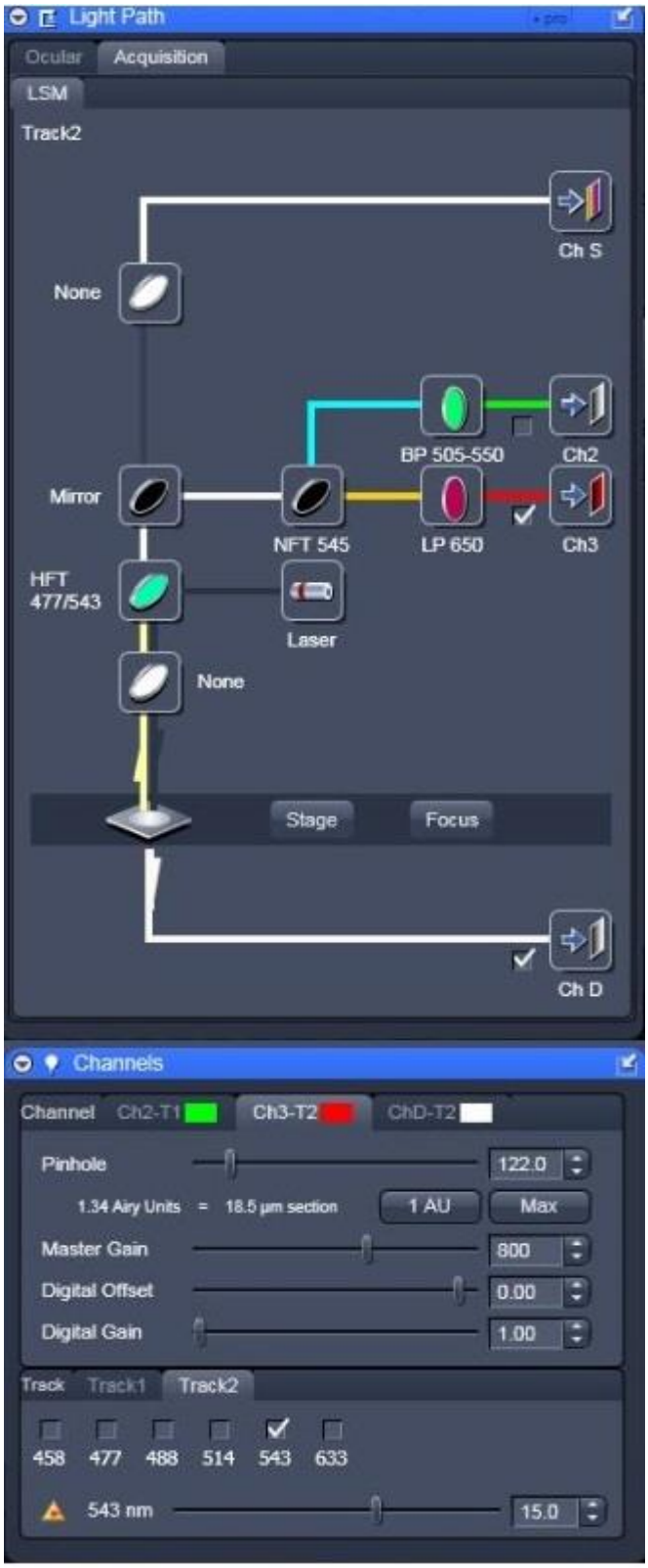

Figure 2.5 Configuration settings for mCherry visualization by confocal microscope

CHAPTER 3

RESULTS AND DISCUSSION

3.1. Cloning mCherry into pBY011 Gateway Expression Vector Using PCR Integration Method

Aiming at generating organelle markers which aid in determination of intracellular trafficking route of yeast membrane proteins labeled with EGFP and especially determining the localization of dimerization of Ste2p, yeast GPCR; we chose four genes of organelle markers at first to fuse with mCherry, red fluorescent protein. The chosen markers were Snf7p, late endosome marker; Sec13p, COPII vesicle marker; Anp1p, the Golgi marker and Pex3p, peroxisome marker (Huh *et al.*, 2003). All the genes were received in pBY011, gateway expression clone, whose promoter is Gal1-10; selection marker for *E. coli* is ampicillin, uracil for *S. cerevisiae* (Figure C 3).

To begin with, insertion of mCherry in frame immediately preceding the each marker gene was planned. Since the sequence of the plasmid was not known, primers complementary to coding region of *SNF7* were designed first so as to learn the upstream and downstream regions of the genes. Using SP1 and SP2, whose sequences are shown at Table D2, that there are spacer sequences flanking the gene was detected.

Then, considering the information, primers which contain homology to mCherry at 3' end were designed. Forward primers possess complementary sequences to specific gene at 5' end while reverse primer consists of complementary region to the immediate downstream of each gene (spacer). Primer 1 and 2, listed at the Table D 1, were used for cloning of mCherry to the 3' end of *SNF7*. Primer 1 and 3 (Table D 1) were used for *SEC13* marker generation. Using the primers, mCherry sequences with appropriate flankings were amplified.

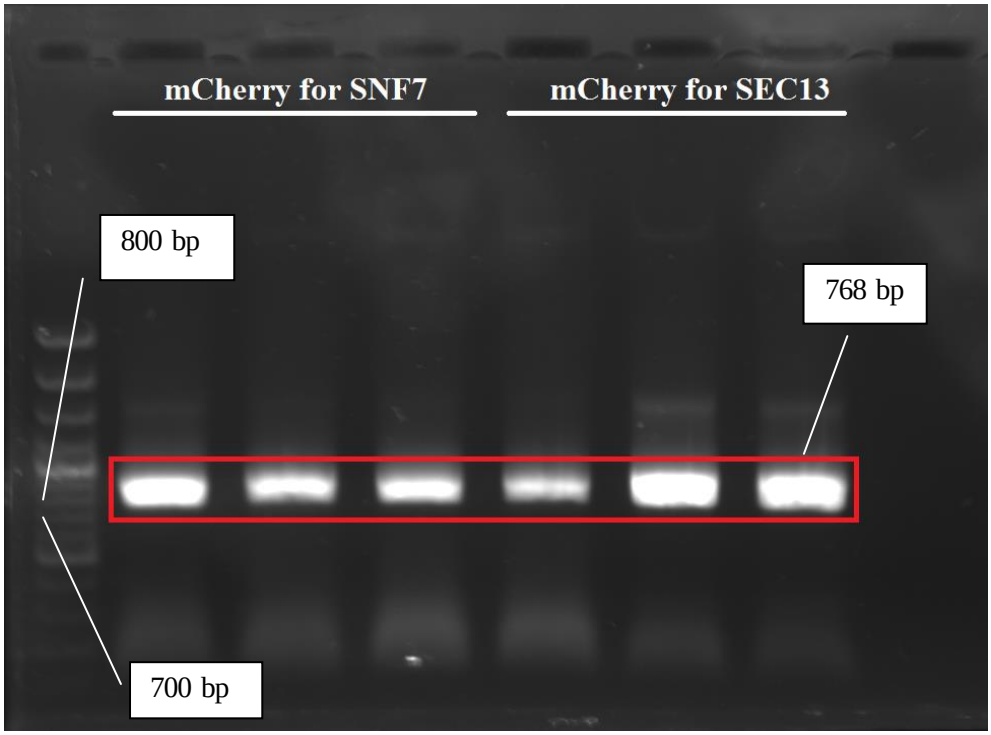

Figure 3.1 mCherry amplified with 30 bp flankings. Lane 1: GeneRuler 100 bp Plus DNA Ladder. Lane 2-4. mCherry amplified with overhangs homologous to SNF7-containing pBY011. Lane 5-7: mCherry with overhangs homologous to SEC13-containing pBY011.

mCherry coding sequence is 708 bp without code for stop. The flankings homologous to both gene and plasmid to be inserted are 30 bp-long. The expected size of the PCR product was controlled by 1% agarose gel run at 90 V (Figure 3.1). Then, the DNA fragments were excised from the gel and purified from the gel components. The gel extraction products were in turn served as primers for the successive PCR, in which PBY011 containing either SNF7 or SEC13 is receiver vector. After the second PCR, products were transformed to competent *E. coli* TOP10 cells to increase the plasmid concentration. At least two transformants were picked up and grown in liquid LB containing ampicillin overnight at 200 rpm. Afterwards, plasmids were isolated and screened through PCR with the primers previously used for amplification and PCR products were run on the 1% agarose gel (Figure 3.2).

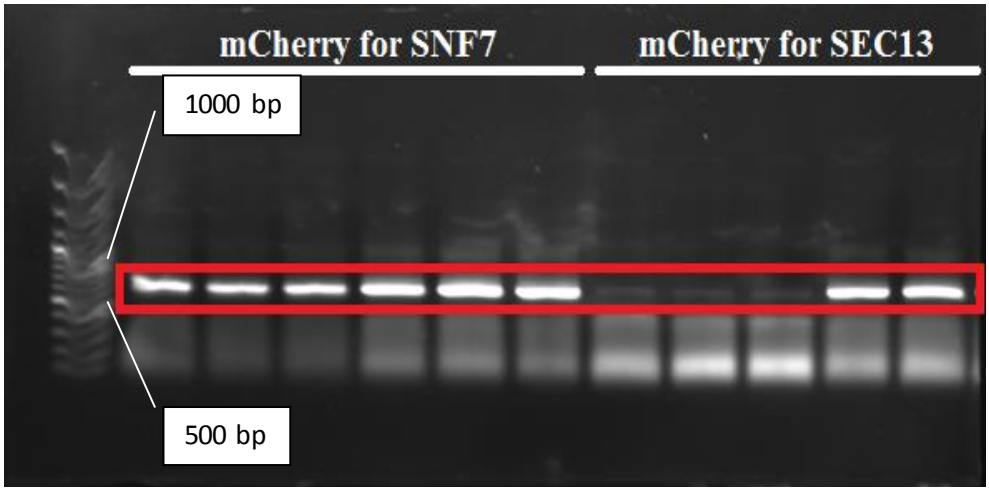

Figure 3.2 Control PCR for insertion of mCherry. Lane 1: GeneRuler 100 bp Plus DNA Ladder. Lane 2-7: mCherry flanked with regions complementary to SNF7 and downstream of SNF7. Lane 8-13: mCherry flanked with regions homologous to SEC13 and its downstream.

According the results, *S. cerevisiae* DK102 cells were transformed with the confirmed plasmids for screening the red fluorescent signal. The cells were grown on MLU for 3 days and then, colonies were chosen to grow in liquid MLU. The cells that were shaken overnight at 200 rpm and 30°C were visualized under confocal and inverted wide field fluorescent microscope. The cells were excited at 543 nm, which is near the excitation maximum of mCherry, and then the signal was collected at 585 nm. However, the entire signal was localized to vacuole rather than any expected subcellular compartment for each marker. Moreover, the signal was lower than expected and it may be because of low pH nature of the vacuole lumen as suggested (Nelson *et al.*, 2007) (Figure 3.3). As suspecting that mCherry may contain any yeast vacuole targeting sequences, using subcellular localization tools like WoLFPSORT (Horton *et al.*, 2007), only mCherry protein sequence was examined and predicted to localize to mostly cytoplasm as well as vacuole but with low possibility. To ensure that fusion did not disrupt the targeting domains of the marker genes, ExPASy tools were used and no clear evidence of the disruption was obtained.

Since the characteristics of the pBY011 were not fully known, it was the other target to be changed. Furthermore, the plasmid does not contain any useful restriction enzyme sites, which can be either used for control or directly for cloning. Therefore, transfers of fusions for SNF7-mCherry and SEC13-mCherry from pBY011 to pBEC were decided.

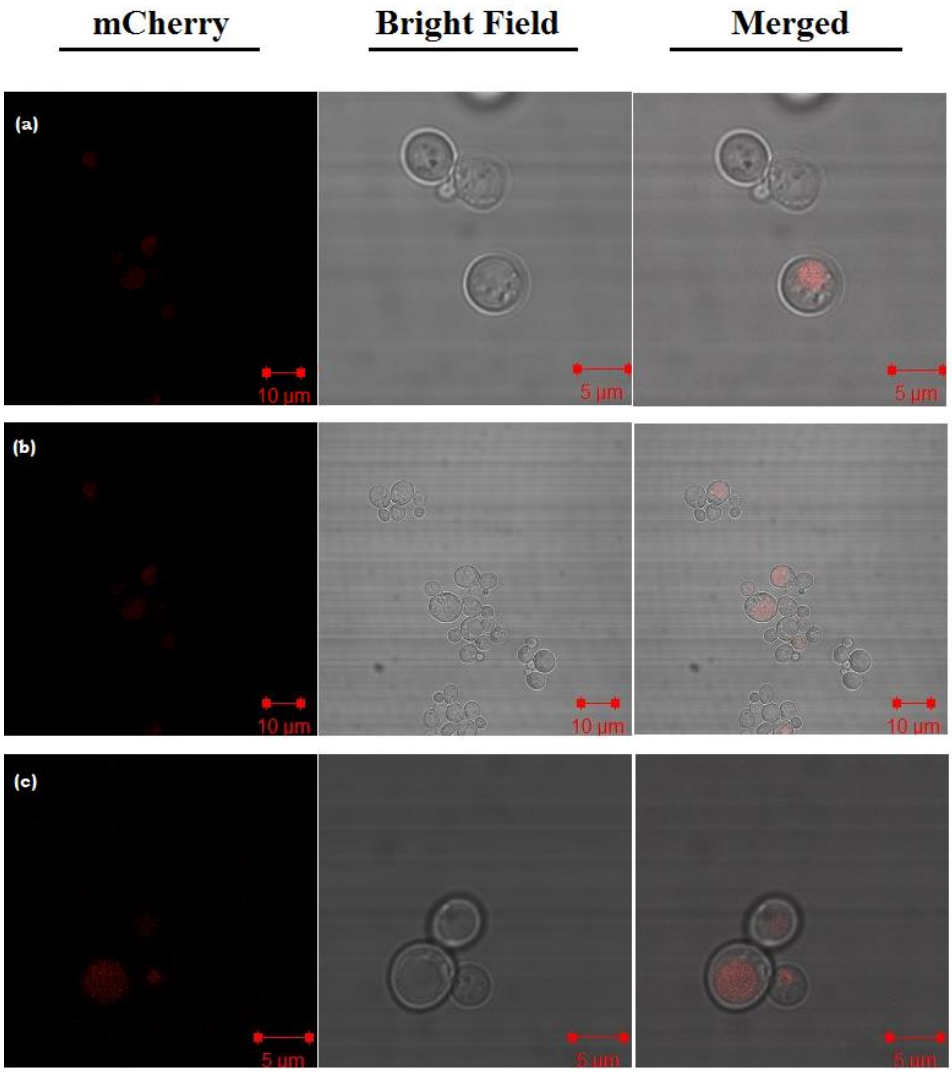

Figure 3.3 *S. cerevisiae* transformed with pBY011 vector containing either SNF7-mCherry (a and b) or SEC13-mCherry (c).

3.2. Transfer of Gene Fusions from pBY011 to pBEC Vector

3.2.1. Transfer of SNF7-mCherry from pBY011 to pBEC Vector

In order to insert the gene fusion into the BamHI and KpnI cut sites in pBEC, primer 4 and 5 were designed to amplify the fusion. The forward primer (4) is complementary at 3' end to the first 21 bps of SNF7 while BamHI cut site precedes the homology. Moreover, BamHI needs one nucleotide before its activity; thus, six bases, which do not complement any

regions in the plasmid, were also added for BamHI activity. The reverse primer had homology at 3' end to last 21 bases of mCherry and KpnI cut site flanked the homology region. As BamHI, KpnI activity requires one nucleotide before its cut site and so six nucleotides were present at 5' end of the primer. Using the primer set, SNF7-mCherry was amplified at expected size of 1455-bp (720 bp of SNF7, 711 bp of mCherry and 24 bp for flankings).

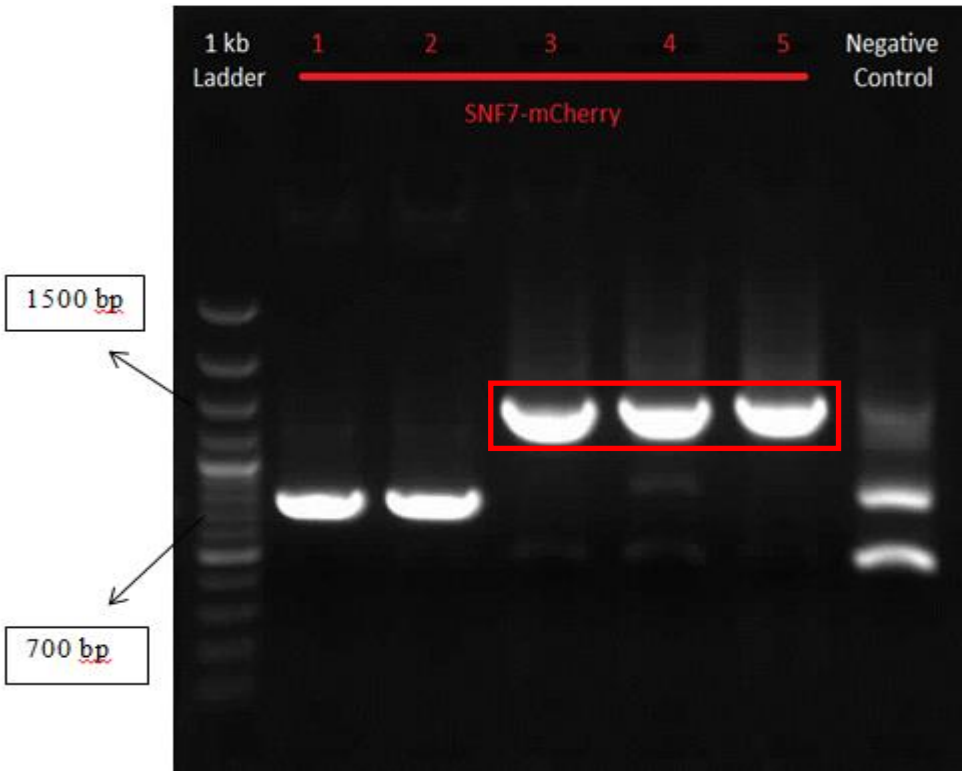

Figure 3.4 SNF7-mCherry with BamHI and KpnI cut site flankings. Lane 1: GeneRuler 1 kb DNA ladder. Lane 2-6: Amplified SNF7-mCherry fusion flanked with BamHI and KpnI cut sites. Lane 7: Negative control.

PCR products were run on the gel and visualized under UV light. As seen from the agarose gel photo (Figure 3.4), SNF7-mCherry was amplified with 5' end BamHI cut site and 3'end KpnI cut site at the expected size. The gel extraction products successively digested with BamHI-HF and KpnI-HF enzymes for 1 hour as well as pBEC vector. The digestion products were, in turn, run on the gel to verify the sizes (Figure 3.5).

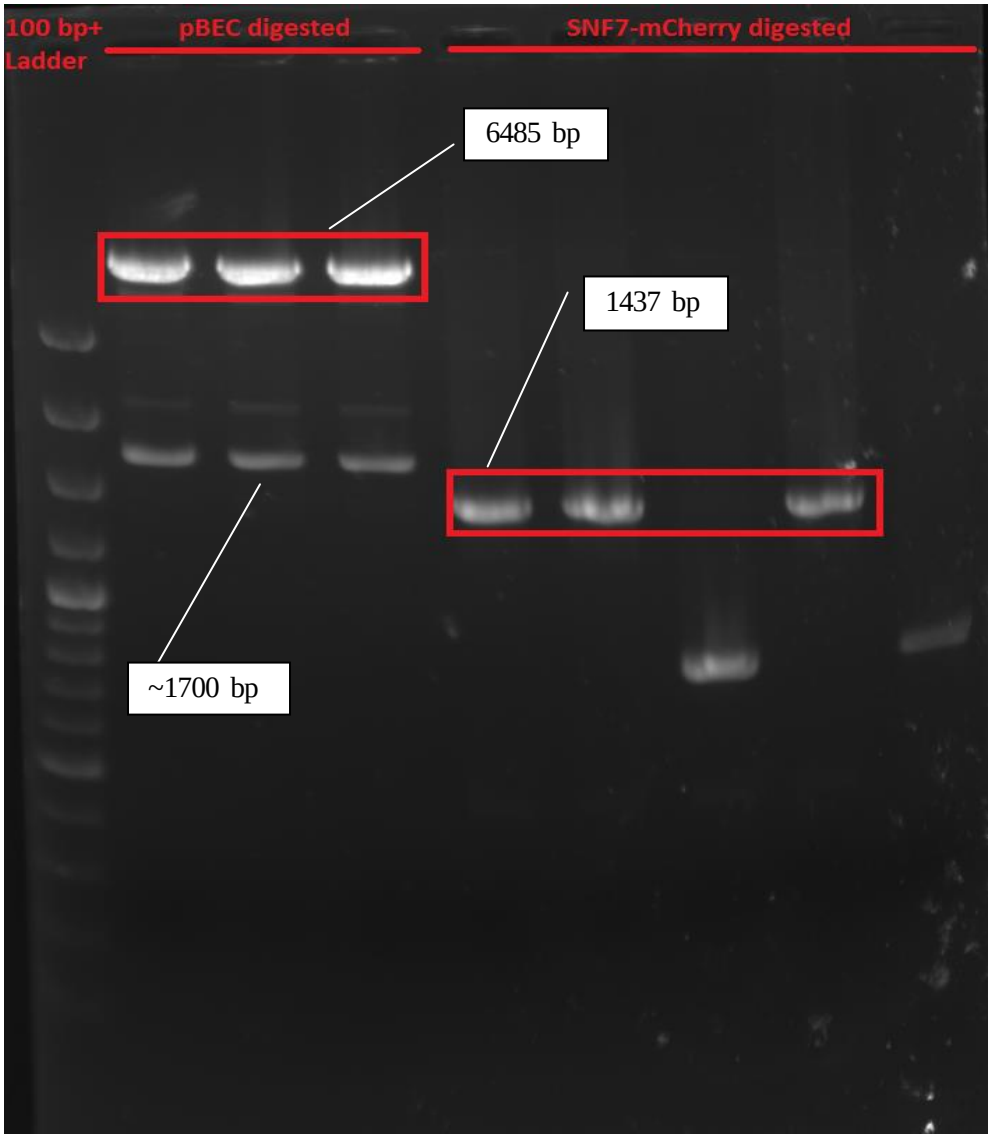

Figure 3.5 pBEC and SNF7-mCherry cut with BamHI and KpnI. Lane 1: GeneRuler 100 bp plus DNA ladder. Lane 2-4: pBEC digested with BamHI and KpnI. Lane 5-9: SNF7-mCherry fusion digested with BamHI and KpnI.

Between BamHI and KpnI cut sites, there was a gene at around 1700 bp. Therefore, all the pBEC bands visualized were at the correct size. Then, the fragments were extracted from the agarose gel and ligated to each other. Competent *E. coli* TOP10 were transformed with the ligation products and then colonies on the plates were grown in LB-Ampicillin broth overnight at 37°C. Plasmids from the cultures were isolated by Thermo Scientific® GeneJet Plasmid Miniprep Kit. After plasmid isolation, plasmids were undergone simultaneous cut by BamHI and KpnI and run on 1% agarose gel.

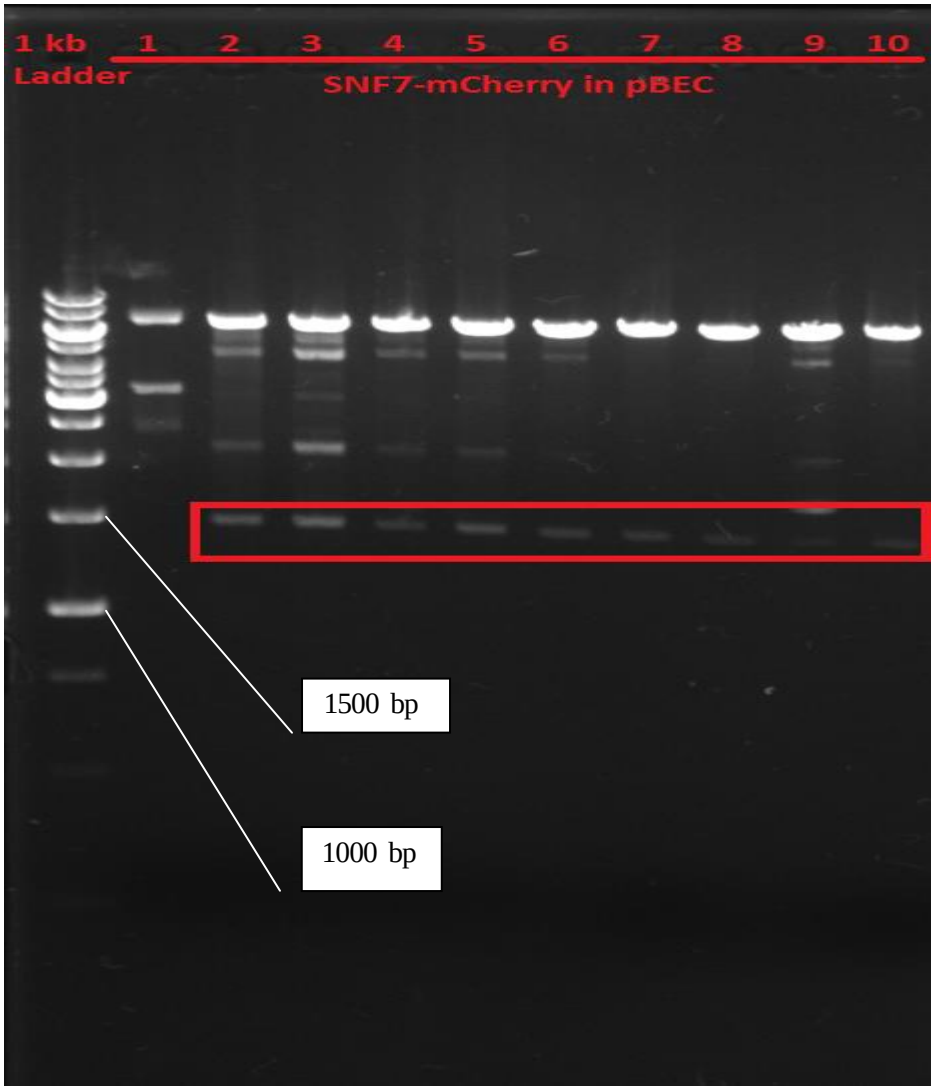

Figure 3.6 Digestion control by BamHI and KpnI restriction enzymes. Lane 1: GeneRuler 1 kb DNA ladder. Lane 2-11: Constructs digested with BamHI and KpnI.

Verified plasmids by size control, were transferred to *Saccharomyces cerevisiae* DK102 cells and visualized under laser scanning confocal and inverted wide field fluorescence microscope. As before, the cells were exposed to light at 543 nm and the signal was collected at 585 nm. After signal verification, corresponding plasmids were sequenced using the primers listed in Table D 2.

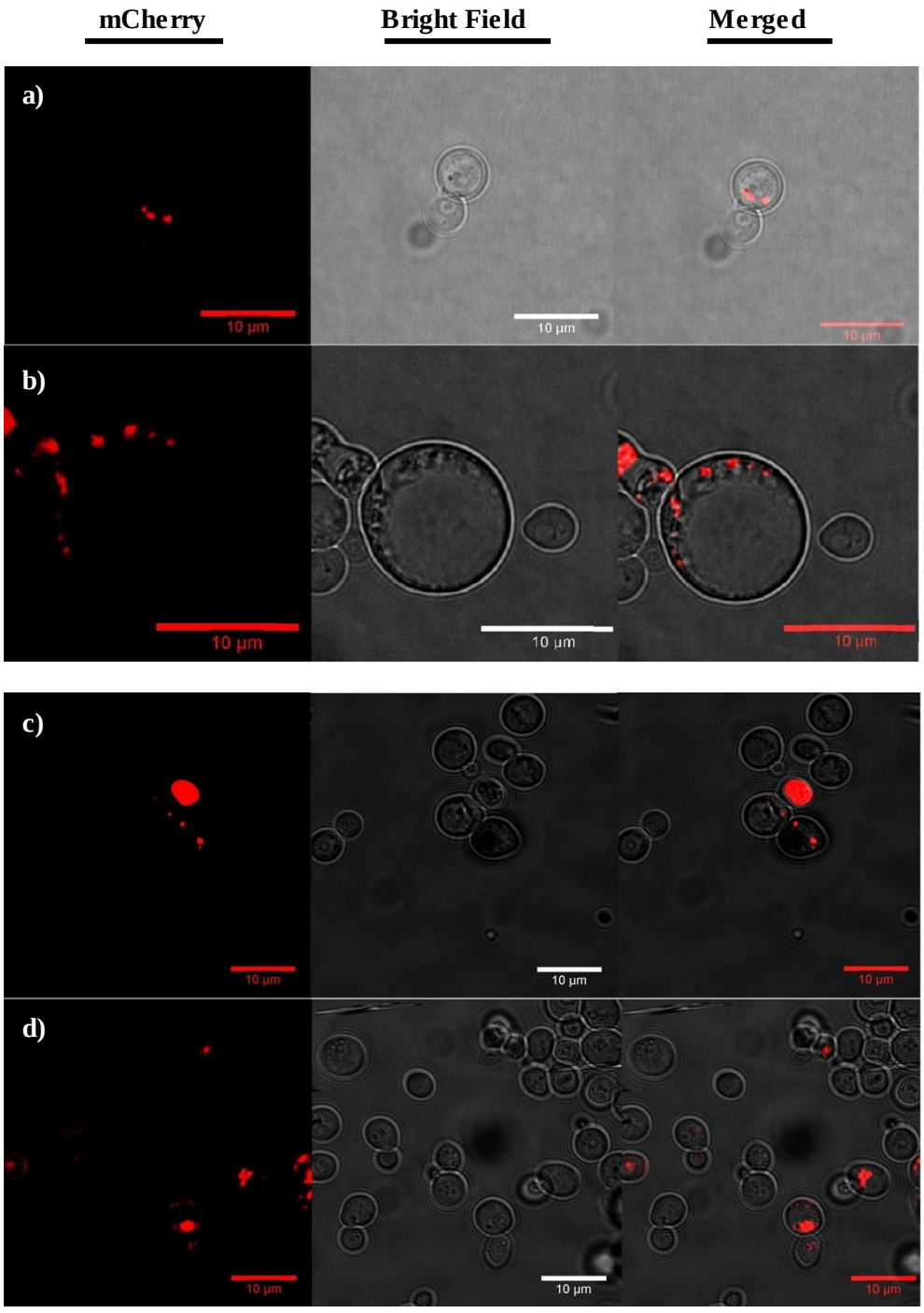

Figure 3.7 Yeast cells expressing Snf7p labeled with mCherry. mCherry labels late endosomes in the cells depicted in the images. Cells were visualized under inverted wide field microscope (a and b) and confocal microscope (c and d).

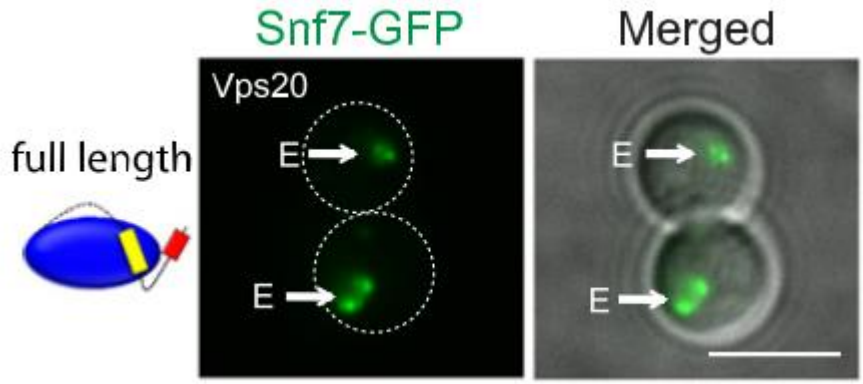

Figure 3.8 Expected result for Snf7 distribution in live yeast cells (William Mike Henne, Buchkovich, Zhao, & Emr, 2012).

Consistent with the characteristic morphology of yeast late endosome and the images of GFP tagged Snf7p (Figure 3.8), the mCherry tagged Snf7 is localized to late endosome as a part of ESCRT III (Babst *et al.*, 2002; William Mike Henne *et al.*, 2012). The signal dots were generally larger and brighter (Figure 3.7 c) when cells were large and seemed not to be healthy.

3.2.2. Transfer of SEC13-mCherry from pBY011 to pBEC

Primers used for the cloning approach were designed in exactly same way with ones for SNF7-mCherry. The primers 6 and 7 (Table D 1) were for amplification of SEC13-mCherry flanked with BamHI cut site at 5' end and KpnI cut site at 3' end. According to the PCR program and mixture explained in the Methods part, PCR was conducted. Then, the products were run on 1% agarose gel and visualized under UV light (Figure 3.9).

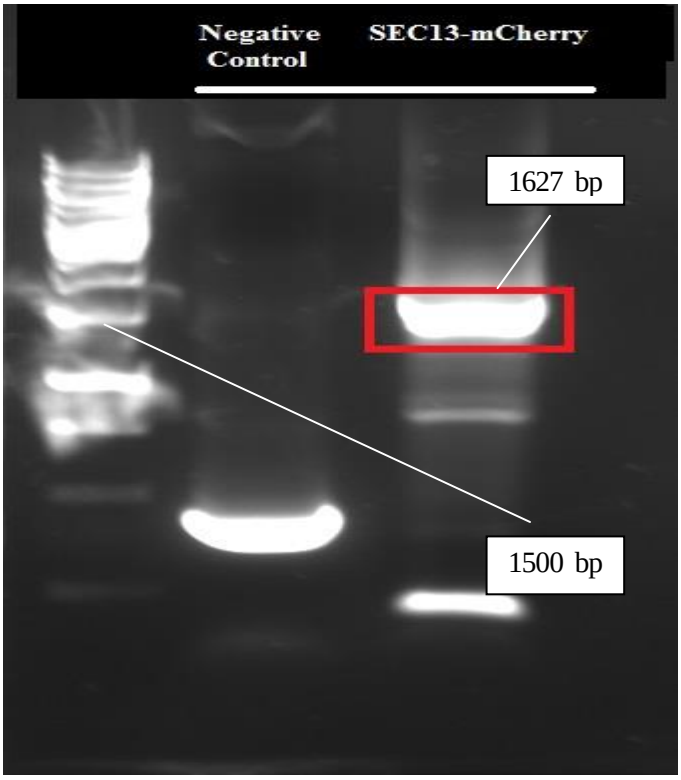

Figure 3.9 SEC13-mCherry flanked with BamHI and KpnI cut sites. Lane 1: GeneRuler 1 kb DNA ladder. Lane 2: Negative control. Lane 3: SEC13-mCherry fusion flanked with BamHI and KpnI cut sites.

SEC13 gene is 891 bp long without the code for stop and when amplified as fusion with the primers, the product was expected to be 1627 bp-long. Therefore, it was verified that SEC13-mCherry flanked with the target cut sites was acquired at expected amount. Then, the DNA fragments were collected from the gel and digested with BamHI and KpnI with the plasmid of interest, pBEC. Afterwards, the digestion products were put in a ligation reaction for 1-2 hours and then competent *E. coli* cells were transformed with the ligation product. Upon plasmid isolation, they were cut by BamHI and KpnI to control size (Figure 3.9).

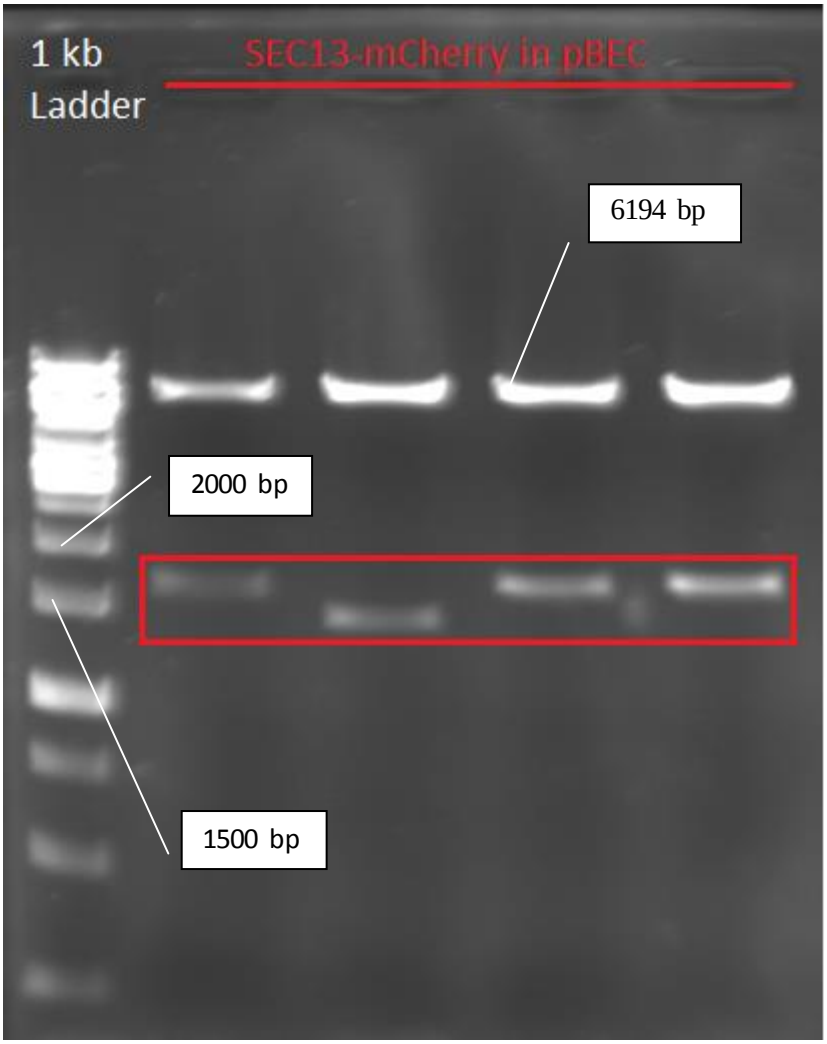

Figure 3.10 SEC13-mCherry in pBEC. Lane 1: GeneRuler 1 kb DNA ladder. Lane 2-5: Construct digested with BamHI and KpnI for control.

Except lane 2, all bands seemed to be at the correct size. Thus, *S. cerevisiae* DK102 cells were transformed with the plasmid by Gietz *et al.* method and the cells grown in MLT broth were examined under both fluorescence and confocal microscope.

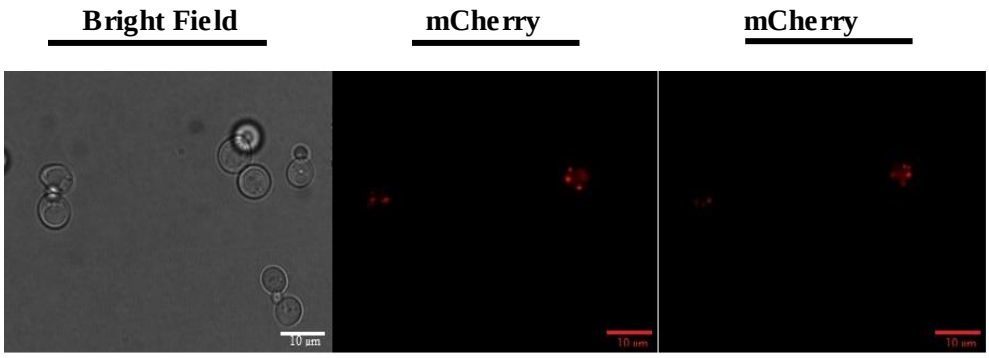

Figure 3.11 *S. cerevisiae* DK102 cells expressing mCherry tagged Sec13 visualized under inverted wide field fluorescence microscope. mCherry image in the middle and at right were acquired from the same cells but the focus was changed.

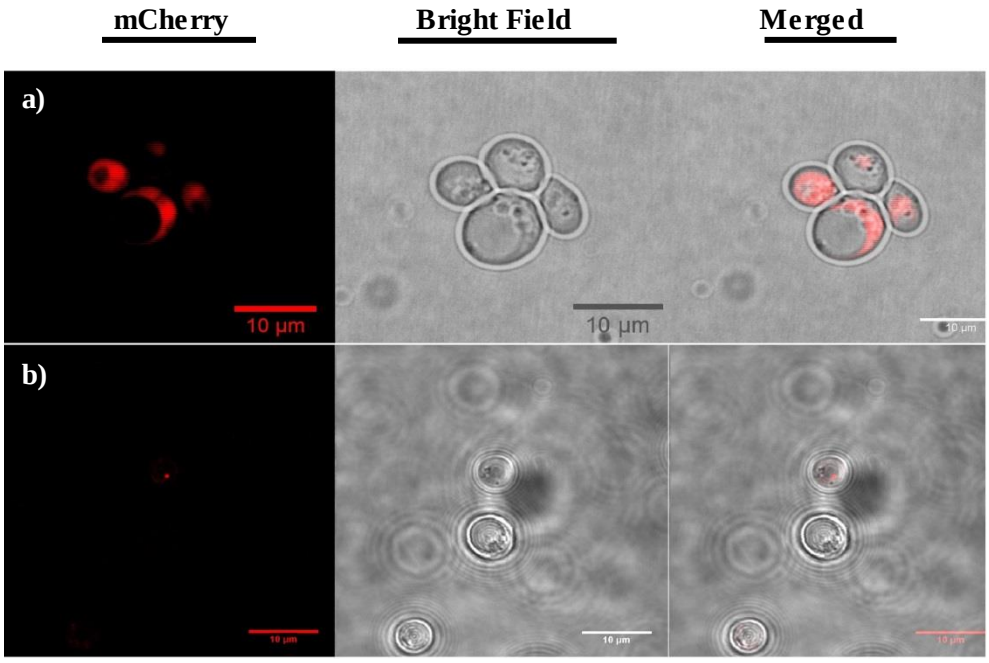

Figure 3.12 *Saccharomyces cerevisiae* cells expressing mCherry tagged Sec13p visualized under a) inverted wide field fluorescence microscope and b) laser scanning confocal microscope.

COPII vesicles carry proteins that are processed and folded enough to continue further modifications in the Golgi apparatus. The vesicle components recycle back and forth from the ER to the Golgi. Therefore, the signal was expected from the ER and the Golgi also. Moreover, a recent study suggests that the distance between the compartments in yeast may be as small as in mammalian cells. In addition, the average diameter of the vesicles is 70-80 nm. Therefore, we do not expect punctate pattern but rather a bit spacious distribution. As expected, images shown in Figure 3.12 presents what we expect.

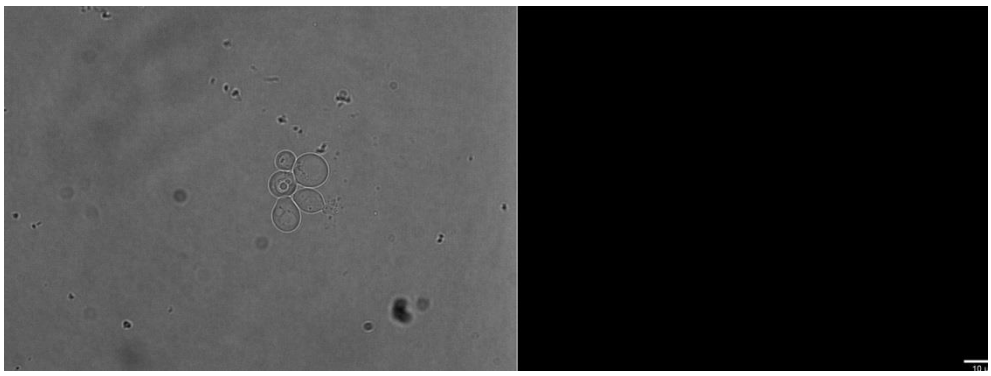

Figure 3.13 Yeast cells that contain pBEC vector but do not express any fluorescent protein.

Figure 3.13 represents that cells containing empty pBEC vector does not fluorescence as expected.

Since red fluorescent signal was acquired from the cells expressing either SNF7-mCherry or SEC13-mCherry, it was decided that all the other fluorescent markers should be built in pBEC vector.

3.3. Construction of ER Marker

3.3.1. Cloning mCherry into pBEC Vector

The strategy was to insert mCherry between BamHI and EcoRI cut sites and then to add targeting sequences or marker gene to pBEC containing mCherry sequence. Firstly, primers were designed in order to insert mCherry coding sequence to pBEC vector between EcoRI

and BamHI. Since there will be HDEL DNA sequence at downstream of mCherry we designed a primer set to insert mCherry without the stop codon. To generate mCherry without stop, primer 8 and 9 (Table D 1) were used for the amplification by PCR and PCR products were run on 1% agarose gel (Figure 3.14).

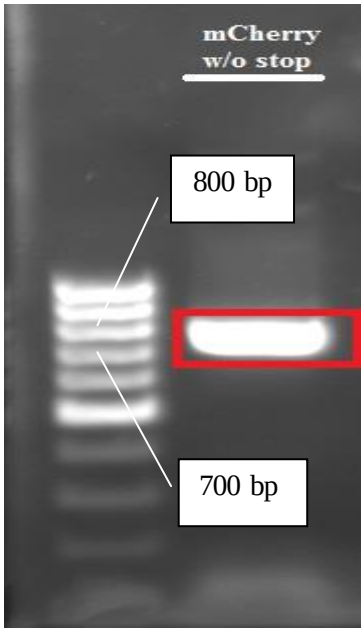

Figure 3.14 mCherry (without stop) flanked with BamHI and EcoRI cut sites. Lane 1: GeneRuler 100 bp DNA ladder. Lane 2: mCherry fragment (no code for stop codon) flanked with BamHI and EcoRI cut sites.

mCherry sequence except the stop codon compromises 708 base pairs. Considering BamHI and EcoRI cut sites and 6 bp for the activity of the restriction enzymes, mCherry band was expected to be 732 bp long. The band at expected size was excised from the gel and mCherry was cut by BamHI-HF and EcoRI-HF simultaneously together with pBEC plasmid. Then, the digestion products were run on 0.8% agarose gel and the gel was photographed under UV light (Figure 3.15).

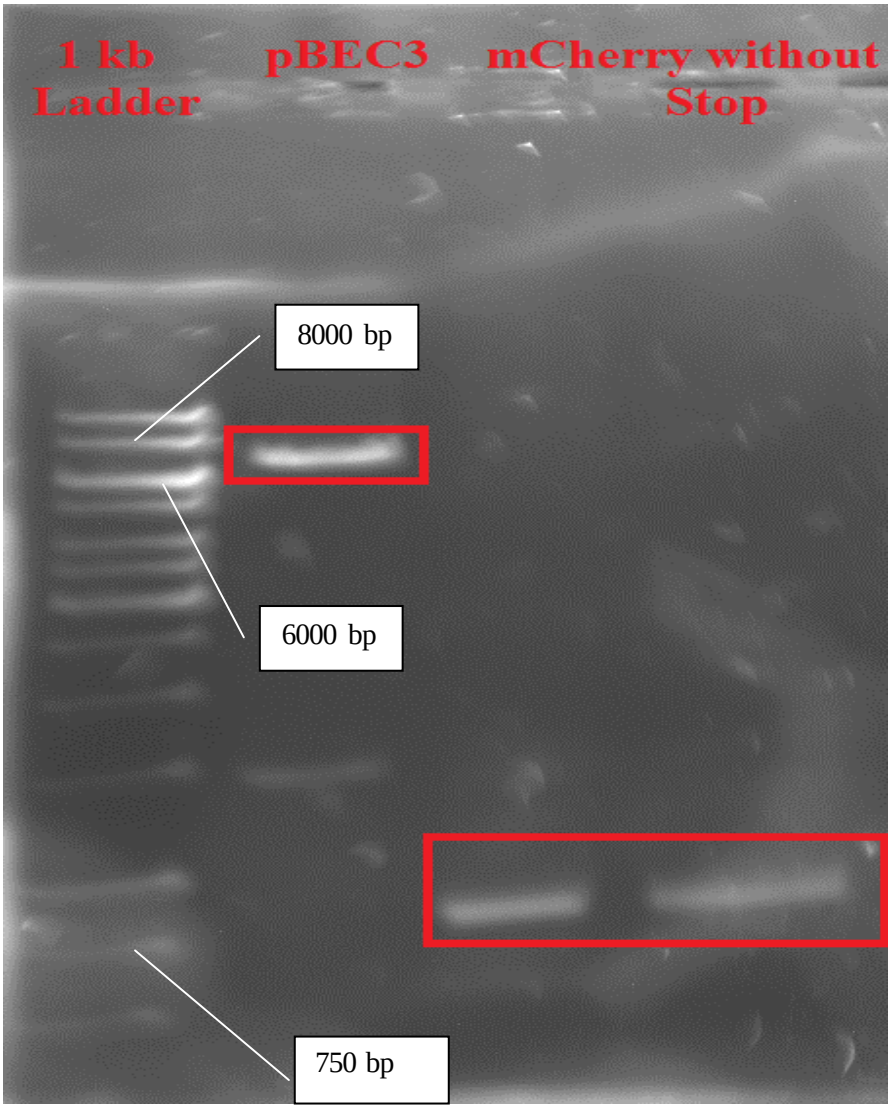

Figure 3.15 Digestion products of pBEC and mCherry. Lane 1: GeneRuler 1 kb ladder. Lane 2: pBEC digested with BamHI and EcoRI. Lane 3-5: mCherry digested with BamHI and EcoRI.

Since all the products were at the desired sizes, gel extraction products were ligated and then competent *E. coli* cells were transformed with the ligation product to increase the amount of new construct. When plasmids were isolated from chosen transformants, they were digested again with BamHI-HF and EcoRI-HF for verification of the size and the digestion products were run on 1% agarose gel (Figure 3.16).

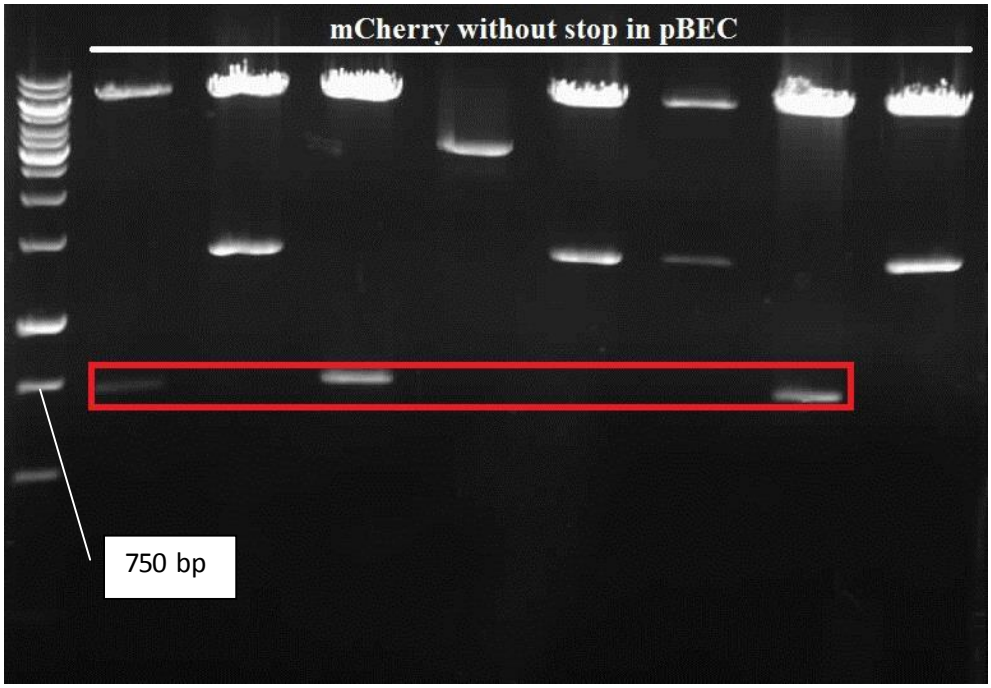

Figure 3.16 Size control of mCherry in pBEC by digestion. Lane 1: GeneRuler 1 kb ladder. Lane 2-9: pBEC, which contains mCherry, digested with BamHI and EcoRI.

As depicted in Figure 3.16, the bands at lane 2, 4 and 8 were at the expected size. Therefore, the corresponding plasmids were sequenced for confirmation (Table D 2).

3.3.2 Insertion of Signal Sequence (SS) of SUC2 to N terminus of mCherry Using PCR Integration Method

In order to generate an ER marker with targeting sequences, HDEL amino acid sequence and signal sequence of SUC2 gene were determined to be added to C and N-terminus of protein, respectively (Carlson *et al.*, 1983; Nelson *et al.*, 2007; Pelham *et al.*, 1988). The signal sequence of the invertase gene (Carlson *et al.*, 1983; Rothe & Lehle, 1998) was determined. Since we do not have SUC2, a primer pair, whose dimer would be the signal sequence of interest, was designed. By PCR, a primer dimer was constructed after many optimization trials. Then, the products were run on 3% agarose gel and examined under UV light (Figure 3.17).

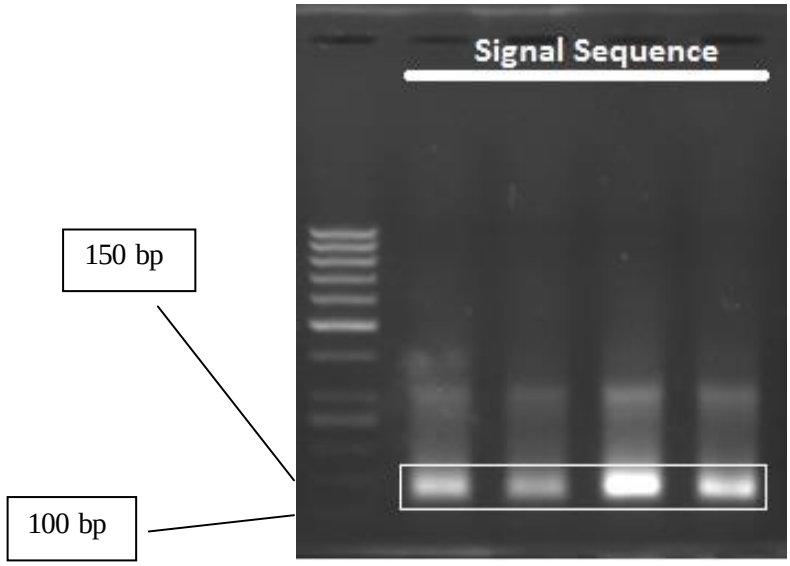

Figure 3.17 SS fragments to be inserted to N terminus of mCherry. Lane 1: GeneRuler 50 bp DNA ladder. Lane 2-5: Coding region of signal sequence of SUC2 amplified with flankings homologous to upstream of mCherry in pBEC.

Since the primers (Primer 13 and 14) also possess homology to the upstream of mCherry in pBEC vector, the DNA fragments were expected to be 118 bp-long while the signal sequence of SUC2 is 63 bp long. The bands were as expected; therefore, gel extraction was conducted and second PCR of the technique was carried out using mCherry (without stop) in pBEC as receiver plasmid and the gel extraction products as insert. The second PCR products, in turn, were digested with DpnI to get rid of plasmids that are not products of the PCR. DpnI recognized methylated GATC sequences, which can be present only if a plasmid is amplified in *E. coli* rather than by PCR. Afterwards, the PCR products, which are purified by digestion, were used for *E. coli* transformation. After growing the chosen transformant colonies in selective LB medium, plasmids were isolated and then digested with BamHI-HF and SpeI in order to control the size. Sizes were examined by agarose gel electrophoresis and successively visualization under UV light (Figure 3.18).

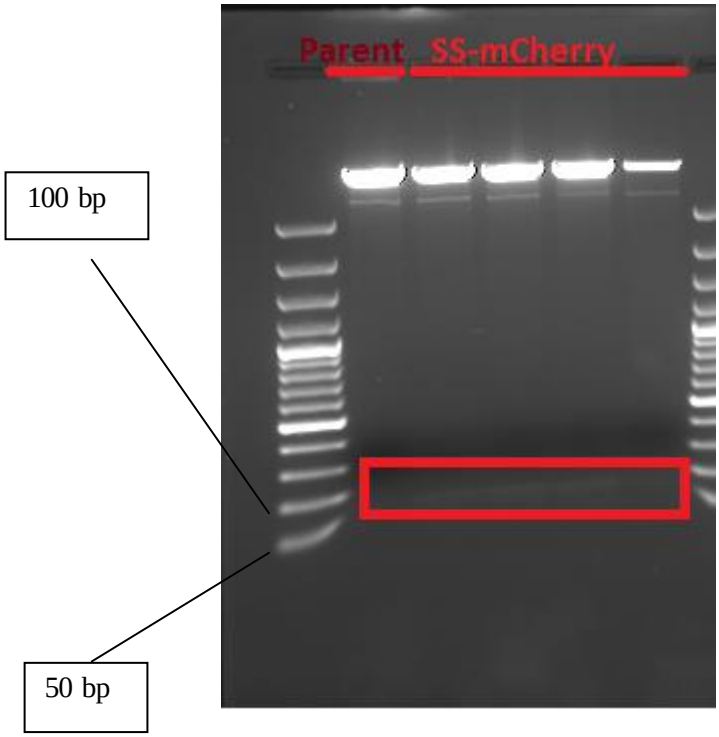

Figure 3.18 Size control by digestion for SS addition. Lane 1: GeneRuler 50 kb ladder. Lane 2-6: SS-mCherry fusion obtained BamHI and SpeI digestion of pBEC.

As seen from the figure, there is no band at the expected size for parent vector since SpeI and BamHI cut sites are successively located. However, for the next three wells, there are bands at the expected size of 66 bp despite being slight.

3.3.3. Insertion of HDEL to C terminus of mCherry Using PCR Integration Method

According to codon bias in *S. cerevisiae*, I determined the DNA sequence of HDEL as 5'-GTGGTCTTCCAA-3'. Furthermore, the sequence was blasted and confirmed that it is present at the C termini of many ER resident proteins.

Since this sequence is short and we do not have any sequence to take HDEL from, I designed a primer pair (Primer 11 and 12, shown at Table D 1) annealing to each other. This double stranded fragment is HDEL expressing sequence flanked with regions homologous to downstream of mCherry (w/o stop) in pBEC. There are papers (Nelson *et al.*, 2007; Pelham *et al.*, 1988) suggesting addition of HDEL after a small polylinker added to the C terminus of protein of interest since they show that there are proteins whose, for instance, secretion is not affected by HDEL addition if it was added immediately after C terminus. They think that because HDEL is a short sequence, it's masked by the protein. Although

there are some papers with successful ER markers generated by direct addition of KDEL I did not want to take risk of masking and inserted HDEL's code to 33 bp downstream of mCherry in order to avoid it. Therefore, according to the aforementioned protocol, PCR was carried out to amplify the primer dimer of HDEL sequence.

HDEL is tetrapeptide encoded by 12 nucleotides. Primer set amplifying the 12 bp-long DNA fragment contain 27-30 bp at the 5' end in order to anneal to targeted upstream of mCherry in pBEC. Hence, the expected size of the primer dimer was 69 bp. As shown in the Figure 3.19, the ER retention sequence was obtained.

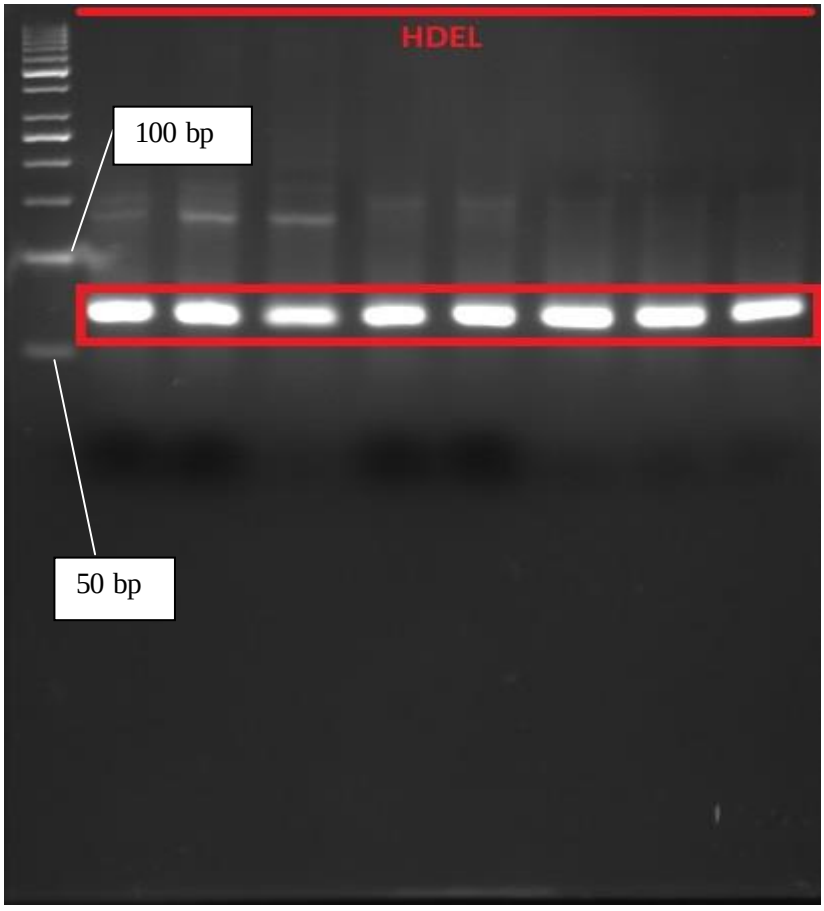

Figure 3.19 HDEL sequence to be inserted to the C terminus of mCherry in pBEC. Lane 1: GeneRuler 50 bp DNA ladder. Lane 2-9: HDEL DNA sequence with overhangs complementary to downstream of mCherry in pBEC.

Then, the DNA fragments were isolated from the gel and used as primer in the successive PCR while previously constructed plasmid, which consists of SS-mCherry fusion, is parent vector. In order to remove plasmids that are not PCR constructs, DpnI digestion was carried out and competent *E.coli* TOP10 cells were transformed with the true constructs. Chosen colonies from each plate of ER markers were grown in liquid LB+Amp at 37°C overnight. Plasmids from the overnight grown cultures were isolated and controlled by double digestion with SpeI and KpnI-HF. The digestion products were loaded onto 1.5% agarose gel and photographed under UV light (Figure 3.20).

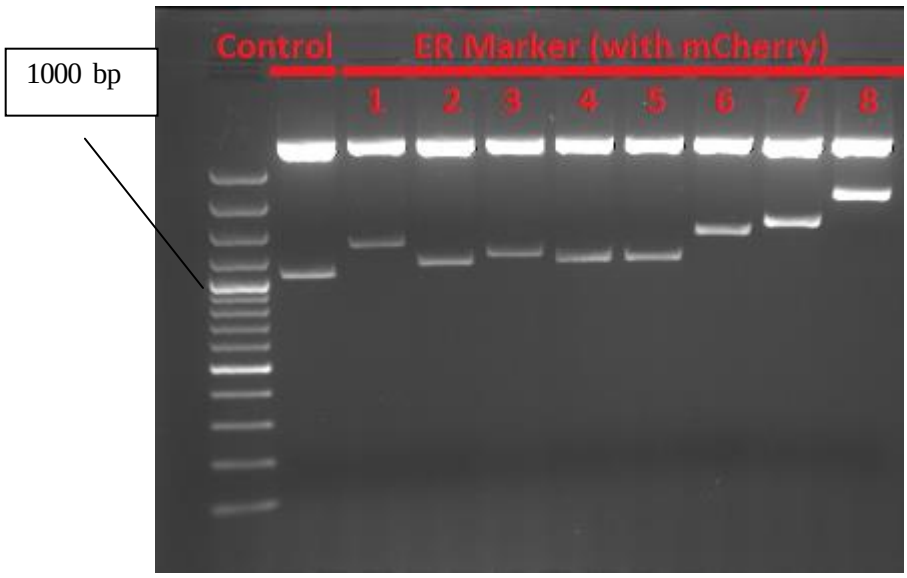

Figure 3.20 Digestion control for ER markers. Lane 1: GeneRuler 100 bp plus DNA ladder. Lane 2: SS-mCherry in pBEC as control. Lane 3-10: ER marker in pBEC digested with SpeI and KpnI.

The expected size of digestion products of the ER marker is 1095 bp. The control, on the other hand, is 1011 bp long. According to the gel photo, the constructs run on lane 2, 4 and 5 seemed to be correct. Based on the assumption, *S. cerevisiae* DK102 cells were transformed with the constructs, grown on selective media and then examined under confocal and fluorescence microscope exciting the cells for mCherry emission. The constructs were sequenced using the primers mentioned at Table D 2.

The cells expressing mCherry with SS or mCherry with HDEL did not fluoresce differing much from cytosolic mCherry as expected. Although SS directs proteins into ER lumen, due to lack of ER retention signal, some processed proteins can exit from the ER for degradation

or for cytosolic localization. mCherry with HDEL may not even enter to the ER and their distribution is the same with the sole mCherry (Figure 3.21).

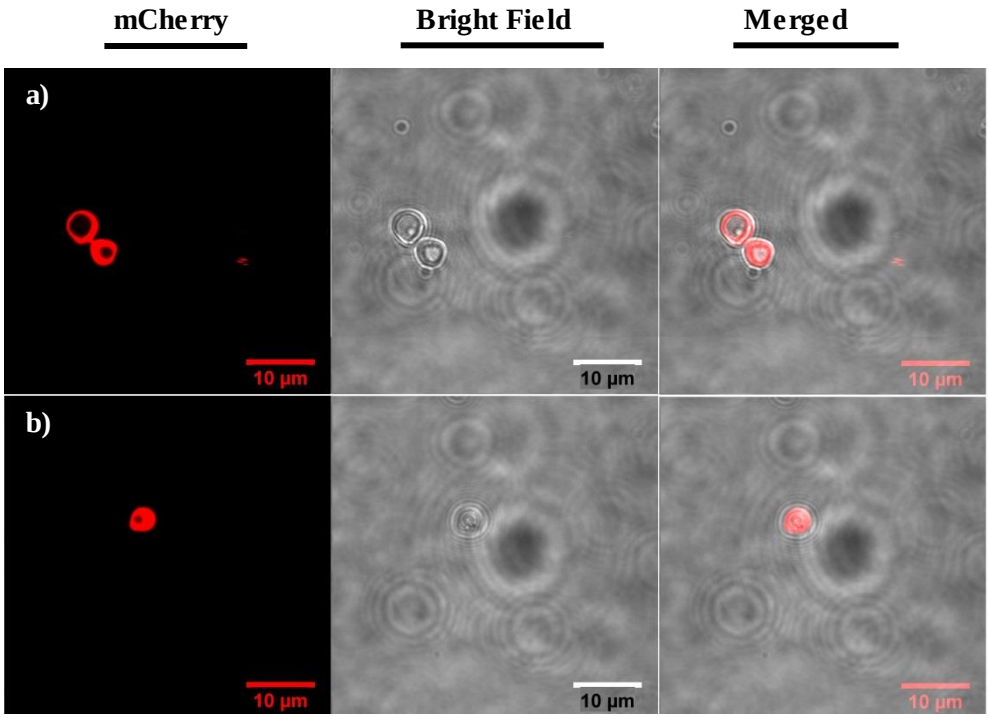

Figure 3.21 The images were acquired from cells expressing mCherry with HDEL (a) and mCherry with SS (b).

Figure 3.27 illustrates *S. cerevisiae* cells that only express mCherry protein which is cytosolic if not targeted. When compared the images depicted in Figure 3.21 with Figure 3.27, we clearly suggest that only SS or HDEL does not localize mCherry to the ER; instead, they distribute to cytoplasm without opportunity of distinguishing a special pattern for the organelle.

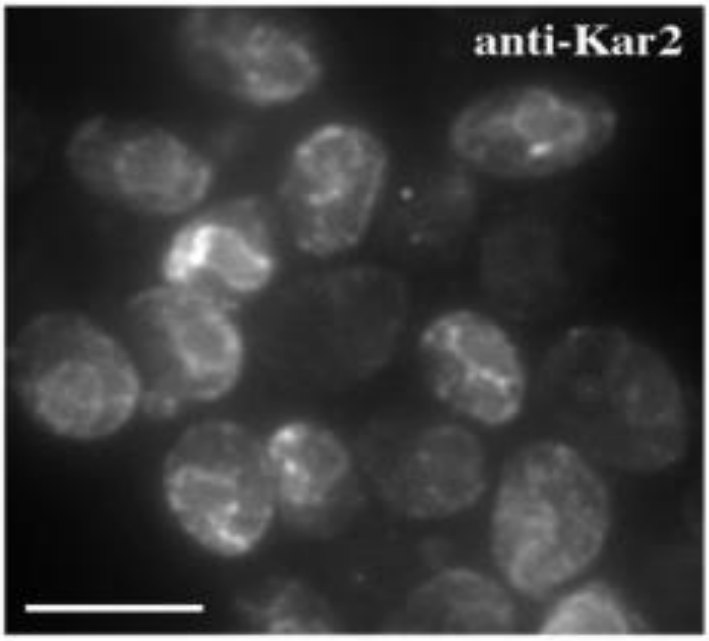

Figure 3.22 Expected labeling of the endoplasmic reticulum in *S. cerevisiae*. Immunoflourescence labeling of Kar2p, ER resident protein.

Figure 3.22 shows the distribution of Kar2p, which is heat shock protein localized to the ER in budding yeast. The image was taken visualizing the protein by use of antibodies targeting the Kar2 protein. Since the ER marker generated in budding yeast is the first for Saccharomyces cerevisiae, this image can serve as reference to compare the morphology and distribution of the compartment with the cells expressing the ER marker constructed.

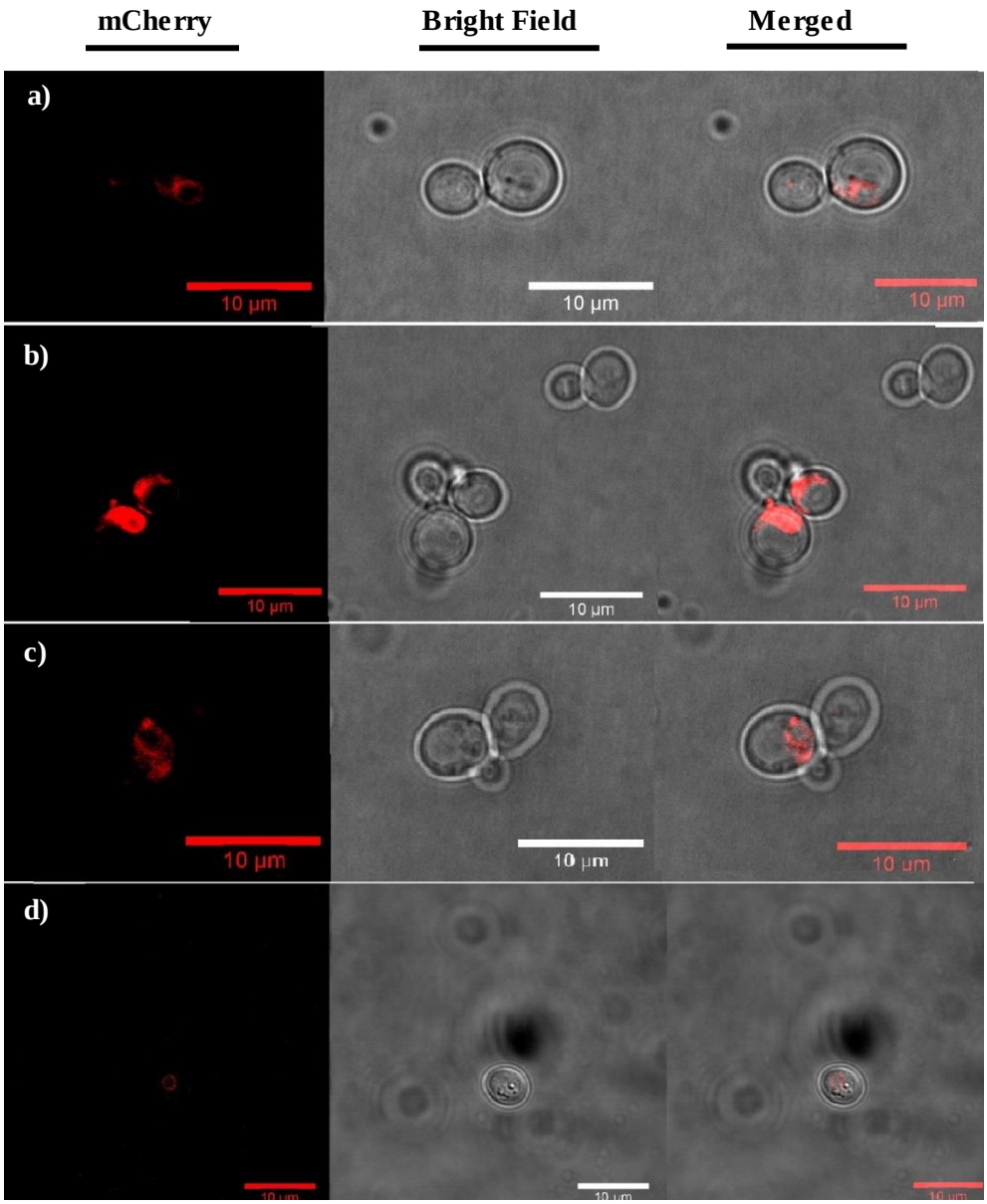

Figure 3.23 *Saccharomyces cerevisiae* cells, which express red fluorescent ER marker, visualized under (a, b and c) fluorescence microscope and (d) confocal microscope.

The ER stretches around the nucleus and extends in a sheet like manner in budding yeast. As expected, the periphery and around of the nucleus was labeled by the marker. The subtle changes, such as non-hollow like pattern, between the images seemed to be due to overexpression. The changes in the nucleus morphology also suggest that the marker can also serve for monitoring the dynamics of the nucleus.

3.4. Construction of Golgi Marker

3.4.1. Cloning mCherry into pBEC Vector

Primer 8 and 10 were used to add BamHI and EcoRI cut sites to 5' and 3' end of mCherry, respectively and to amplify the coding sequence as such. The PCR products were run on 1% agarose gel and whether the DNA fragments were at the expected size was controlled. mCherry coding sequence is 711 bp long and with the addition of the cut sites and nucleotides for the activity of the restriction enzymes, the expected size is 735 bp long (Figure 3.24).

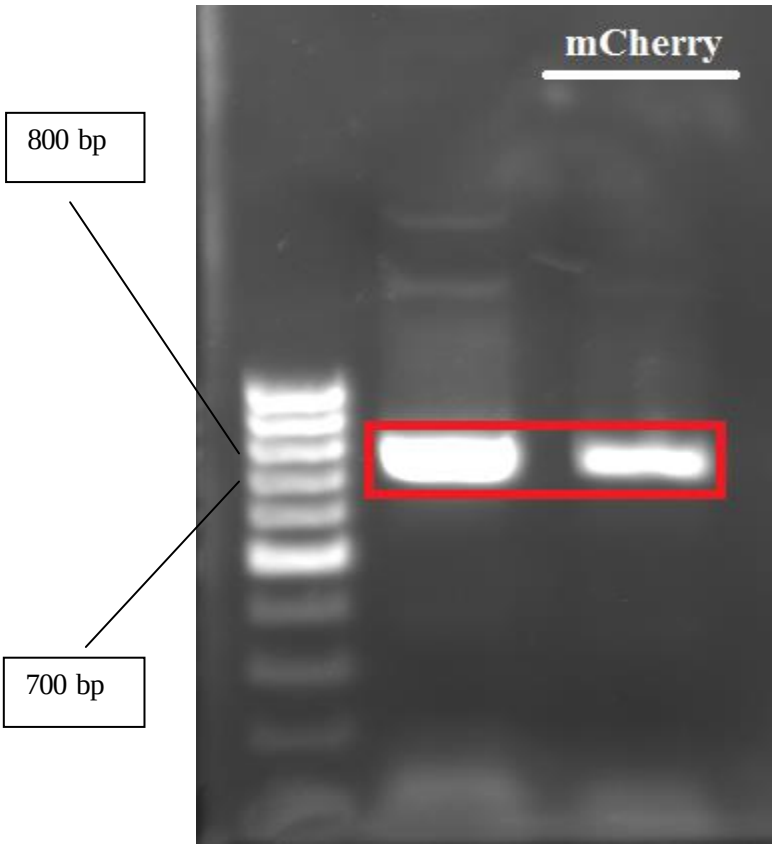

Figure 3.24 mCherry with BamHI and EcoRI cut site flankings to be cloned to pBEC vector. Lane 1: GeneRuler 100 bp ladder. Lane 2-3: mCherry amplified with overhangs containing BamHI and EcoRI cut sites.

The mCherry was then extracted from the gel and, as pBEC, digested by BamHI-HF and EcoRI-HF. After digestion, mCherry and pBEC were loaded onto agarose gel and run. The gel was photographed and the sizes of the digestion products were verified (Figure 3.25)

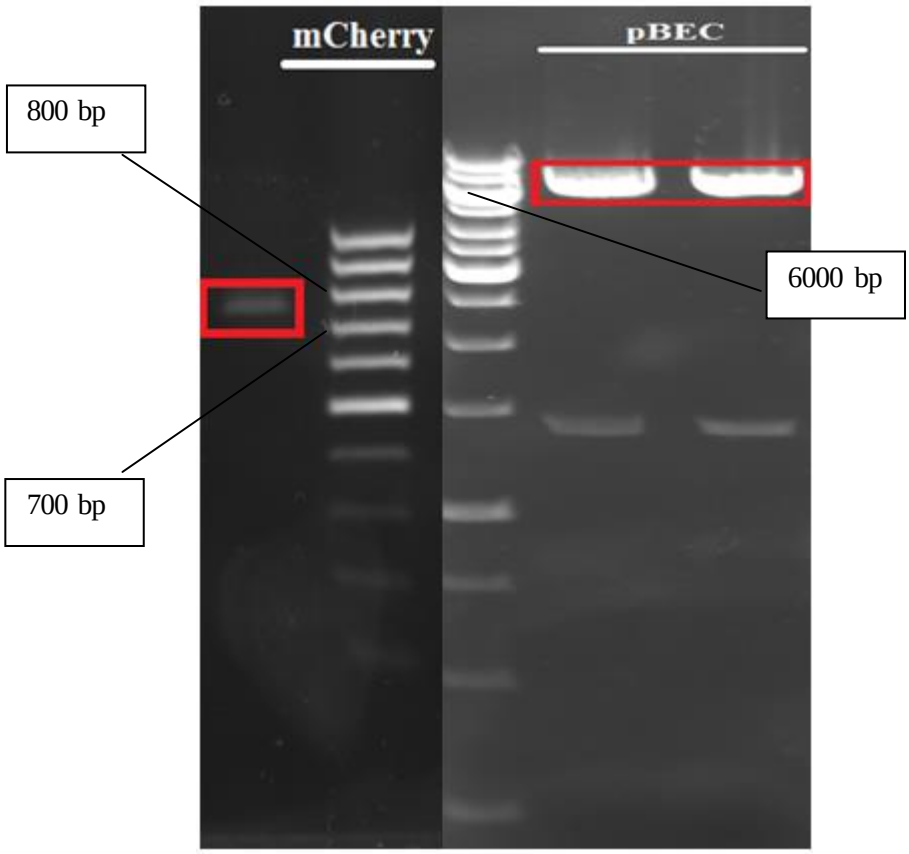

Figure 3.25 mCherry and pBEC digested with BamHI-HF and EcoRI-HF. Lane 1: mCherry digested with BamHI and EcoRI. Lane 2: GeneRuler 100 bp DNA ladder. Lane 3: GeneRuler 1 kb DNA ladder. Lane 4-5: pBEC digested with BamHI and EcoRI.

As seen from the figure, the bands were at the correct size; thus, they were purified and then ligated. The ligation products were used for transformation of competent *E. coli* TOP10 cells. After increasing plasmid number and selecting the transformants, plasmids were isolated and their sizes were controlled by BamHI-HF and EcoRI-HF double digestion (Figure 3.26).

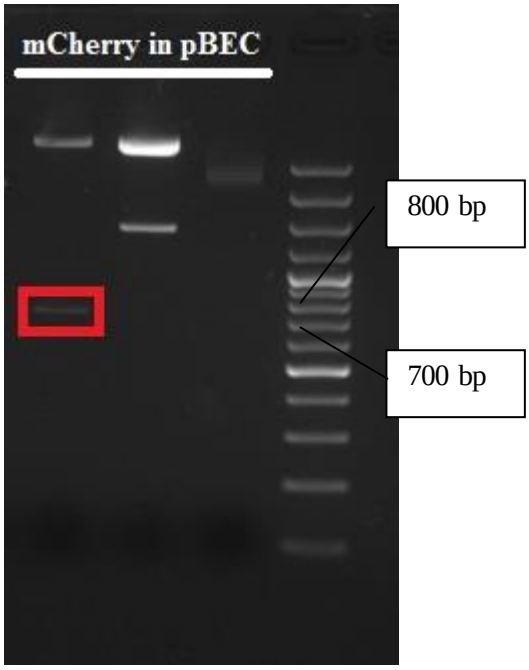

Figure 3.26 Size control of mCherry in pBEC by digestion. Lane 1-3: pBEC containing mCherry digested with BamHI and EcoRI. Lane 4: GeneRuler 100 bp plus DNA ladder).

The figure depicts that only the construct loaded onto the lane 1 was at the expected size. Therefore, *Saccharomyces cerevisiae* DK102 cells were transformed with the construct and examined under fluorescence and confocal microscope. mCherry was expected to be distributed throughout the cytoplasm excluding the membrane bound organelles as seen in Figure 3.27.

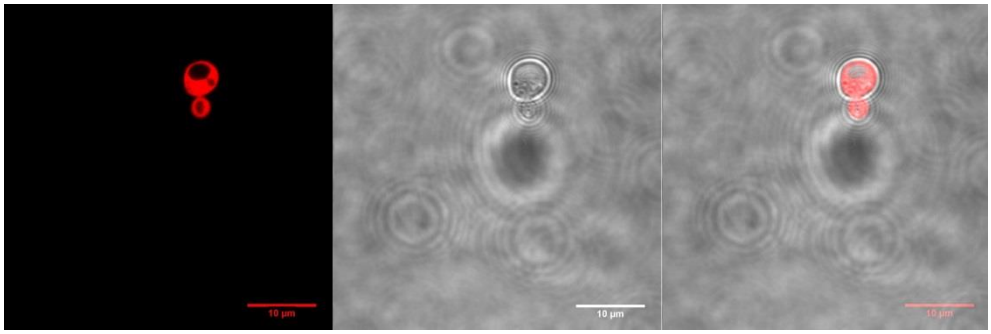

Figure 3.27 Cells expressing only mCherry generate cytosolic signal.

3.4.2. Insertion of ANP1 to Upstream of mCherry in pBEC Vector

Anp1p is mannosyl transferase located in the Golgi apparatus in *Saccharomyces cerevisiae* and is expected to be dispersed due to the nature of the Golgi in the budding yeast (Wooding & Pelham, 1998) (Figure 1.6).

Gene of the golgi marker was aimed at inserting between SpeI and BamHI cut sites at immediate upstream of mCherry in pBEC. Thus, using Primer 15 and 16 (Table D 1), SpeI and BamHI cut sites were added to respectively 5' and 3' end of the coding sequence owing to amplification by PCR. The PCR products were run on agarose gel and visualized (Figure 3.28).

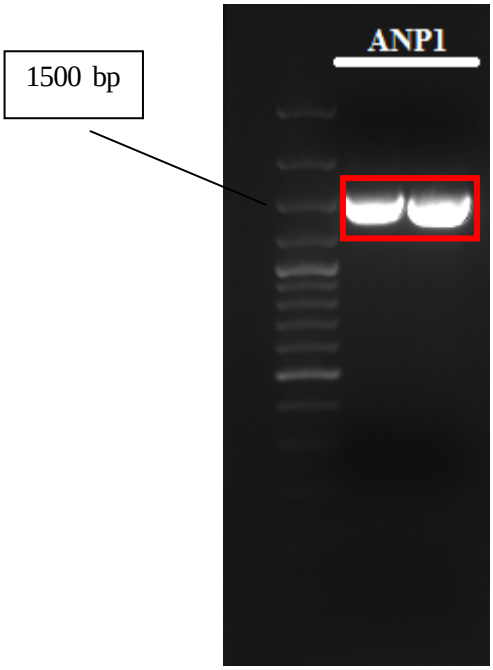

Figure 3.28 ANP1 amplified for cloning into pBEC. Lane 1: GeneRuler 100 bp plus DNA ladder. Lane 2-3: ANP1 DNA fragment amplified with BamHI and SpeI cut sites flanking the coding region.

With stop, ANP1 is 1503 bp long. When amplified with the cut sites, the product was expected to be 1524 bp long. Although the bands seemed to belong to a shorter DNA

fragment, it was due to high concentration of DNA and the bands later digested would verify that they were at the expected size.

In addition to pBEC, the gel extraction products of ANP1 were digested with SpeI and BamHI. Then, they were run on 1% agarose to check the size and reliability of the double digestion process (Figure 3.29).

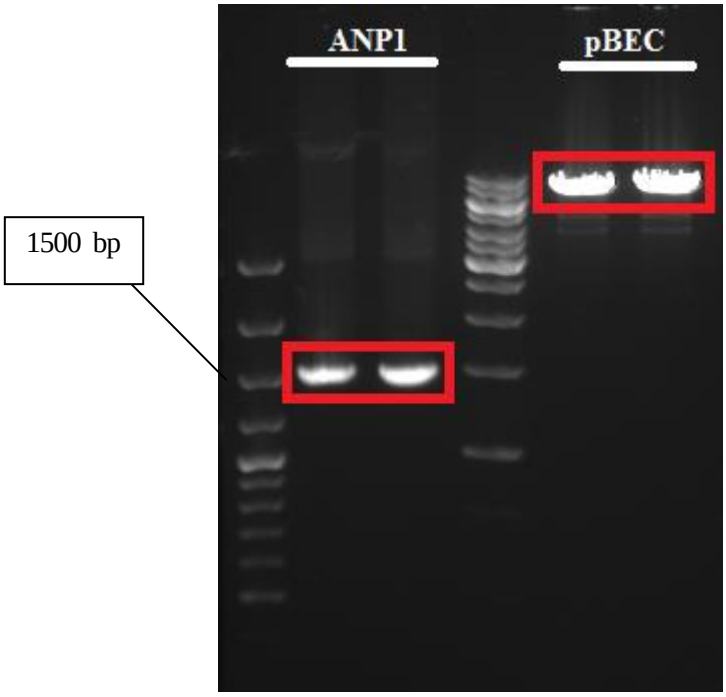

Figure 3.29 ANP1 and mCherry-containing pBEC digested with SpeI and BamHI. Lane 1: GeneRuler 100 bp plus DNA ladder. Lane 2-3: ANP1 PCR product digested with SpeI and BamHI. Lane 4: GeneRuler 1 kb DNA ladder. Lane 5-6: pBEC digested with SpeI and BamHI.

There is no sequence between SpeI and BamHI cut sites in pBEC; thus, it was expected to be 7196 bp long. ANP1 digested with SpeI and BamHI was to be around 1506 bp long. As seen from the figure above, all the sizes appeared to be correct. Consequently, the bands were purified from agarose and then ligated. Then, the newly constructed plasmid was used for transformation of competent *E.coli* TOP10 cells. Cells were grown on selective medium and then transformants were picked up and sent for sequencing (Table D 2) due to that the whole fusion cannot be digested for control by appropriate combination of restriction

enzymes. The verified plasmids were used for yeast transformation and visualized under fluorescence microscope for screening of red fluorescent signal.

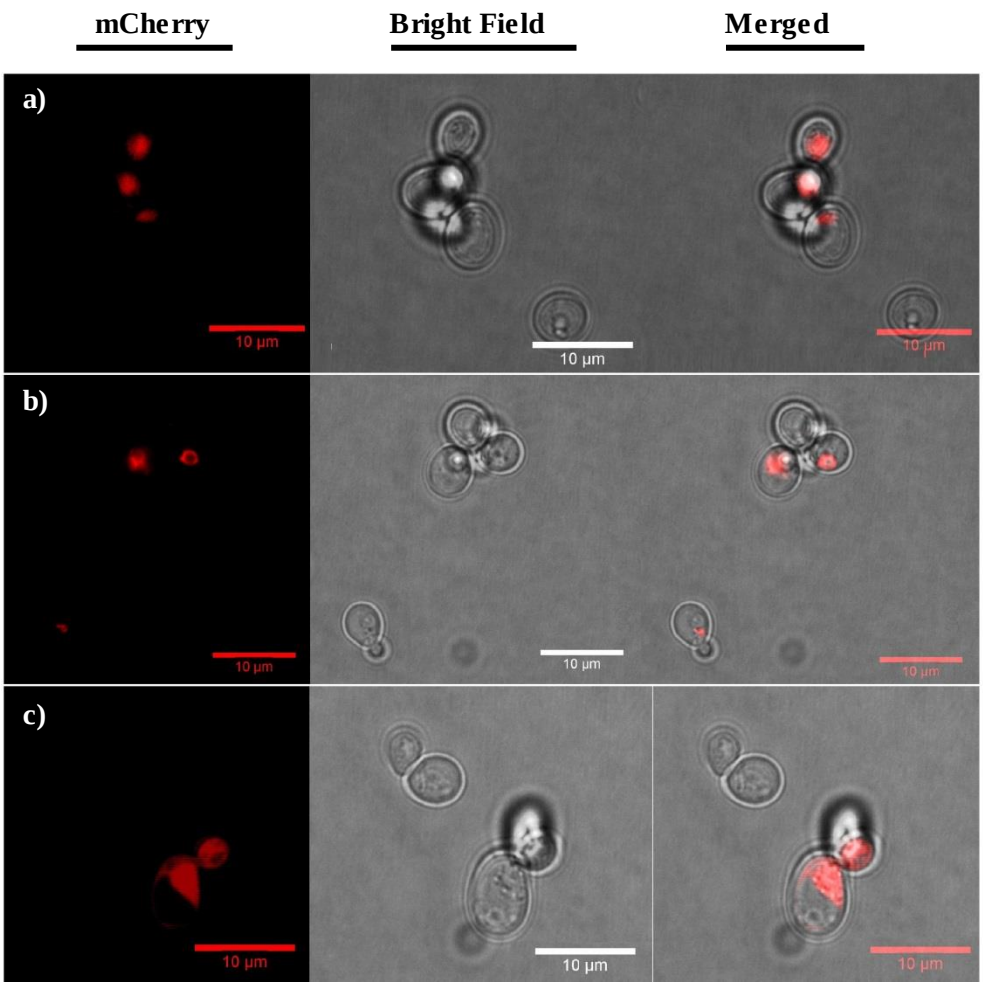

Figure 3.30 Yeast cells expressing red fluorescent Golgi marker under inverted wide field fluorescence microscope (a, b, c).

Figure 3.30 shows the distribution of the Golgi when a mannosyl transferase is tagged with red fluorescent protein. In *S. cerevisiae*, the Golgi apparatus is dispersed throughout the cells (Papanikou & Glick, 2009; Wooding & Pelham, 1998) (Figure 1.6). Due to resolution limits of microscope, the punctates were hard to detect; however, the distribution is clear to suggest that the red fluorescent Golgi marker has a unique distribution pattern and differs from vacuole or any other labeling.

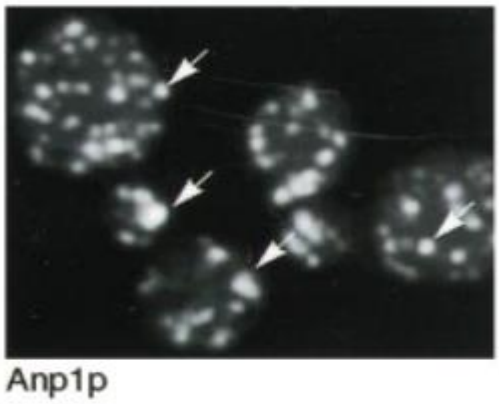

Figure 3.31 Immunofluorescent staining of the Golgi apparatus in live yeast cells (Wooding & Pelham, 1998).

3.5. Construction of Peroxisome Marker Using PCR Integration Method

For the generation of peroxisome marker, Pex3, which is integral membrane protein of peroxisome, was selected to be used (Agrawal, Joshi, & Subramani, 2011; Tam, Fagarasanu, Fagarasanu, & Rachubinski, 2005).

Using primer 17 and 18 (Table D 1), PEX3 was amplified with overhangs which are homologous the immediate upstream and 5' end of mCherry in pBEC. PCR products were in turn run on agarose gel and gel image was taken under UV light (Figure 3.32).

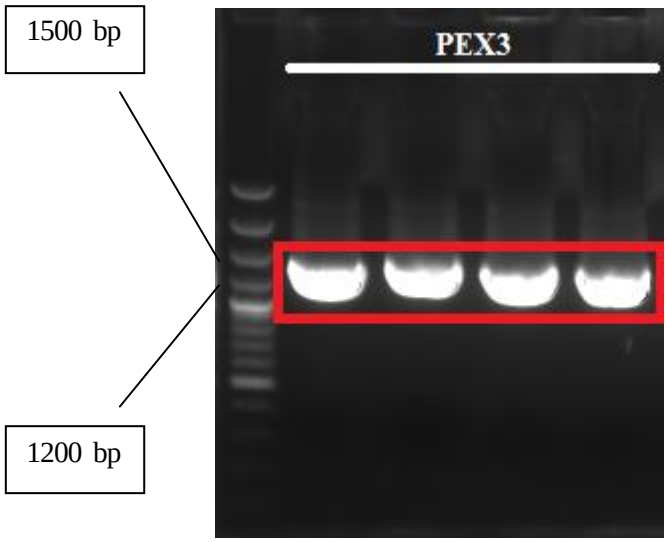

Figure 3.32 PEX3 amplified with overhangs complementary to immediate upstream and 5' end of mCherry in pBEC. Lane 1: GeneRuler 100 bp plus DNA ladder. Lane 2-5: PEX3 coding region amplified with overhangs homologous to upstream of mCherry in pBEC.

PEX3 is 1326 bp long. Excluding the code for stop and considering the flankings, the bands were expected to 1386 bp. The DNA fragments were extracted from the gel and used as primer for another PCR of PCR integration method. Previously constructed pBEC, which has mCherry between BamHI and EcoRI cut sites, was receiver plasmid. The second PCR products were digested with DpnI to get rid of nontransformant plasmids and then digestion products were transferred to competent *E.coli* TOP10 cells. The transformant colonies were screened from selective medium and grown for plasmid isolation. The plasmids were in turn verified by sequencing. Then, DK102 yeast cells were transformed with the plasmids and peroxisome pattern was examined under confocal and fluorescence microscope when excited at 543 nm and the emission was collected at 585 nm.

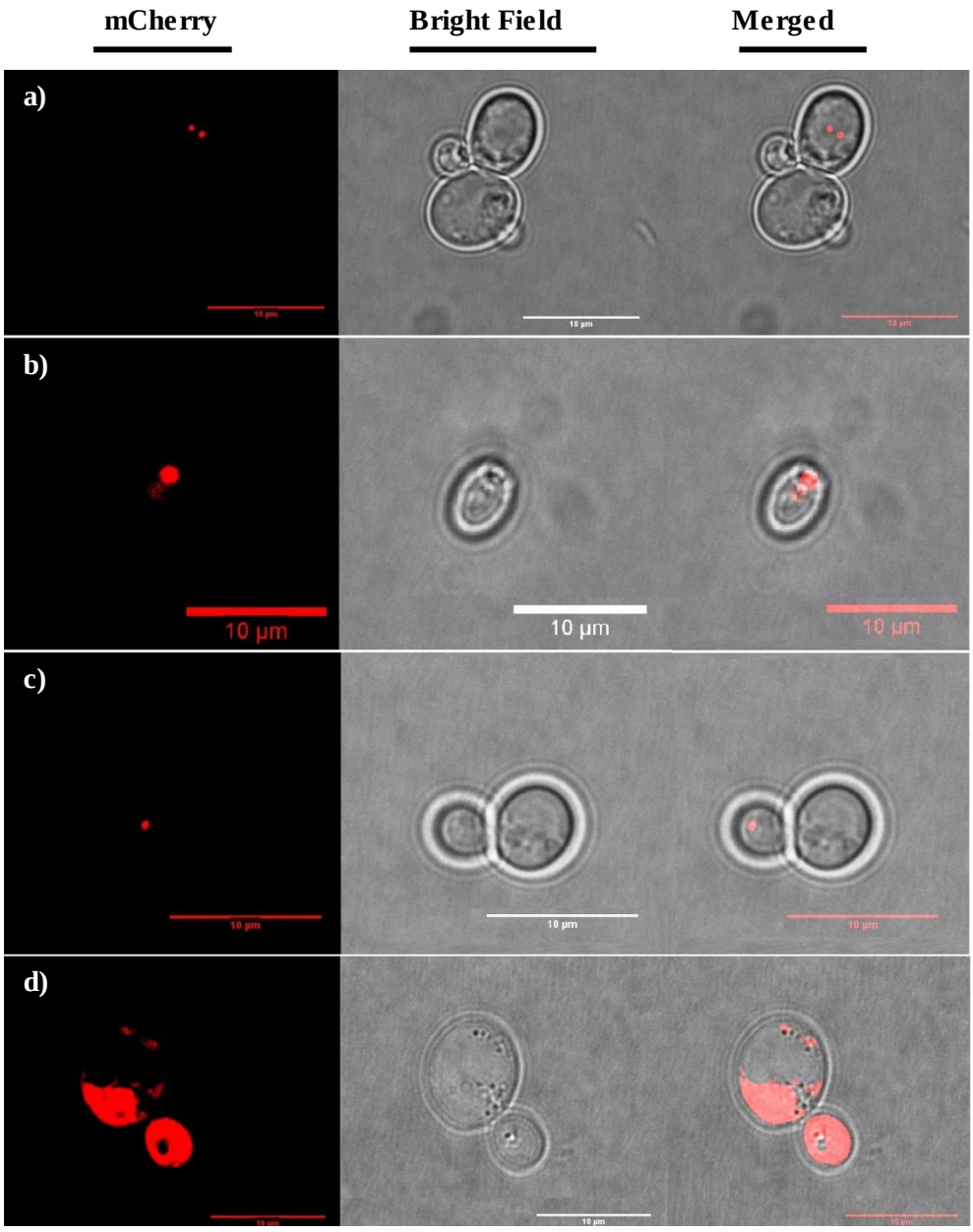

Figure 3.33 *Saccharomyces cerevisiae* cells expressing mCherry tagged Pex3p examined under inverted wide field fluorescence microscope (a, b and c) and laser scaning confocal microscope (d).

Peroxisomes in budding yeast are generally a few in number but small (Figure 3.33 a and c. Some studies show that cells grown in many fatty acid containing media have larger and more dispersed peroxisomes as depicted in Figure 3.33 b and d (Agrawal *et al.*, 2011).

3.6. Cloning EGFP Tagged Ste2p into pNED Vector

Although all the marker coding sequences were constructed in pBEC vector, whose yeast selection marker is trypthopan, the STE2 genes were also labeled with EGFP in the same vector. In order to effectively select the transformants, STE2-EGFP fusions were cloned into pNED vector, whose selection marker is uracil. Thus, transformants containing both marker and labeled receptor would be selected in MLTU.

For the purpose, pBEC vectors containing EGFP labeled full-length STE2 were digested with BamHI and EcoRI since the fusion genes were between the cut sites in pBEC. To manage the transfer to pNED vector, pNED was also digested with the enzymes. The digestion products were run on 1% agarose gel and visualized under UV light (Figure 3.34).

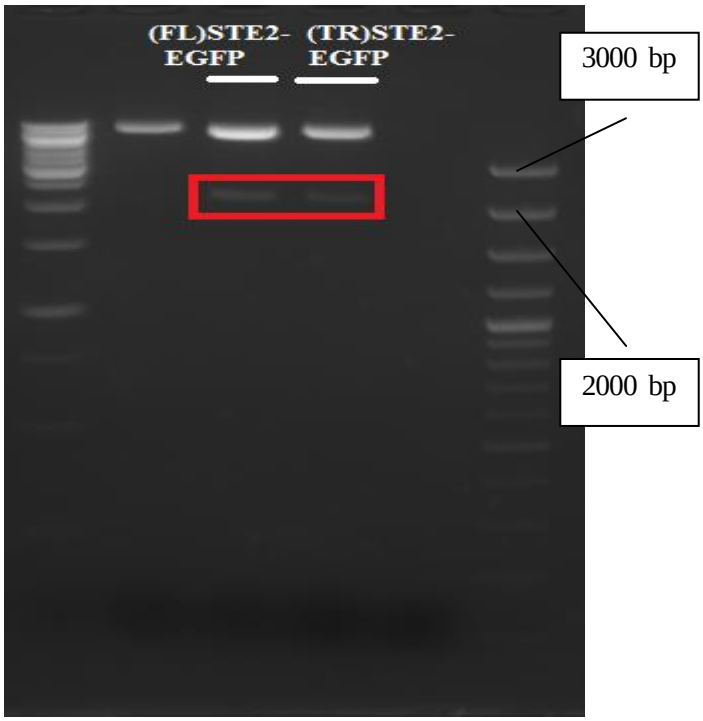

Figure 3.34 Full-length (FL) STE2 and truncated (TR) STE2 fused with EGFP in pBEC. Lane 1: GeneRuler 1 kb DNA ladder. Lane 2-3: EGFP fused to full-length STE2. Lane 4-5: EGFP fused to truncated STE2. Lane 6: GeneRuler 1 kb DNA ladder.

Between BamHI and EcoRI cut sites, there are 912 bp of STE2, 714 (717) bp of EGFP and the C-tail, His and FLAG tags were present. For truncated STE2 construct, after EGFP there is stop to terminate the translation at the point whereas stop is before EcoRI cut sites for full length EGFP. Therefore, the digestion products differed only in 3 base pairs, which cannot be distinguished by agarose gel electrophoresis but the sizes were as expected. Therefore, the digestion products were extracted from the gel and ligated to pNED which was also double digested with BamHI and EcoRI. The ligation products in turn were used for transformation of *E.coli* TOP10 cells. From chosen transformants grown on selective medium, plasmids were isolated and digested again with BamHI and EcoRI to control size of the gene fusions (Figure 3.35).

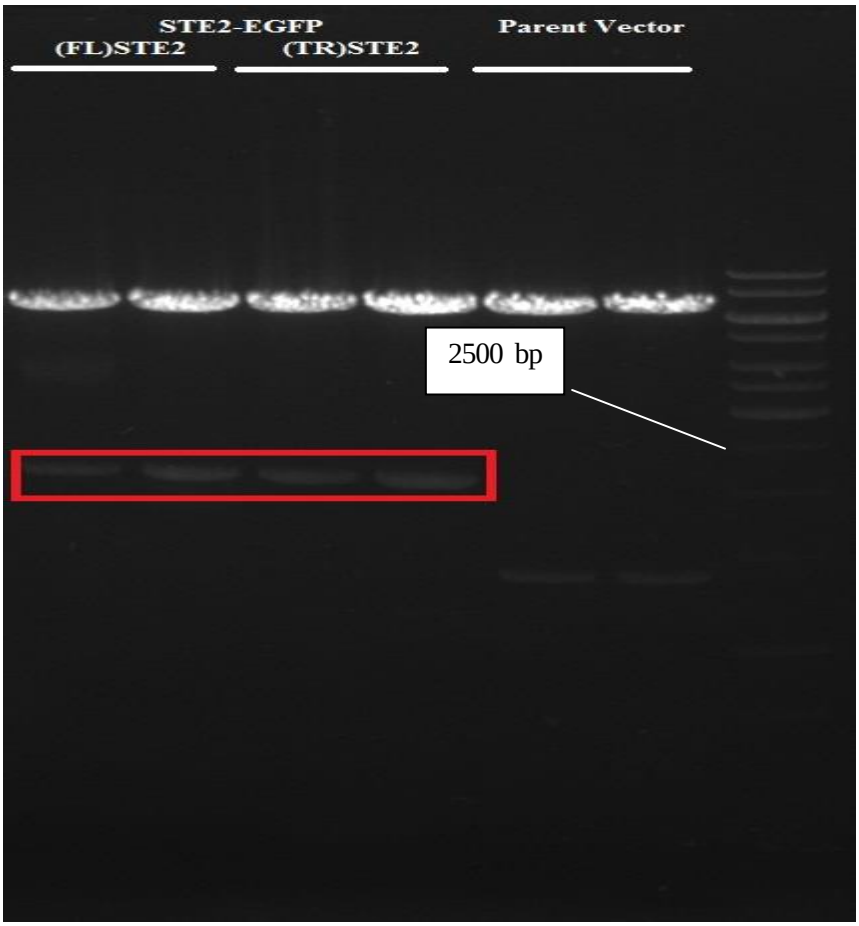

Figure 3.35 Size control of EGFP tagged STE2s by digestion. Lane 1-2: Full-length (FL) STE2-EGFP. Lane 3-4: Truncated (TR) STE2-EGFP. Lane 5-6: pBEC as control. Lane 7: GeneRuler 1 kb DNA ladder).

As shown at Figure 3.35, the bands for EGFP tagged STE2 were at the expected size. pNED only containing STE2 was used as negative control and gave bands at around 1400 bp as expected.

Then, the new constructs were sequenced and transferred into *Saccharomyces cerevisiae* DK102 cells. Transformants grown on MLU medium were visualized under laser scanning confocal microscope and inverted wide field fuorescent microscope exciting EGFP at 458 nm and the emission was collected in the range of 505-580 nm.

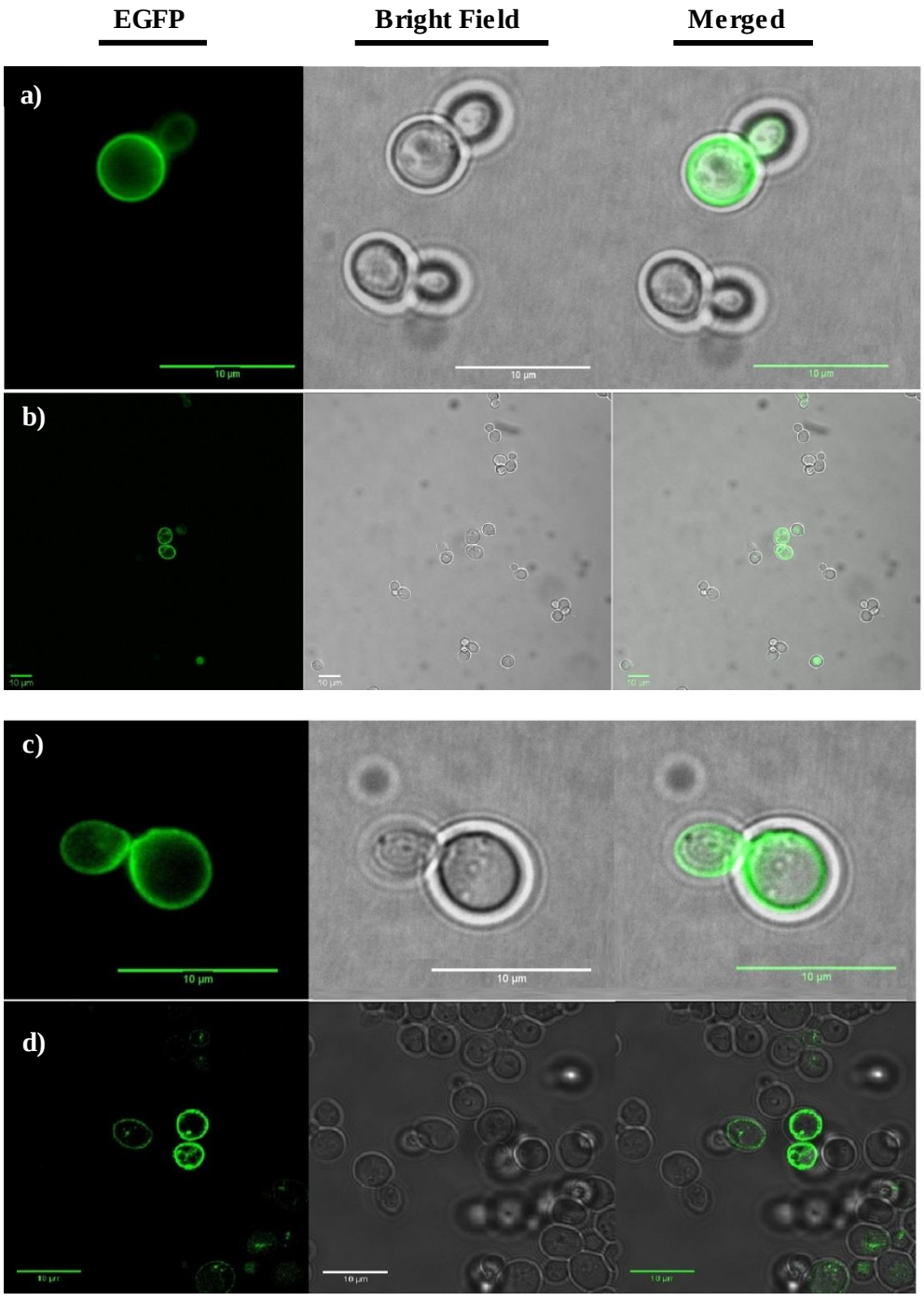

Figure 3.36 The images were acquired from yeast cells expressing EGFP tagged truncated Ste2p (a and b) or full-length Ste2p (c and d). a and c are laser scanning confocal microscope images whereas b and d are inverted wide field fluorescence microscope images.

3.7. Co-localization of Fluorescent Organelle Markers with EGFP Tagged Gpr1p

Gpr1p, GPCR that participate in glucose sensing in *Saccharomyces cerevisiae*, had been tagged with EGFP by one of my labmates and yeast were transformed with the construct in pNED vector.

Then, *S. cerevisiae* cells expressing EGFP labeled Gpr1p were transformed with pBEC vector containing mCherry fused with the organelle marker gene or targeting sequence. The transformants were screened on MLTU media and chosen colonies were examined under inverted wide field fluorescence microscope.

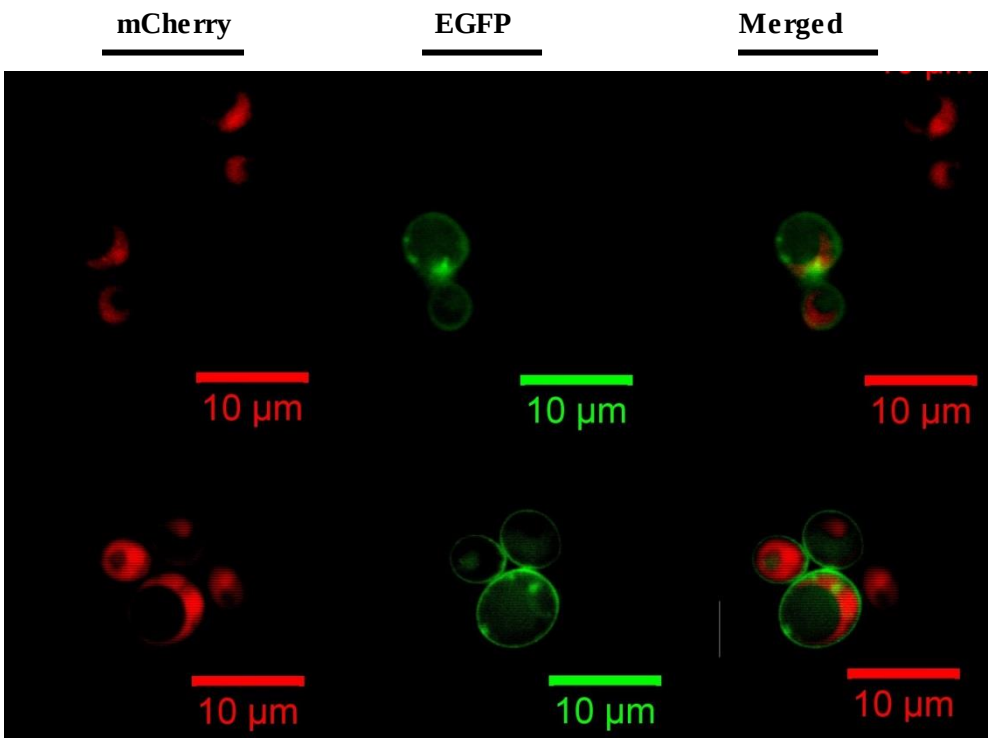

Figure 3.37 Cells co-expressing Gpr1p-EGFP and COPII marker under inverted wide field fluorescence microscope (a) and laser scanning confocal microscope (b).

Figure 3.37 depicts the colocalization of Gpr1p with COPII vesicle. While there is yellow signal for a) image, there is not so for b one. Due to that the anterograde transport is fairly

fast action, it can be expected that colocalization is hard to detect. However, the images suggest that Gpr1 is trafficked to PM by passing through COPI vesicles.

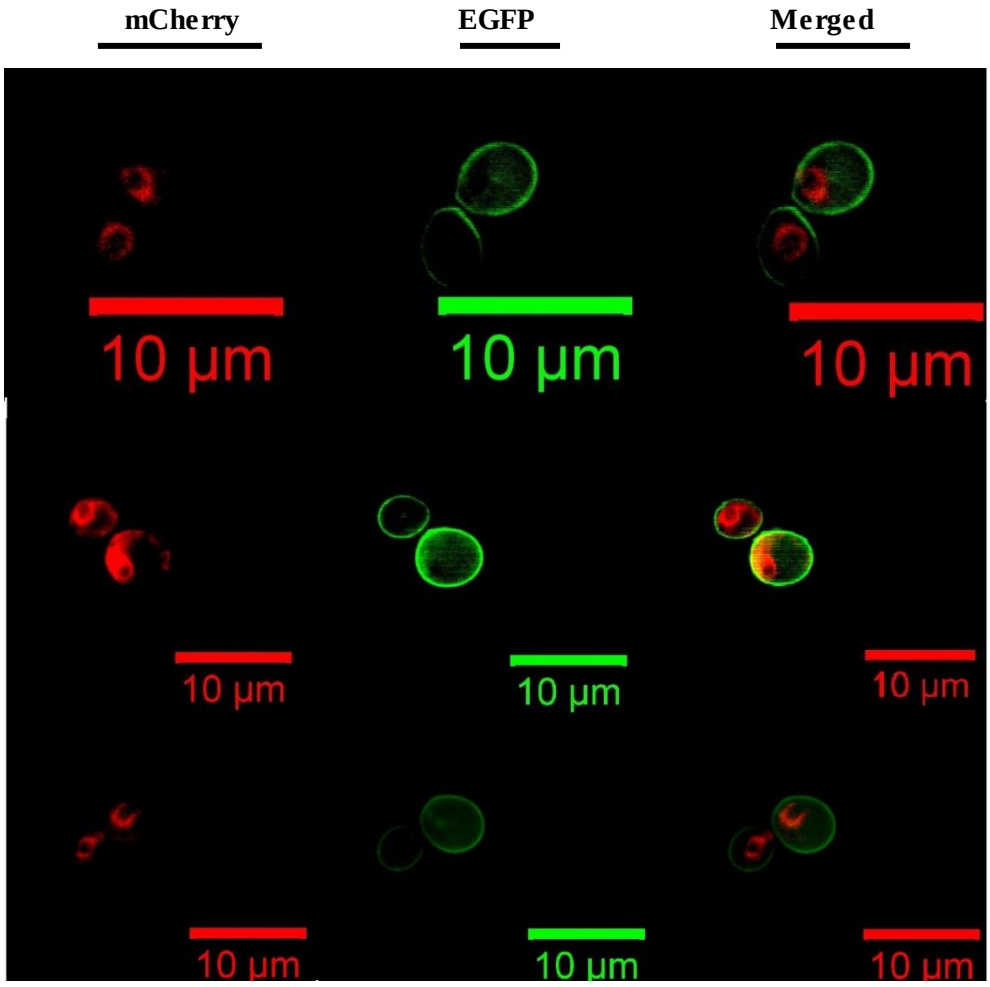

Figure 3.38 Yeast cells co-expressing Gpr1p and ER marker under inverted wide field fluorescence microscope (a, b) and laser scanning confocal microscope (c).

Although it is known that membrane proteins are processed in the ER we could not get any positive co-localization data for Gpr1p. This may be because of the maturation rate of EGFP. Until EGFP fluoresce Gpr1 may be trafficked to the ER. This can later be studied using ER exit mutants, which prevent the exit of folded proteins from the ER.

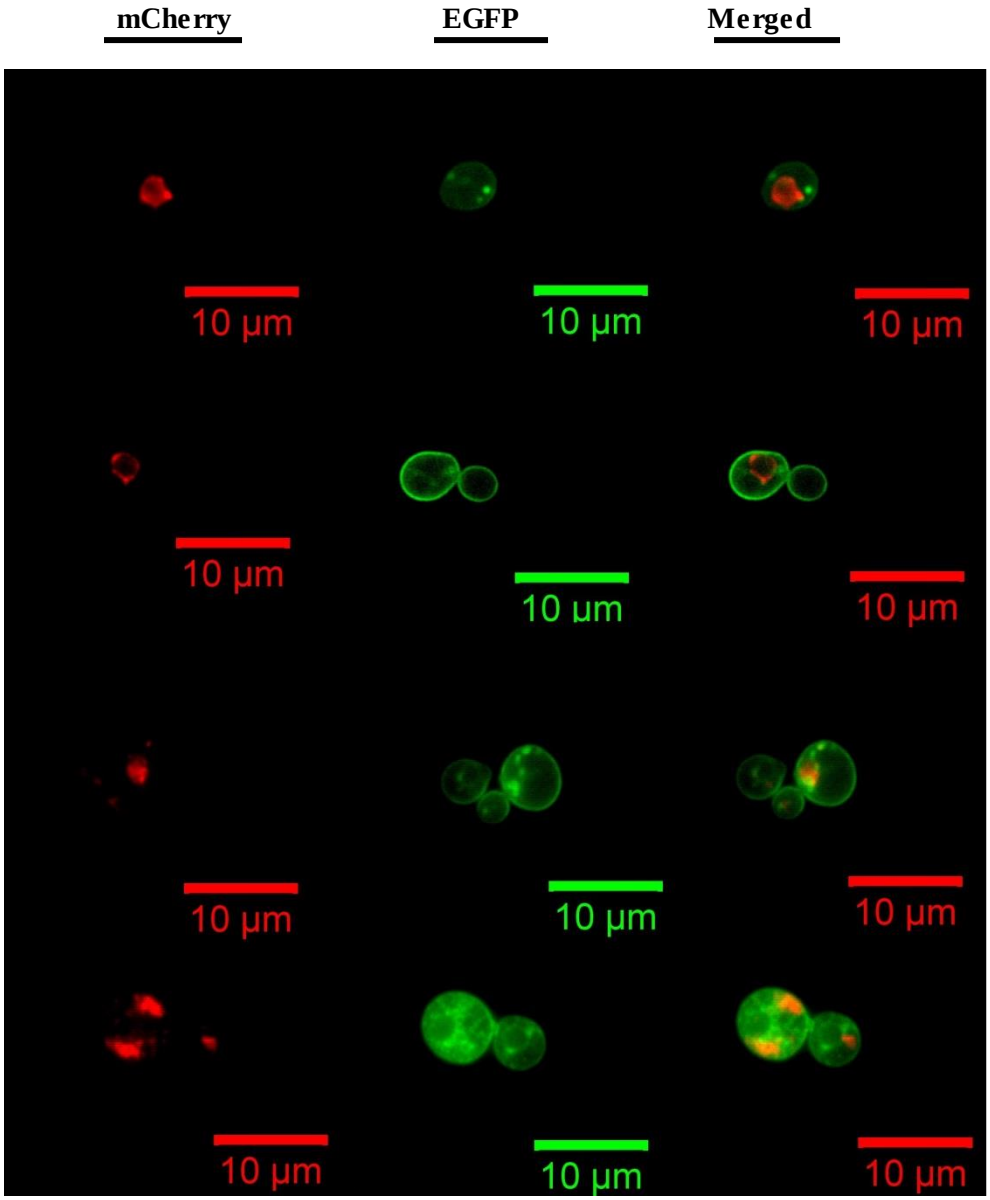

Figure 3.39 *S. cerevisiae* cells co-expressing Gpr1p-EGFP and late endosome marker inverted wide field fluorescence microscope (a,c) and laser scanning confocal microscope (b,d).

As illustrated in the figure above (a, c and d), Gpr1 co-localizes with late endosome marker. This may be proof of that Gpr1 is internalized by endocytic vesicles and then the vesicle maturates to form late endosomes. Although the signal was acquired from the late endosome, which seemed to localize around vacuole especially in Figure 3.39 a and b, no green signal was obtained inside the vacuole. This may be due to acidity of vacuole or late endosome transports the internalized receptors to the Golgi or any other destination for processing rather than degradation.

3.8. Co-localization of Fluorescent Organelle Markers with EGFP Tagged Ste2p

Truncated Ste2p lacks its C tail, which possesses endocytosis signal. The absence leads to failure in internalization of the receptor. The cells containing the plasmid which has truncated STE2 coding sequence as EGFP fusion were transformed with organelle markers.

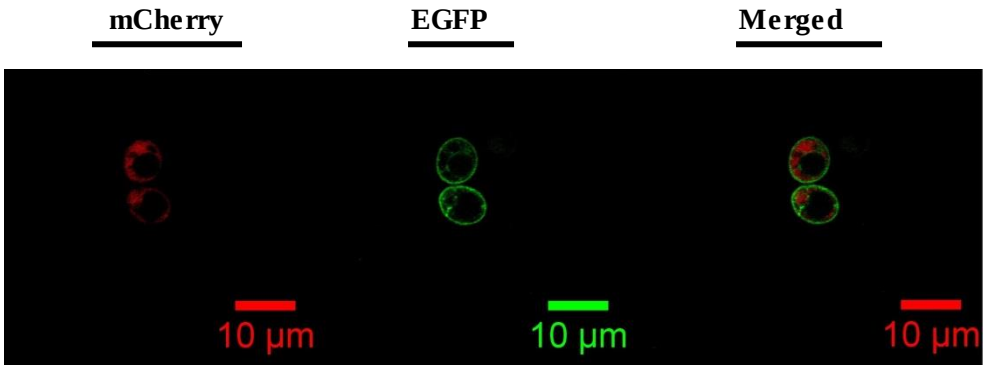

Figure 3.40 Cells co-expressing EGFP tagged truncated Ste2 with COPII marker.

There are not many images for the co-localization; thus, it is hard to conclude. However, it can be said that even if EGFP tagged truncated Ste2 fluoresce during anterograde transport the transient nature of the vesicle leads to difficulty in determination.

Full-length Ste2 tagged with EGFP containing yeast cells were transformed with organelle markers for examination of the trafficking of the receptor.

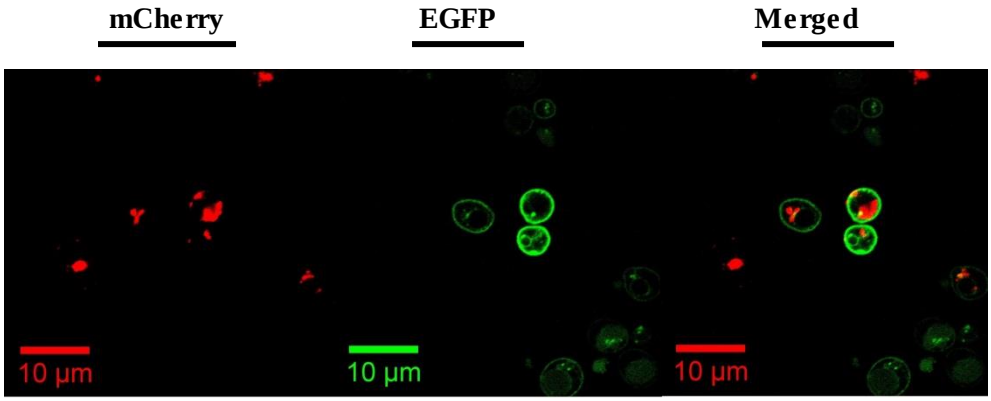

Figure 3.41 *S. cerevisiae* cells co-expressing EGFP tagged full-length Ste2 and late endosome marker.

It is expected that cells expressing full-length Ste2p endocytose the receptor upon ligand binding or for processing. As depicted in the Figure 3.41, it is clear that EGFP labeled full-length Ste2 co-localize with mCherry tagged Snf7.

The co-localization data are consistent with the expectations and known facts on intracellular trafficking of GPCRs. Therefore, they suggest that the co-localization data with all the markers generated and Ste2 and Ste2 dimer will elucidate the difference between trafficking of Ste2 and Ste2 homodimers.

Overexpression of fluorescent proteins was the major pitfall of the approach. The overexpression sometimes led to mislocalization of the markers, mainly to cytosol. In addition, it was reported that the overexpression may differentiate the transport of natural residents of the organelle and so cause disruption of characteristic morphology of subcellular compartment (Nelson *et al.*, 2007). However, these problems generally bring about negative effects on yeast growth and development. Therefore, before visualization of the yeast cells they were grown as always, growth conditions were strictly remained the same and only healthy cells were photographed.

While choosing the images presented in the study, the images representing the characteristic distribution or co-localization pattern of majority of cells were preferred.

CHAPTER IV

CONCLUSION

The aim of the study was to generate fluorescent proteins that are markers of the ER, Golgi, late endosome, COPII vesicle and peroxisome in *Saccharomyces cerevisiae* for co-localization studies in live cells with wide range of yeast proteins including GPCRs. These markers were chosen for the purpose of tracking of intracellular trafficking of fluorescently labeled yeast G-protein-coupled receptors and especially their dimers. For the excellent combination with EGFP tagged receptors, all the markers were constructed with fusion of mCherry, e red fluorescent protein, in pBEC vectors for suitable selection of double transformants. The construction in the same vector also eliminated the expression differences due to plasmid copy number and promoter strength.

As a result, late endosome marker was constructed by tagging Snf7p at C terminus with mCherry. The DNA sequence of the construct was verified and used for transformation of *S. cerevisiae* DK102 cells. The distribution of the marker was compared with previous descriptions of the characteristic morphology of the subcellular compartment and the distribution pattern of GFP labeled Snf7p which was described in literature.

Anterograde transport vesicles were also managed to visualize in live cells by tagging Sec13 with mCherry fluorescent protein. Budding yeast was transformed with the plasmids containing SEC13-mCherry fusion and examined under inverted wide field fluorescence microscope and laser scanning confocal microscope. The distribution pattern of COPII marker was evaluated by making comparison with GFP form of the markers generated and presented before.

For the first time, a yeast ER marker was constructed fusing well established targeting and retention signals at N and C terminus, respectively, with a fluorescent marker in yeast. For the purpose, signal sequence of SUC2 was inserted to the upstream of mCherry coding sequence and retention/retrieval sequence was embedded to downstream of mCherry. The distribution of the marker was compared with ER antibodies labeling fixed cells and verified the marker by sequencing and the comparison.

The golgi marker was prepared tagging Anp1 from C terminus with mCherry. The sequence was controlled by sequencing and yeast cells expressing the marker were excited to collect mCherry signal. Although the Golgi apparatus in S. cerevisae is suggested to be dispersed,

the signal obtained from the transformant cells appeared to be localized to point. Considering resolution limits of light microscopes, it cannot be confidently said but the fluorescent signal seemed to be from stack localized to a point of cell.

The last organelle marker was mCherry tagged Pex3p. Using PCR integration method, the construct was generated and in turn sequenced for verification. Images were taken from yeast cells expressing the tagged peroxisome integral membrane proteins and compared with previously reported peroxisome markers. The organelle marker can be used for co-localization studies with any proteins whose fatty acid chains were degraded in the peroxisomes from now on.

All the markers are valuable resources for co-localization studies in live yeast cells. Moreover, they can serve for identification of localization and thus function of unidentified proteins and monitoring the distribution and dynamics of organelles.

In order to assess the functionality of the organelle markers, they were co-localized with EGFP tagged Ste2p and Gpr1p. All the results were consistent with expectation based on knowledge on membrane protein trafficking. Therefore, it can be confidently suggest that these markers can be used for determination of trafficking of any proteins in *Saccharomyces cerevisiae*. In our case, if split-EGFP tagged STE2s are managed to clone into a vector containing double promoter the organelle markers can elucidate where Ste2 homodimerizes. During the study, cloning of the split-EGFP tagged Ste2 receptors has been started into a double-promoter vector; however, the approach cannot be succeeded up to now. Therefore, the co-localization data of Ste2 dimers with the organelle markers could not be obtained yet. In a further study, the co-localization data with Ste2 and Gpr1 receptors can be used for comparison of dimer and monomer trafficking.

REFERENCES

Agrawal, G., Joshi, S., & Subramani, S. (2011). Cell-free sorting of peroxisomal membrane proteins from the endoplasmic reticulum. *Proceedings of the National Academy of Sciences of the United States of America*, *108*(22), 9113–8. doi:10.1073/pnas.1018749108

Akiyama, N., Ghaedi, K., & Fujiki, Y. (2002). A novel pex2 mutant: catalase-deficient but temperature-sensitive PTS1 and PTS2 import. *Biochemical and biophysical research communications*, *293*(5), 1523–9. doi:10.1016/S0006-291X(02)00419-9

Attwood, T. K., & Findlay, J. B. C. (1994). Fingerprinting G-protein-coupled receptors. *Protein Eng*. Retrieved August 05, 2013, from http://peds.oxfordjournals.org/cgi/content/long/7/2/195

Babst, M., Katzmann, D. J., Estepa-Sabal, E. J., Meerloo, T., & Emr, S. D. (2002). Escrt-III: an endosome-associated heterooligomeric protein complex required for mvb sorting. *Developmental cell*, *3*(2), 271–82. Retrieved from http://www.ncbi.nlm.nih.gov/pubmed/12194857

Bardwell, L. (2004). A walk-through of the yeast mating pheromone response pathway, *25*, 1465–1476. doi:10.1016/j.peptides.2003.10.022

Barlowe, C. K., & Miller, E. a. (2013). Secretory protein biogenesis and traffic in the early secretory pathway. *Genetics*, *193*(2), 383–410. doi:10.1534/genetics.112.142810

Bouvier, M. (2001). Oligomerization of G-protein-coupled transmitter receptors. *Nature reviews. Neuroscience*, *2*(4), 274–86. doi:10.1038/35067575

Busti, S., Coccetti, P., Alberghina, L., & Vanoni, M. (2010). Glucose signaling-mediated coordination of cell growth and cell cycle in Saccharomyces cerevisiae. *Sensors (Basel, Switzerland)*, *10*(6), 6195–240. doi:10.3390/s100606195

Cai, Y., Chin, H., Lazarova, D., Menon, S., & Fu, C. (2008). The structural basis for activation of the Rab Ypt1p by the TRAPP membrane-tethering complexes. *Cell*, *133*(7), 1202–1213. Retrieved from http://www.sciencedirect.com/science/article/pii/S0092867408006818

Carlson, M., Taussig, R., Kustu, S., & Botstein, D. (1983). The secreted form of invertase in Saccharomyces cerevisiae is synthesized from mRNA encoding a signal sequence. *Molecular and cellular biology*, *3*(3), 439–47. Retrieved from http://www.pubmedcentral.nih.gov/articlerender.fcgi?artid=368553&tool=pmcentrez&rendertype=abstract

Chabre, M., Deterre, P., & Antonny, B. (2009). The apparent cooperativity of some GPCRs does not necessarily imply dimerization. *Trends in pharmacological sciences*, *30*(4), 182–7. doi:10.1016/j.tips.2009.01.003

Chabre, M., & Maire, M. (2005). Current Topics Monomeric G-Protein-Coupled Receptor as a Functional Unit, *44*(27).

Dixit, R., Cyr, R., & Gilroy, S. (2006). Using intrinsically fluorescent proteins for plant cell imaging. *The Plant journal : for cell and molecular biology*, *45*(4), 599–615. doi:10.1111/j.1365-313X.2006.02658.x

Dohlman, H G, Goldsmith, P., Spiegel, a M., & Thorner, J. (1993). Pheromone action regulates G-protein alpha-subunit myristoylation in the yeast Saccharomyces cerevisiae. *Proceedings of the National Academy of Sciences of the United States of America*, *90*(20), 9688–92. Retrieved from http://www.pubmedcentral.nih.gov/articlerender.fcgi?artid=47635&tool=pmcentrez&rendertype=abstract

Dohlman, Henrik G, & Thorner, J. W. (2001). Regulation f G-Protein – Iniated signal transduction in yeast: Paradigms and Principles. *Annual review of Biochemistry*, 70, 703-54.

Dowell, S. J., Bishop, a L., Dyos, S. L., Brown, a J., & Whiteway, M. S. (1998). Mapping of a yeast G protein betagamma signaling interaction. *Genetics*, *150*(4), 1407–17. Retrieved from http://www.pubmedcentral.nih.gov/articlerender.fcgi?artid=1460424&tool=pmcentrez&rendertype=abstract

Emanuelsson, O., & von Heijne, G. (2001). Prediction of organellar targeting signals. *Biochimica et biophysica acta*, *1541*(1-2), 114–9. Retrieved from http://www.ncbi.nlm.nih.gov/pubmed/11750667

Ferré, S., Baler, R., Bouvier, M., & Caron, M. (2009). Building a new conceptual framework for receptor heteromers. *Nature chemical …*, *5*(3), 131–134. doi:10.1038/nchembio0309-131.Building

Fischer-Parton, S., Parton, R. M., Hickey, P. C., Dijksterhuis, J., Atkinson, H. a, & Read, N. D. (2000). Confocal microscopy of FM4-64 as a tool for analysing endocytosis and vesicle trafficking in living fungal hyphae. *Journal of*

microscopy, *198*(Pt 3), 246–59. Retrieved from http://www.ncbi.nlm.nih.gov/pubmed/10849201

Fotiadis, D., Liang, Y., Filipek, S., Saperstein, D. a, Engel, A., & Palczewski, K. (2004). The G protein-coupled receptor rhodopsin in the native membrane. *FEBS letters*, *564*(3), 281–8. doi:10.1016/S0014-5793(04)00194-2

Gehret, A. U., Bajaj, A., Naider, F., & Dumont, M. E. (2006). Oligomerization of the yeast alpha-factor receptor: implications for dominant negative effects of mutant receptors. *The Journal of biological chemistry*, *281*(30), 20698–714. doi:10.1074/jbc.M513642200

Giepmans, B. N. G., Adams, S. R., Ellisman, M. H., & Tsien, R. Y. (2006). The fluorescent toolbox for assessing protein location and function. *Science (New York, N.Y.)*, *312*(5771), 217–24. doi:10.1126/science.1124618

Gietz, D., St Jean, a, Woods, R. a, & Schiestl, R. H. (1992). Improved method for high efficiency transformation of intact yeast cells. *Nucleic acids research*, *20*(6), 1425. Retrieved from http://www.pubmedcentral.nih.gov/articlerender.fcgi?artid=312198&tool=pmcentrez&rendertype=abstract

Harford, J., & Bonifacino, J. (2009). Subcellular Fractionation and Isolation of Organelles. *Current Protocols in Cell Biology*, (December). doi:10.1002/0471143030.cb0300s45

Hartwell, L. H. (1980). Mutants of Saccharomyces cerevisiae unresponsive to cell division control by polypeptide mating hormone. *The Journal of cell biology*, *85*(3), 811–22. Retrieved from http://www.pubmedcentral.nih.gov/articlerender.fcgi?artid=2111434&tool=pmcentrez&rendertype=abstract

Heldin, C. H. (1995). Dimerization of cell surface receptors in signal transduction. *Cell*, *80*(2), 213–23. Retrieved from http://www.ncbi.nlm.nih.gov/pubmed/7834741

Henne, William M, Buchkovich, N. J., & Emr, S. D. (2011). The ESCRT pathway. *Developmental cell*, *21*(1), 77–91. doi:10.1016/j.devcel.2011.05.015

Henne, William Mike, Buchkovich, N. J., Zhao, Y., & Emr, S. D. (2012). The endosomal sorting complex ESCRT-II mediates the assembly and architecture of ESCRT-III helices. *Cell*, *151*(2), 356–71. doi:10.1016/j.cell.2012.08.039

Herskowiitz, I. (1989). A regulatory hierarchy for cell specialization in yeast. *Nature*, *342*, 749–757.

Hicke, L. (1997). Ubiquitin-dependent internalization and down-regulation of plasma membrane proteins. *FASEB journal : official publication of the Federation of American Societies for Experimental Biology*, *11*(14), 1215–26. Retrieved from http://www.ncbi.nlm.nih.gov/pubmed/9409540

Hipser, C., Bushlin, I., & Gupta, A. (2010). Role of Antibodies in Developing Drugs That Target G-Protein-Coupled Receptor Dimers. *Mount Sinai Journal of …*, *77*(4), 374–380. doi:10.1002/msj.20199.ROLE

Horton, P., Park, K.-J., Obayashi, T., Fujita, N., Harada, H., Adams-Collier, C. J., & Nakai, K. (2007). WoLF PSORT: protein localization predictor. *Nucleic acids research*, *35*(Web Server issue), W585–7. doi:10.1093/nar/gkm259

Huber, L. a, Pfaller, K., & Vietor, I. (2003). Organelle proteomics: implications for subcellular fractionation in proteomics. *Circulation research*, *92*(9), 962–8. doi:10.1161/01.RES.0000071748.48338.25

Huh, W.-K., Falvo, J. V, Gerke, L. C., Carroll, A. S., Howson, R. W., Weissman, J. S., & O'Shea, E. K. (2003, October 16). Global analysis of protein localization in budding yeast. *Nature*. doi:10.1038/nature02026

Javois, L. (1999). *Immunocytochemical: Methods and Protocols* (Vol. 115). Retrieved from http://books.google.com/books?hl=en&lr=&id=Ch4J7FxmzI0C&oi=fnd&pg=PR5&dq=Immunocytochemical+methods+and+protocols&ots=b2-J-egOw2&sig=lbN0zxggXOMy6iCfwH4nY-qqx9A

Jordan, B., & Devi, L. (1999). G-protein-coupled receptor heterodimerization modulates receptor function. *Nature*, *399*(6737), 697–700. doi:10.1038/21441.G-protein-coupled

Kaupmann, K., Malitschek, B., Schuler, V., Heid, J., Froestl, W., Beck, P., … Bettler, B. (1998). GABA(B)-receptor subtypes assemble into functional heteromeric complexes. *Nature*, *396*(6712), 683–7. doi:10.1038/25360

Kniazeff, J., Bessis, A.-S., Maurel, D., Ansanay, H., Prézeau, L., & Pin, J.-P. (2004). Closed state of both binding domains of homodimeric mGlu receptors is required for full activity. *Nature structural & molecular biology*, *11*(8), 706–13. doi:10.1038/nsmb794

Kobilka, B. (2013). The Structural Basis of G-Protein-Coupled Receptor Signaling (Nobel Lecture). *Angewandte Chemie (International ed. in English)*, *94305*, 6380–6388. doi:10.1002/anie.201302116

Laboissière, M. C. A., Sturley, S. L., & Raines, R. T. (1995). The Essential Function of Protein-disulfide Isomerase Is to Unscramble Non-native Disulfide Bonds.

Journal of Biological Chemistry, *270*(47), 28006–28009. doi:10.1074/jbc.270.47.28006

Latek, D., Modzelewska, A., Trzaskowski, B., Palczewski, K., & Filipek, S. (2012). G protein-coupled receptors--recent advances. *Acta biochimica Polonica*, *59*(4), 515–29. Retrieved from http://www.ncbi.nlm.nih.gov/pubmed/23251911

Lee, M. C. S., Hamamoto, S., & Schekman, R. (2002). Ceramide biosynthesis is required for the formation of the oligomeric H+-ATPase Pma1p in the yeast endoplasmic reticulum. *The Journal of biological chemistry*, *277*(25), 22395–401. doi:10.1074/jbc.M200450200

Li, X., Staszewski, L., Xu, H., Durick, K., Zoller, M., & Adler, E. (2002). Human receptors for sweet and umami taste. *Proceedings of the National Academy of Sciences of the United States of America*, *99*(7), 4692–6. doi:10.1073/pnas.072090199

Lohse, M. J. (2010). Dimerization in GPCR mobility and signaling. *Current opinion in pharmacology*, *10*(1), 53–8. doi:10.1016/j.coph.2009.10.007

Lunn, J. E. (2007). Compartmentation in plant metabolism. *Journal of experimental botany*, *58*(1), 35–47. doi:10.1093/jxb/erl134

Madden, K., & Snyder, M. (1998). Cell polarity and morphogenesis in budding yeast. *Annual review of microbiology*, *52*, 687–744. doi:10.1146/annurev.micro.52.1.687

Martínez-Pastor, M. T., Marchler, G., Schüller, C., Marchler-Bauer, a, Ruis, H., & Estruch, F. (1996). The Saccharomyces cerevisiae zinc finger proteins Msn2p and Msn4p are required for transcriptional induction through the stress response element (STRE). *The EMBO journal*, *15*(9), 2227–35. Retrieved from http://www.pubmedcentral.nih.gov/articlerender.fcgi?artid=450147&tool=pmcentrez&rendertype=abstract

Milligan, G. (2007). G protein-coupled receptor dimerisation: molecular basis and relevance to function. *Biochimica et biophysica acta*, *1768*(4), 825–35. doi:10.1016/j.bbamem.2006.09.021

Nelson, B. K., Cai, X., & Nebenführ, A. (2007). A multicolored set of in vivo organelle markers for co-localization studies in Arabidopsis and other plants. *The Plant journal : for cell and molecular biology*, *51*(6), 1126–36. doi:10.1111/j.1365-313X.2007.03212.x

Neuman-Silberberg, F. S., Bhattacharya, S., & Broach, J. R. (1995). Nutrient availability and the RAS/cyclic AMP pathway both induce expression of ribosomal protein genes in Saccharomyces cerevisiae but by different

mechanisms. *Molecular and cellular biology*, *15*(6), 3187–96. Retrieved from http://www.pubmedcentral.nih.gov/articlerender.fcgi?artid=230551&tool=pmcentrez&rendertype=abstract

Overton, M., & Blumer, K. (2000). G-protein-coupled receptors function as oligomers in vivo. *Current biology : CB*, *10*(6), 341–4. Retrieved from http://www.ncbi.nlm.nih.gov/pubmed/10744981

Overton, M. C., & Blumer, K. J. (2002). The extracellular N-terminal domain and transmembrane domains 1 and 2 mediate oligomerization of a yeast G protein-coupled receptor. *The Journal of biological chemistry*, *277*(44), 41463–72. doi:10.1074/jbc.M205368200

Overton, M. C., Chinault, S. L., & Blumer, K. J. (2005). MINIREVIEW Oligomerization of G-Protein-Coupled Receptors : Lessons from the Yeast Saccharomyces cerevisiae, *4*(12), 1963–1970. doi:10.1128/EC.4.12.1963

Papanikou, E., & Glick, B. S. (2009). The yeast Golgi apparatus: insights and mysteries. *FEBS letters*, *583*(23), 3746–51. doi:10.1016/j.febslet.2009.10.072

Pausch, M. H. (1997). G-protein-coupled receptors in high-throughput screening assays for drug discovery. *Trends in biotechnology*, *15*, 487–494.

Peeters, T., Versele, M., & Thevelein, J. M. (2007). Directly from Galpha to protein kinase A: the kelch repeat protein bypass of adenylate cyclase. *Trends in biochemical sciences*, *32*(12), 547–54. doi:10.1016/j.tibs.2007.09.011

Pelham, H. R., Hardwick, K. G., & Lewis, M. J. (1988). Sorting of soluble ER proteins in yeast. *The EMBO journal*, *7*(6), 1757–62. Retrieved from http://www.pubmedcentral.nih.gov/articlerender.fcgi?artid=457164&tool=pmcentrez&rendertype=abstract

Peter, M., & Herskowitz, I. (1994). Direct inhibition of the yeast cyclin-dependent kinase Cdc28-Cln by Far1. *Science*, *265*, 1228–1231. Retrieved from http://www.sciencemag.org/content/265/5176/1228.abstract

Reneke, J., Blumer, K., Courchesne, W., & Thorner, J. (1988). The carboxy-terminal segment of the yeast alpha-factor receptor is a regulatory domain. *Cell*, *55*(2), 221–234. Retrieved from http://www.ncbi.nlm.nih.gov/pubmed/?term=The+carboxy-terminal+segment+of+the+yeast+alpha-factor+receptor+is+a+regulatory+domain.

Rolland, F., Winderickx, J., & Thevelein, J. M. (2002). Glucose-sensing and -signalling mechanisms in yeast. *FEMS yeast research*, *2*(2), 183–201. Retrieved from http://www.ncbi.nlm.nih.gov/pubmed/12702307

Rothe, C., & Lehle, L. (1998). Sorting of invertase signal peptide mutants in yeast dependent and independent on the signal-recognition particle. *European journal of biochemistry / FEBS*, *252*(1), 16–24. Retrieved from http://www.ncbi.nlm.nih.gov/pubmed/9523707

Salahpour, A., Angers, S., & Bouvier, M. (2000). Functional significance of oligomerization of G-protein-coupled receptors. *Trends in Endocrinology & Metabolism*, *11*(5). Retrieved from http://www.sciencedirect.com/science/article/pii/S1043276000002605

Salahpour, A., Angers, S., Mercier, J.-F., Lagacé, M., Marullo, S., & Bouvier, M. (2004). Homodimerization of the beta2-adrenergic receptor as a prerequisite for cell surface targeting. *The Journal of biological chemistry*, *279*(32), 33390–7. doi:10.1074/jbc.M403363200

Sato, K., & Nakano, A. (2007). Mechanisms of COPII vesicle formation and protein sorting. *FEBS letters*, *581*(11), 2076–82. doi:10.1016/j.febslet.2007.01.091

Schöneberg, T., Schulz, A., Biebermann, H., Hermsdorf, T., Römpler, H., & Sangkuhl, K. (2004). Mutant G-protein-coupled receptors as a cause of human diseases. *Pharmacology & therapeutics*, *104*(3), 173–206. doi:10.1016/j.pharmthera.2004.08.008

Shaner, N., Steinbach, P., & Tsien, R. (2005). A guide to choosing fluorescent proteins. *Nature methods*, *2*(12), 905–909. doi:10.1038/NMETH819

Shi, C., Paige, M. F., Maley, J., & Loewen, M. C. (2009). In vitro characterization of ligand-induced oligomerization of the S. cerevisiae G-protein coupled receptor, Ste2p. *Biochimica et biophysica acta*, *1790*(1), 1–7. doi:10.1016/j.bbagen.2008.10.003

Sikorski, R. S., & Hieter, P. (1989). A System of Shuttle Vectors and Yeast Host Strains Designed for Efficient Manipulation of DNA in, (1 979).

Smith, M. H., Ploegh, H. L., & Weissman, J. S. (2011). Road to ruin: targeting proteins for degradation in the endoplasmic reticulum. *Science (New York, N.Y.)*, *334*(6059), 1086–90. doi:10.1126/science.1209235

Solinger, J. a, & Spang, A. (2013). Tethering complexes in the endocytic pathway: CORVET and HOPS. *The FEBS journal*, *280*(12), 2743–57. doi:10.1111/febs.12151

Spang, a. (2008). The life cycle of a transport vesicle. *Cellular and molecular life sciences : CMLS*, *65*(18), 2781–9. doi:10.1007/s00018-008-8349-y

Surma, M. a, Klose, C., & Simons, K. (2012). Lipid-dependent protein sorting at the trans-Golgi network. *Biochimica et biophysica acta*, *1821*(8), 1059–67. doi:10.1016/j.bbalip.2011.12.008

Tam, Y. Y. C., Fagarasanu, A., Fagarasanu, M., & Rachubinski, R. a. (2005). Pex3p initiates the formation of a preperoxisomal compartment from a subdomain of the endoplasmic reticulum in Saccharomyces cerevisiae. *The Journal of biological chemistry*, *280*(41), 34933–9. doi:10.1074/jbc.M506208200

Terasaki, M., Loew, L., Lippincott-Schwartz, J., & Zaal, K. (2001). Fluorescent staining of subcellular organelles: ER, Golgi complex, and mitochondria. *Current protocols in cell biology / editorial board, Juan S. Bonifacino ... [et al.]*, *Chapter 4*, Unit 4.4. doi:10.1002/0471143030.cb0404s00

Terasaki, M., Song, J., Wong, J. R., Weiss, M. J., & Chen, L. B. (1984). Localization of endoplasmic reticulum in living and glutaraldehyde-fixed cells with fluorescent dyes. *Cell*, *38*(1), 101–108.

Venkatakrishnan, a J., Deupi, X., Lebon, G., Tate, C. G., Schertler, G. F., & Babu, M. M. (2013). Molecular signatures of G-protein-coupled receptors. *Nature*, *494*(7436), 185–94. doi:10.1038/nature11896

Versele, M., Lemaire, K., & Thevelein, J. M. (2001). Sex and sugar in yeast: two distinct GPCR systems. *EMBO reports*, *2*(7), 574–9. doi:10.1093/embo-reports/kve132

Vilardaga, J.-P., Agnati, L. F., Fuxe, K., & Ciruela, F. (2010). G-protein-coupled receptor heteromer dynamics. *Journal of cell science*, *123*(Pt 24), 4215–20. doi:10.1242/jcs.063354

Wang, H. X., & Konopka, J. B. (2009). Identification of amino acids at two dimer interface regions of the alpha-factor receptor (Ste2). *Biochemistry*, *48*(30), 7132–9. doi:10.1021/bi900424h

Wang, Y., Xuan, Y., Zhang, P., Jiang, X., Ni, Z., Tong, L., & Zhou, X. (2009). Targetingexpressionofthe catalyticdomainofthe kinaseinsert domainreceptor(KDR) intheperoxisomesof Pichia pastoris, *9*, 732–741. doi:10.1111/j.1567-1364.2009.00521.x

White, J. M., & Rose, M. D. (2001). Yeast mating: getting close to membrane merger. *Current biology : CB*, *11*(1), R16–20. Retrieved from http://www.ncbi.nlm.nih.gov/pubmed/11166190

Whiteway, M., Hougan, L., Dignard, D., Thomas, D. Y., Bell, L., Saari, G. C., … MacKay, V. L. (1989). The STE4 and STE18 genes of yeast encode potential β and γ subunits of the mating factor receptor-coupled G protein. *Cell*, *56*(3),

467–477. Retrieved from http://www.sciencedirect.com/science/article/pii/0092867489902493

Wilson, S., Bergsma, D. J., Chambers, J. K., Muir, a I., Fantom, K. G., Ellis, C., … Stadel, J. M. (1998). Orphan G-protein-coupled receptors: the next generation of drug targets? *British journal of pharmacology*, *125*(7), 1387–92. doi:10.1038/sj.bjp.0702238

Wollert, T., & Hurley, J. (2010). Molecular mechanism of multivesicular body biogenesis by ESCRT complexes. *Nature*, *464*(7290), 864–869. doi:10.1038/nature08849.Molecular

Wooding, S., & Pelham, H. R. (1998). The dynamics of golgi protein traffic visualized in living yeast cells. *Molecular biology of the cell*, *9*(9), 2667–80. Retrieved from http://www.pubmedcentral.nih.gov/articlerender.fcgi?artid=25539&tool=pmcentrez&rendertype=abstract

Xue, C., Hsueh, Y.-P., & Heitman, J. (2008). NIH Public Access. *FEMS Microbiol Rev.*, *32*(6), 1010–1032. doi:10.1111/j.1574-6976.2008.00131.x.Magnificent

Yesilaltay, A., & Jenness, D. D. (2000). Homo-oligomeric Complexes of the Yeast ␣ -Factor Endocytosis, *11*(September), 2873–2884.

Zabrocki, P., Bastiaens, I., Delay, C., Bammens, T., Ghillebert, R., Pellens, K., … Winderickx, J. (2008). Phosphorylation, lipid raft interaction and traffic of alpha-synuclein in a yeast model for Parkinson. *Biochimica et biophysica acta*, *1783*(10), 1767–80. doi:10.1016/j.bbamcr.2008.06.010

Zaman, S., Lippman, S. I., Zhao, X., & Broach, J. R. (2008). How Saccharomyces responds to nutrients. *Annual review of genetics*, *42*, 27–81. doi:10.1146/annurev.genet.41.110306.130206

Zeller, C. E., Parnell, S. C., & Dohlman, H. G. (2007). The RACK1 ortholog Asc1 functions as a G-protein beta subunit coupled to glucose responsiveness in yeast. *The Journal of biological chemistry*, *282*(34), 25168–76. doi:10.1074/jbc.M702569200

APPENDIX A

COMPOSITION AND PREPARATION OF BACTERIAL CULTURE MEDIUM

Luria Bertani (LB) Medium

10 g/L Tryptone

5 g/L Yeast Extract

5 g/L NaCl

20 g/L agar was added for solid medium.

The pH of the medium was adjusted to 7.0.

APPENDIX B

COMPOSITION AND PREPARATION OF YEAST CULTURE MEDIA

Table B 1 Composition of Drop-out Mix Used in the Preparation of Yeast Selective Media; MLT, MLU and MLTU

Amino Acid	Final Concentration (g/L)
Adenine Sulfate	0.058
Arginine HCl	0.026
Asparagine	0.058
Aspartic Acid	0.14
Glutamic Acid	0.14
Histidine HCl	0.028
Isoleucine	0.028
Leucine	0.083
Lysine	0.042
Methionine	0.028
Phenylalanine	0.69
Serine	0.52
Threonine	0.28
Tyrosine	0.042
Tryptophan*	0.03
Valine	0.21
Uracil*	0.028

*These amino acids were not added while preparation of drop-out mix according to the prepared media.

All the required amino acids were measured precisely and mixed in a dark bottle.

Media Composition

20 g/L D-Glucose

10 g/L Casamino Acids

6.7 g/L Yeast Nitrogen Base without Amino Acids

1.8 g/L Drop-out Mix

20 g/L agar was added for solid media preparation.

YEPD Media Composition

10 g/L Yeast Extract

20 g/L Peptone

20 g/L D-Glucose

20 g/L agar was added for solid YEPD medium.

APPENDIX C

PLASMID MAPS

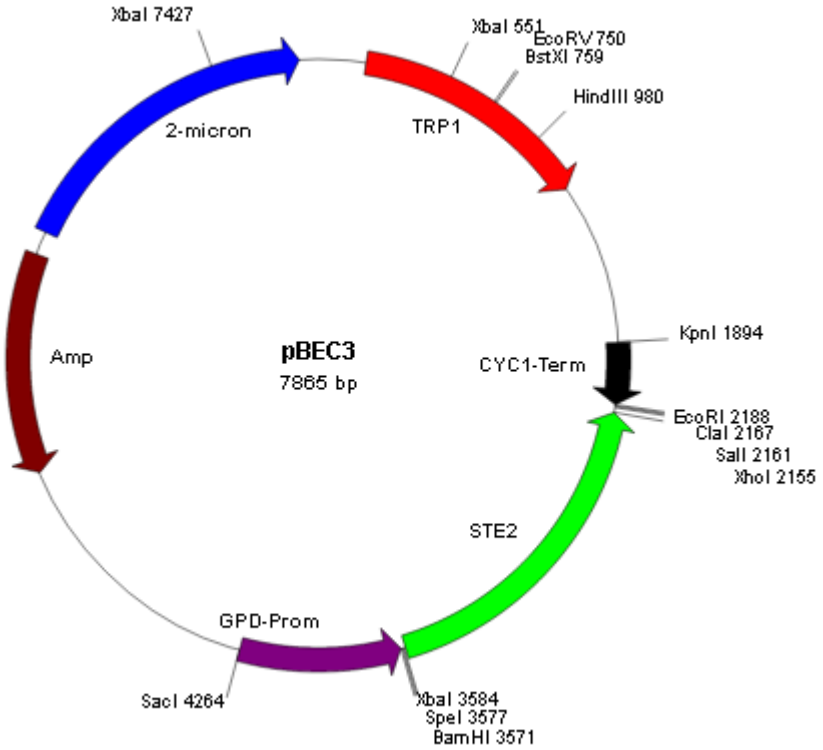

Figure C 1 pBEC1 Vector Containing STE2 Between BamHI and EcoRI Cut Sites

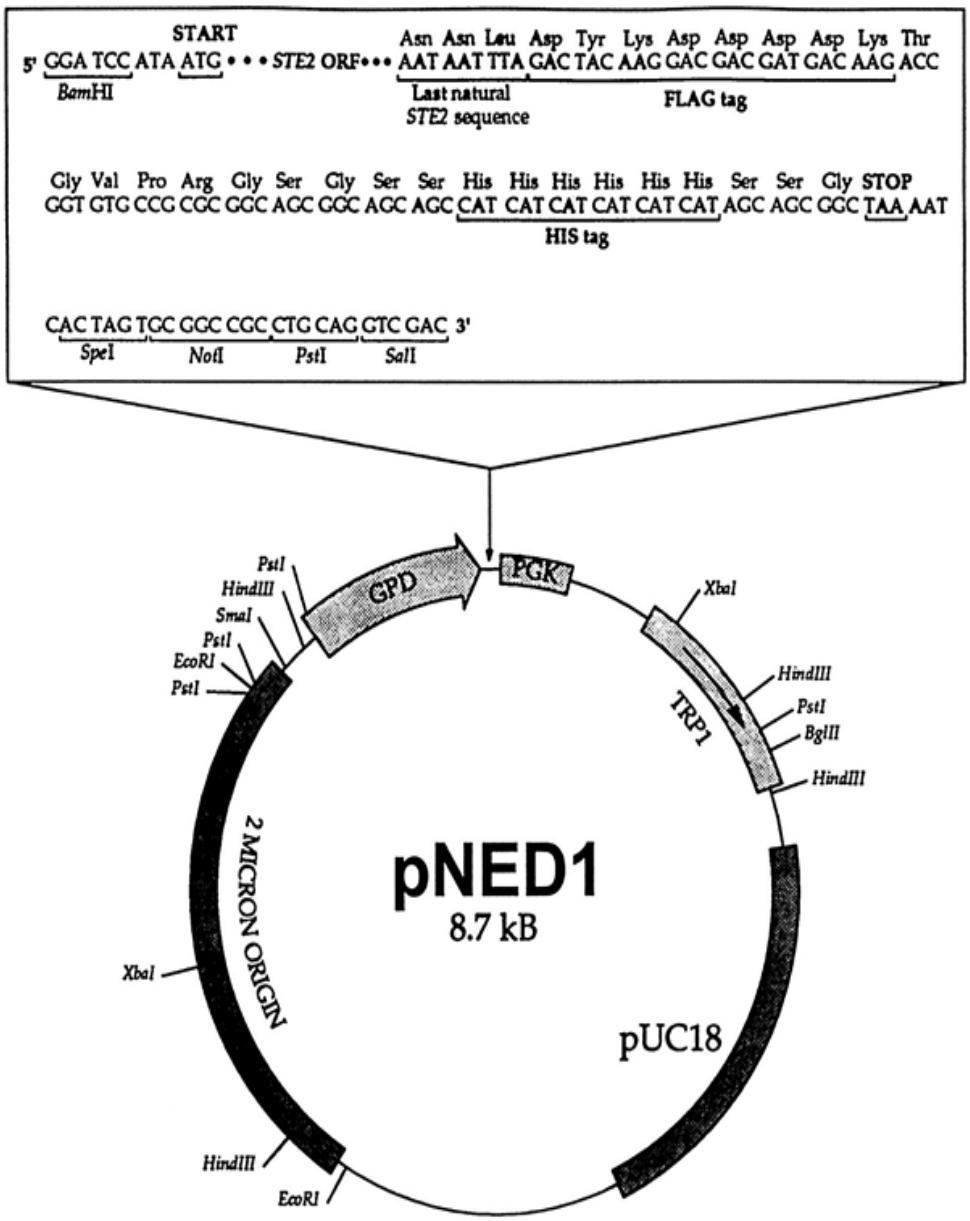

Figure C 2 pNED1 Vector Map

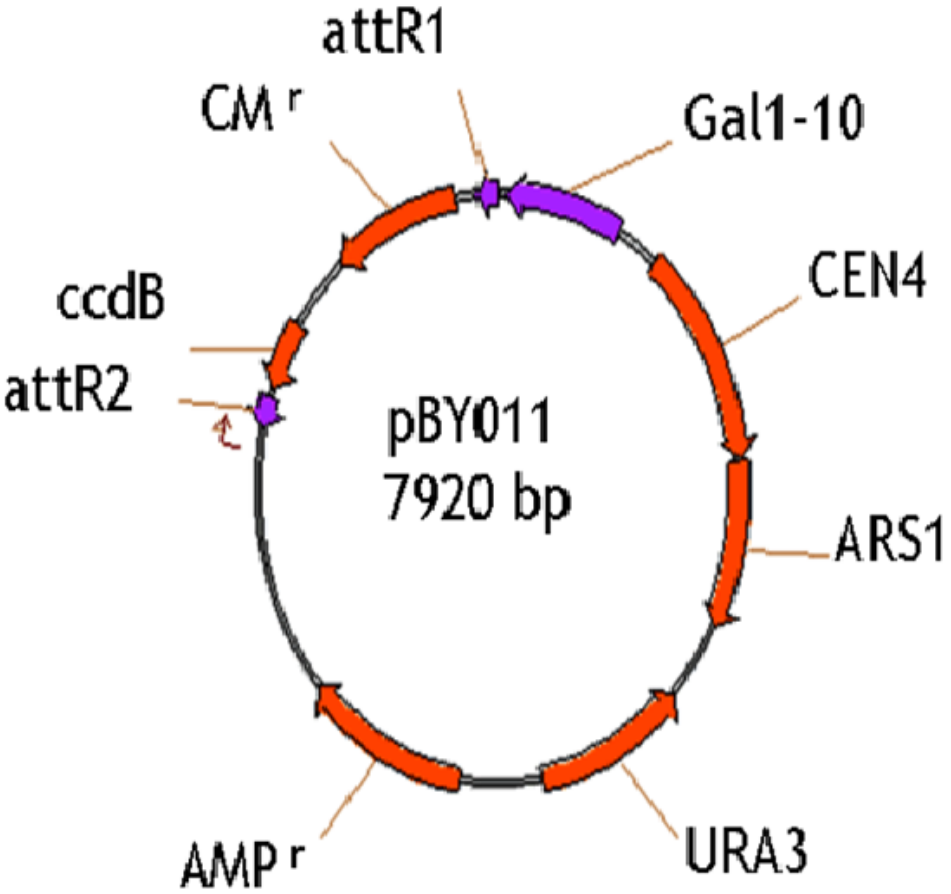

Figure C 3 Map of pBY011 Vector

APPENDIX D

PRIMERS

Table D 1 Primers Used in the Study

Primer	Sequence
1	TTAAGAGAACTACAAGCAGAAATGGGGCTTATGGTGAGCAA GGGCGAGGAG
2	AAATGGGAACCCGCTGGTGAAGTTCATCAGATGGTGAGCAAG GGCGAGGAG
3	AAGCTGGGTATCCCCGGGAATTGCCATGCTATTACTTGTACA GCTCGTCCATGCC
4	AGTACTGGATCCATGGTGAGCAAGGGCGAGGAGGATAACAT G
5	ATGGATGAATTCCTTGTACAGCTCGTCCATGCCGCCGGTGGA
6	ATGGATGAATTCCTACTTGTACAGCTCGTCCATGCCGCCGGT
7	GCACTG**GGATCC**ATGTGGTCATCACTTTTTGGT
8	GCATGA**GGTACC**TTACTTGTACAGCTCGTCCAT
9	GCTAAT**GGATCC**ATGGTCGTCATAGCTAATGCG
10	GCTATA**GGTACC**TTACTTGTACAGCTCGTCCAT
11	GATATCAAGCTTATCGATACCGTCGACGTGGTCTTCCAA
12	GTGACATAACTAATTACATGACTCGAG**TCA**TTGGAAGACCAC
13	gaacttagtttcgaCGGA**TCTAGA**ACTAGTATGCTTTTGCAAGCTTTC CTTTTCCTTTTGGCT
14	CCTCGCCCTTGCTCACCATGGATCCCATTGATGCAGATA TTTTGGCTGCAAAACCAGCCAAAAGG
15	TGATACACTAGTATGAAGTATAATAACAGAAAACTC
16	TGATCAGAATTCGTTTCTATCAGGGTCGAAGTCTAA
17	gaacttagtttcgaCGGA**TCTAGA**ACTAGTATGGCCCCAAATCAAAG ATCACGTTCG
18	CCTCGCCCTTGCTCACCATGGATCCAGGCTTGAAGGAAAACG AGCTGGAGAC

Table D 2 Sequencing Primers Used for Verification

Primer	Sequence
SNF7-mCherry Sequencing Primers	
CmCherry_517F	Aagcagaggctgaagctg
mCherry_22F	ATGGTGAGCAAGGGCGAGGAG
mCherry_RP	ACCTTGAAGCGCATGAACTC
SP1	GTGGATCCATGTGGTCATCA
SP2	GCAAACTTAAATCTAGAGACAATGAGG
SEC13-mCherry Sequencing Primers	
CmCherry_517F	Aagcagaggctgaagctg
mCherry_22F	ATGGTGAGCAAGGGCGAGGAG
mCherry_RP	ACCTTGAAGCGCATGAACTC
SP3	TAGTGGATCCATGGTCGTCA
SP4	TGGTTGCTTCCTCTGATGGT
mCherry and ER Marker Sequencing Primers	
CmCherry_517F	Aagcagaggctgaagctg
mCherry_22F	ATGGTGAGCAAGGGCGAGGAG
mCherry_RP	ACCTTGAAGCGCATGAACTC
ANP1-mCherry Sequencing Primers	
CmCherry_517F	Aagcagaggctgaagctg
mCherry_22F	ATGGTGAGCAAGGGCGAGGAG
mCherry_RP	ACCTTGAAGCGCATGAACTC
SP5	ACCCGTGACGATCAGAAAAG
SP6	GGAGAGCCTACCGAATGCTT
PEX3-mCherry Sequencing Primers	
CmCherry_517F	Aagcagaggctgaagctg
mCherry_22F	ATGGTGAGCAAGGGCGAGGAG
mCherry_RP	ACCTTGAAGCGCATGAACTC
SP7	GTATGGCCCCAAATCAAAGA
SP8	GCAGAGAAAGTTCGCCGTTA
SP9	CACGAATTCCCAAATATTCCA

APPENDIX E

BUFFERS AND SOLUTIONS

1X NEBuffer 4:

20 mM Tris-acetate

50 mM Potassium Acetate

10 mM Magnesium Acetate

1mM Dithiothreitol

pH: 7.9 at 25°C

1X T4 DNA Ligase Reaction Buffer:

50 mM Tris-HCl

10 mM $MgCl_2$

1 mM ATP

10 mM Dithiothreitol

pH: 7.5 at 25°C

10X TBE (Tris-Borate-EDTA) Buffer:

108 g/L Tris Base

55 g/L Boric Acid

40 mL/L 20 mM EDTA

For agarose gel electrophoresis, the stock solution was diluted by a dilution factor of 10.

6X Loading Dye:

10 mM Tris-HCl (pH: 7.6)

0.03% Bromophenol Blue

0.03% Xylene Cyanol FF

60% Glycerol (V/V)

60 mM EDTA

Transformation Buffer I:

100 mL/L 0.3 M KOAc

100 mL/L 1 M $RbCl_2$

10 mL/L 1M $CaCl_2$

50mL/L 1 M $MnCl_2$

15% Glycerol (V/V)

pH: 7.8

It was filter sterilized.

Transformation Buffer II:

50 mL/L 1 M MOPS

37.5 mL/L 1 M $CaCl_2$

50 mL/L 1 M $RbCl_2$

15% Glycerol (V/V)

pH: 6.5

It was filter sterilized.

Single Stranded Carrier DNA:

200 mg of salmon sperm DNA (DNA sodium salt from salmon testes, Sigma D1626) was dissolved in 100 mL of TE buffer (Sigma #93283) mixing by a magnetic stirrer for 2-3 hours. 500 µL aliquots were stored at -20°C.

1 M LiAc Solution:

Lithium acetate was dissolved in distilled water and the final pH was adjusted to be between 8.4 and 8.9. Then, it was filter sterilized and stored at room temperature. 100 mM LiAc solution was diluted from the 1 M stock dilution by dilution factor of 10.

50% (w/V) Polyethylene Glycol 3350:

PEG 3350 (Sigma, #P3640) was dissolved in distilled water and the prepared solution was heat sterilized at 120°C for 20 minutes. In order to prevent water evaporation, cap of the stock was sealed with parafilm and the solution was stored at room temperature.